AD-A133 556 STUDY OF PHASE DIAGRAMS OF TERNARY SEMICONDUCTORS(U) 1/1
HUGHES RESEARCH LABS MALIBU CA R KIKUCHI AUG 83
ARO-17090.3-PH DAAG29-80-C-0116

UNCLASSIFIED F/G 20/12 NL

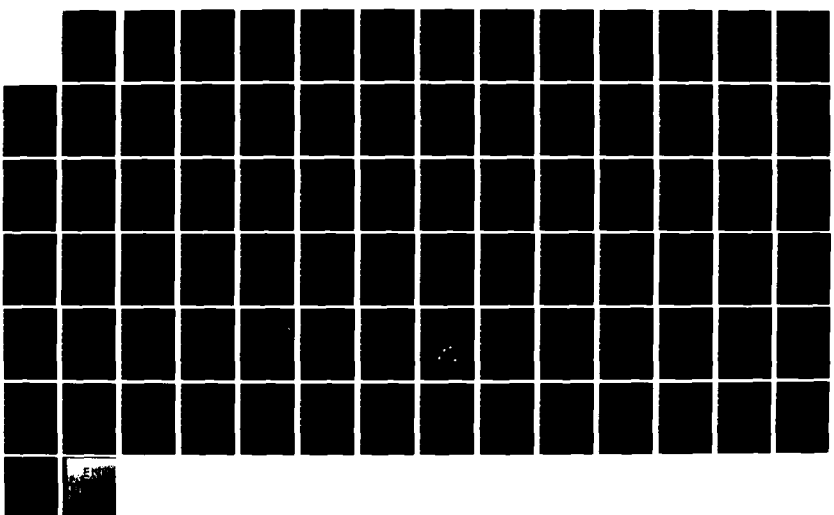

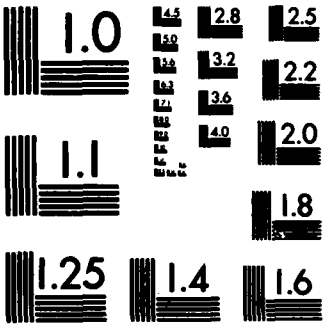

MICROCOPY RESOLUTION TEST CHART
NATIONAL BUREAU OF STANDARDS-1963-A

STUDY OF PHASE DIAGRAMS OF TERNARY SEMICONDUCTORS

R. Kikuchi

Hughes Research Laboratories
3011 Malibu Canyon Road
Malibu, CA 90265

August 1983

DAAG29-80-C-0116
Final Report
20 April 1980 to 19 July 1983

U.S. ARMY RESEARCH OFFICE
P. O. Box 12211
Research Triangle Park, NC 27709

UNCLASSIFIED

SECURITY CLASSIFICATION OF THIS PAGE (When Data Entered)

REPORT DOCUMENTATION PAGE		READ INSTRUCTIONS BEFORE COMPLETING FORM
1. REPORT NUMBER	2. GOVT ACCESSION NO. AD-A133 556	3. RECIPIENT'S CATALOG NUMBER
4. TITLE (and Subtitle) Study of Phase diagrams of Ternary Semiconductors		5. TYPE OF REPORT & PERIOD COVERED Final Report 20 Apr. 1980 - 19 July 1983
		6. PERFORMING ORG. REPORT NUMBER
7. AUTHOR(s) R. Kikuchi		8. CONTRACT OR GRANT NUMBER(s) DAAG 29-80-C-0116
9. PERFORMING ORGANIZATION NAME AND ADDRESS Hughes Research Laboratories 3011 Malibu Canyon Road Malibu, CA 90265		10. PROGRAM ELEMENT, PROJECT, TASK AREA & WORK UNIT NUMBERS
11. CONTROLLING OFFICE NAME AND ADDRESS U.S. Army Research Office P.O. Box 12211 Research Triangle Park, NC		12. REPORT DATE August 1983
		13. NUMBER OF PAGES
14. MONITORING AGENCY NAME & ADDRESS(if different from Controlling Office)		15. SECURITY CLASS. (of this report)
		15a. DECLASSIFICATION/DOWNGRADING SCHEDULE

16. DISTRIBUTION STATEMENT (of this Report)

Approved for public release; distribution unlimited.

17. DISTRIBUTION STATEMENT (of the abstract entered in Block 20, if different from Report)

18. SUPPLEMENTARY NOTES

THE VIEW, OPINIONS, AND/OR FINDINGS CONTAINED IN THIS REPORT ARE THOSE OF THE AUTHOR(S) AND SHOULD NOT BE CONSTRUED AS AN OFFICIAL DEPARTMENT OF THE ARMY POSITION, POLICY, OR DECISION, UNLESS SO DESIGNATED BY OTHER DOCUMENTATION.

19. KEY WORDS (Continue on reverse side if necessary and identify by block number)

20. ABSTRACT (Continue on reverse side if necessary and identify by block number)

In this three-year project on the theoretical studies of Hg-Cd-Te phase diagram, the liquidus and solidus have been calculated using the conditions of thermal coexistence of the liquid and solid.

The pair approximation of the cluster variation method is used throughout, and the energy parameters are always treated as independent of temperature and composition.

DD FORM 1 JAN 73 1473 EDITION OF 1 NOV 65 IS OBSOLETE

UNCLASSIFIED

SECURITY CLASSIFICATION OF THIS PAGE (When Data Entered)

The lattice defects in the solid are neglected in the first treatment. By choosing energy parameters, it is possible to make the theoretical liquidus and solidus agree reasonably well with experiments. In the later formulation, lattice vacancies and antiatoms are taken into account. Then the theory shows that the temperature dependence of Hg vacancies is the same as that of holes in the valence band. The relation between the hole concentration and the partial pressure of Hg can also be derived with good agreement with experiments.

TABLE OF CONTENTS

LIST OF ILLUSTRATIONS

SECTION 1

INTRODUCTION AND SUMMARY

Hg-Cd-Te is a semiconductor material particularly useful as an infrared detector. Although it has been grown for some years, there are still problems in achieving crystals of desired quality. In order to improve the crystal growth technique, the knowledge and understanding of the liquidus-solidus phase diagram are of crucial importance. This study has addressed the theoretical calculation of the phase diagram of HgCdTe.

Heretofore, we have known that the pair approximation of the cluster variation method (CVM) provides a good theoretical phase diagram of III-V compound semiconductors wuch as GaAs and In-As, as reported in Section 2 and Appendix A. In this project we have applied a similar theoretical technique to Hg-Cd-Te, which is a II-VI semiconductor.

The special qualitative features of the II-VI liquidus as compared with the III-V case are that the former is asymmetric with respect to the 50-50 composition, and that the liquidus is sharply peaked at the 50% composition. In order to explain these two features theoretically (Section 3 and Appendix B), we have allowed vacancies in the pseudo-lattice model of the liquid phase, and have included molecular species HgTe and CdTe in the liquid phase. It has been discovered that the peak in the liquidus results when the interaction between an atomic species (Hg, Cd or Te) and a molecular species (HgTe or CdTe) is repulsive.

Using the associated liquid model developed in Section 3, a theoretical treatment of the liquidus of the ternary Hg-Cd-Te has been developed in Section 4 (and in Appendix C). In this treatment no lattice defects are included in the solid phase. The liquidus in both the Te-rich region and that in the Hg-rich region agree with experiments reasonably well. The special feature of the work that differs from the previous regular

solution theory treatment of Brebrick et al. is that the nearest-neighbor interaction parameters used in formulating the free energy of the liquid phase are treated as being independent of temperature and composition.

It is known that the electrical properties of the semiconductor depends greatly on the lattice defects in the Hg-Cd-Te crystal. Thus, in Section 5 we take into account lattice vacancies and antiatoms in the crystal (details are described in Appendix D). The lattice is composed of two fcc sublattices, one for Te atoms and the other for Hg and Cd. The theory uses intersublattice pair probabilities and intrasublattice pair probabilities as the basic variables and includes intersublattice and intrasublattice nearest-neighbor interaction energies.

The method of calculating the liquidus and solidus using the solid with defects (of Section 5) is explained in Section 6, and the details are presented in Appendix E. The main results are the number of Hg vacancies in Figure 10, the Hg partial pressure in Figure 11, and the relation between the two in Figure 12. These results agree well with Vydyanathan's experiments.

Interstitial atoms have not been taken into account in Sections 5 and 6, but their plausibility is discussed in Section 7.

SECTION 2

III-V DIAGRAM CALCULATIONS USING THE "PAIR" METHOD

Calculations of phase diagrams of III-V systems form the basis of the II-VI systems, which are the main concern of this study. Therefore, we have included the main results of III-V calculations in Figures 1, 2, and 3 even though they had been done before this effort was begun. They were calculated by Stringfellow and Greene[1] and also by the author.[2] The formulation in Reference 2 is basic in subsequent work developed in this study. Therefore, Reference 2 is attached as Appendix A in this report.

In modeling and calculating the free energy of the liquid phase, a pseudo-lattice structure is assumed. Configurations of nearest-neighbor pairs on the lattice are chosen as the basic variables, and thus the method is called the "pair" method (which is also called the quasi-chemical approximation or Bethe's approximation).

The excellent agreement between theory and experiments in Figures 1, 2, and 3 supports the usefulness and the reliability of the pair method. Noteworthy features in the liquidus curves in Figure 1 are that the curves are symmetric with respect to the 50% composition, and also well rounded near the maxima.

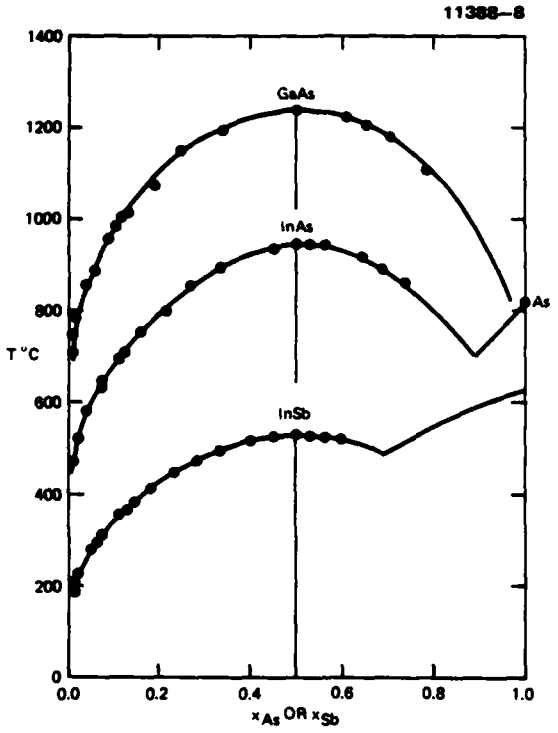

Figure 1. Liquidus curves of III-V semiconductors. Solid curves are theory and circles are experiments.

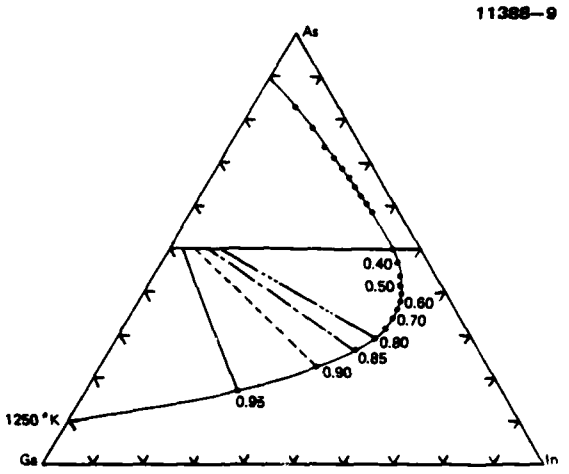

Figure 2. The calculated isothermal liquidus of Ga-In-As ternary system at 1250°K. The numbers along the curve are x in the solid composition, $(GaAs)_{1-x}(InAs)_x$. Four tie lines are shown.

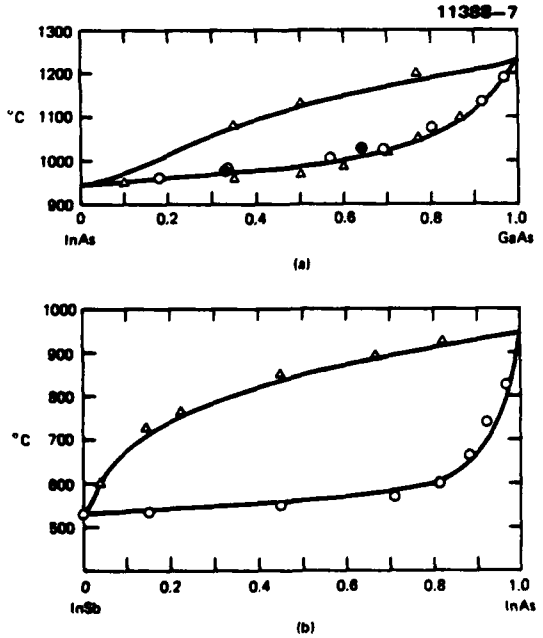

Figure 3. Pseudobinary liquidus and solidus curves of InAs-GaAs (a) and InSb-InAs (b). The solid curves are calculations, and the circles and triangles are experimental results.

SECTION 3

II-VI BINARY LIQUIDUS-SOLIDUS CALCULATIONS USING THE "PAIR" METHOD AND THE ASSOCIATION MODEL

Different from the III-V cases of Figure 1, the liquidus curves of Hg-Te and Cd-Te are not symmetric at right and left and are peaked near the 50% composition. In order to take into account these two features, the model of the liquid phase is modified in two aspects: vacancies are included in the pseudo-lattice structure and molecular species of HgTe or CdTe are added. When the effective interaction of molecular species and atomic species is repulsive, we can explain the sharp peak near the 50% composition. The results are shown in Figures 4 and 5, and are published in Reference 3, which is attached in this report as Appendix B.

The model of the liquid state in which the molecular species are included is called the associated model. In such a model, the number of species is four (i.e., Hg, Te, HgTe and vacancy). The cluster variation method (CVM)[4] formulation of the pair method for such a system has a decisive advantage over the quasi-chemical approximation treatment of the same problem, although the two approaches give exactly the same results, because of the intuitive ease of the CVM formulation.

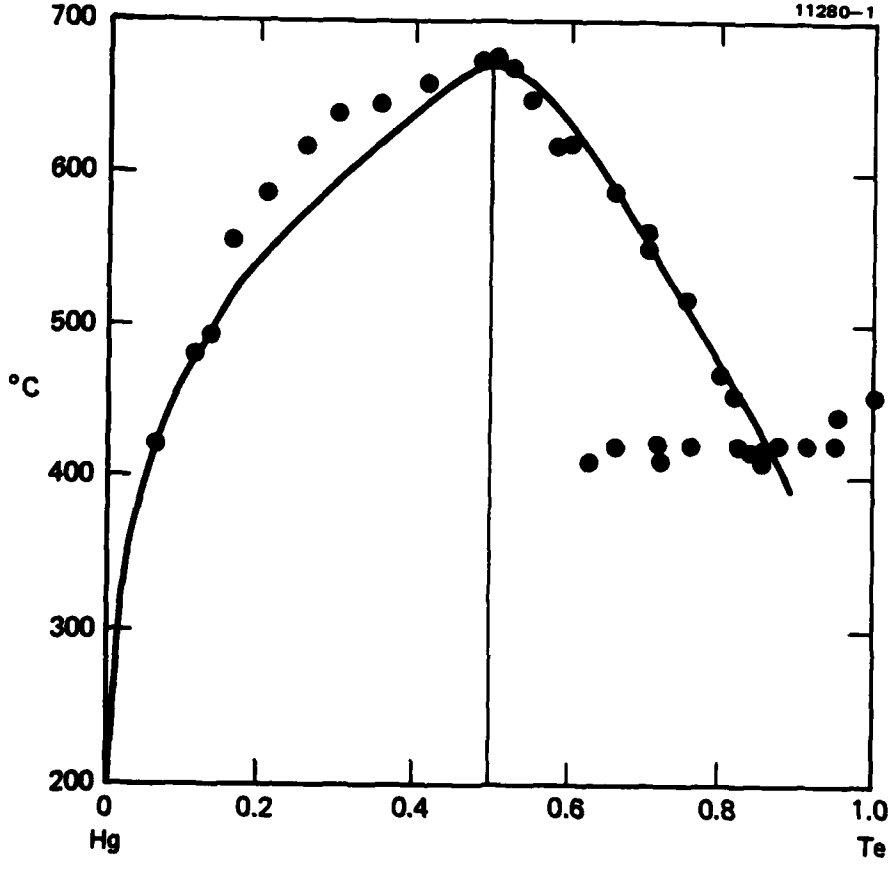

Figure 4. Hg-Te binary liquidus.
Dots are experiments.

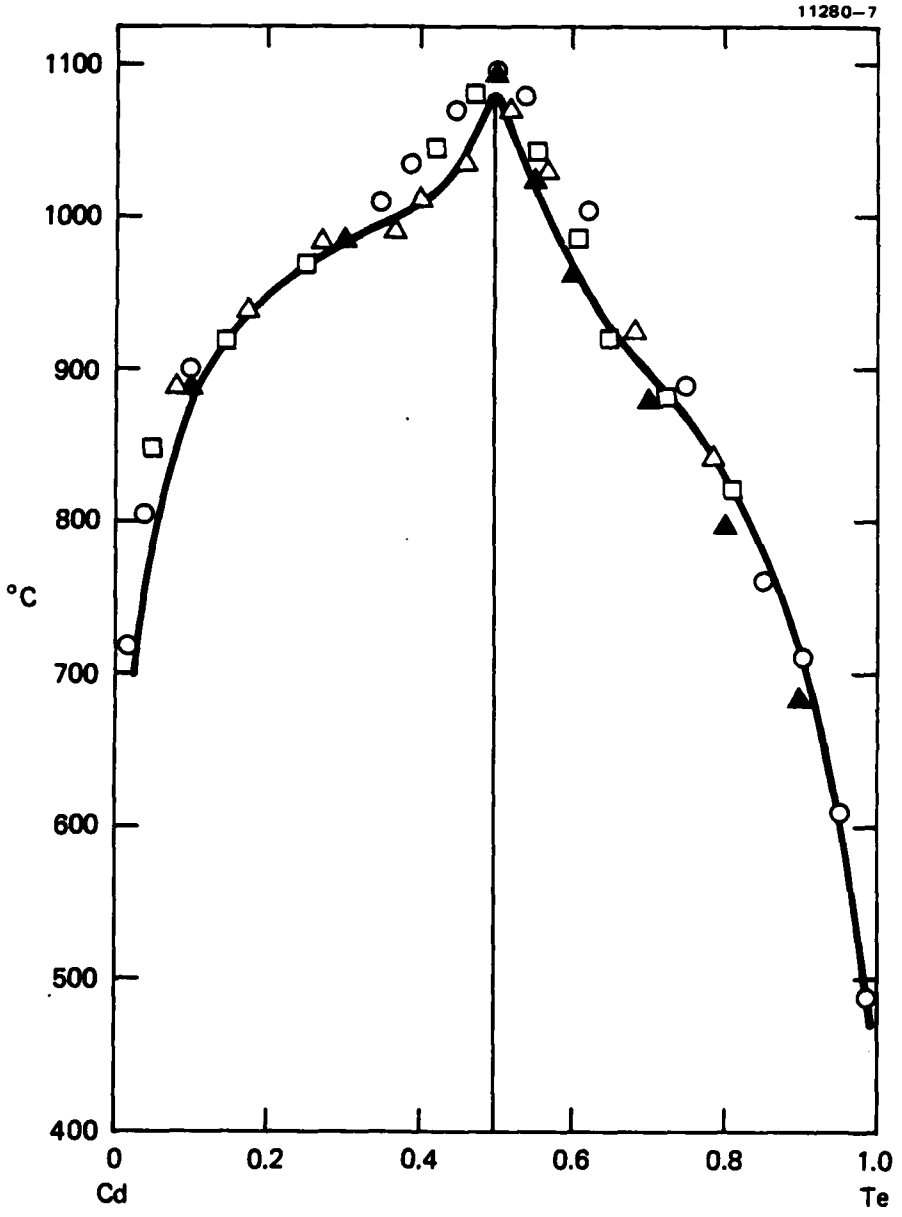

Figure 5. Cd-Te binary liquidus. Points are experiments; curve is the theory.

SECTION 4

Hg-Cd-Te LIQUIDUS-SOLIDUS PHASE DIAGRAM

In the binary cases of Section 3, the main input to the theory are the values of interaction potentials between nearest-neighbor pairs in the pseudo-lattice structure of the liquid phase. These same interaction potential values of binary cases are used for the ternary liquid phases as well.

In the Hg-Cd-Te liquid phase, we work with three atomic species, two molecular species and vacancies on the pseudo-lattice structure. The details are in Reference 5 which is reproduced as Appendix C. The main results are presented in Figures 6, 7 and 8, which indicate good agreement between theory and experiments. Figure 6 shows the Hg corner (of the triangular Gibbs diagram), and Figure 7 and 8 depict the Te corner. As opposed to the regular solution approach which uses the "point" variables only rather than the "pair" variables, the present method treats the energy parameters as being independent of temperature and composition, and common to both the Hg and Te corners.

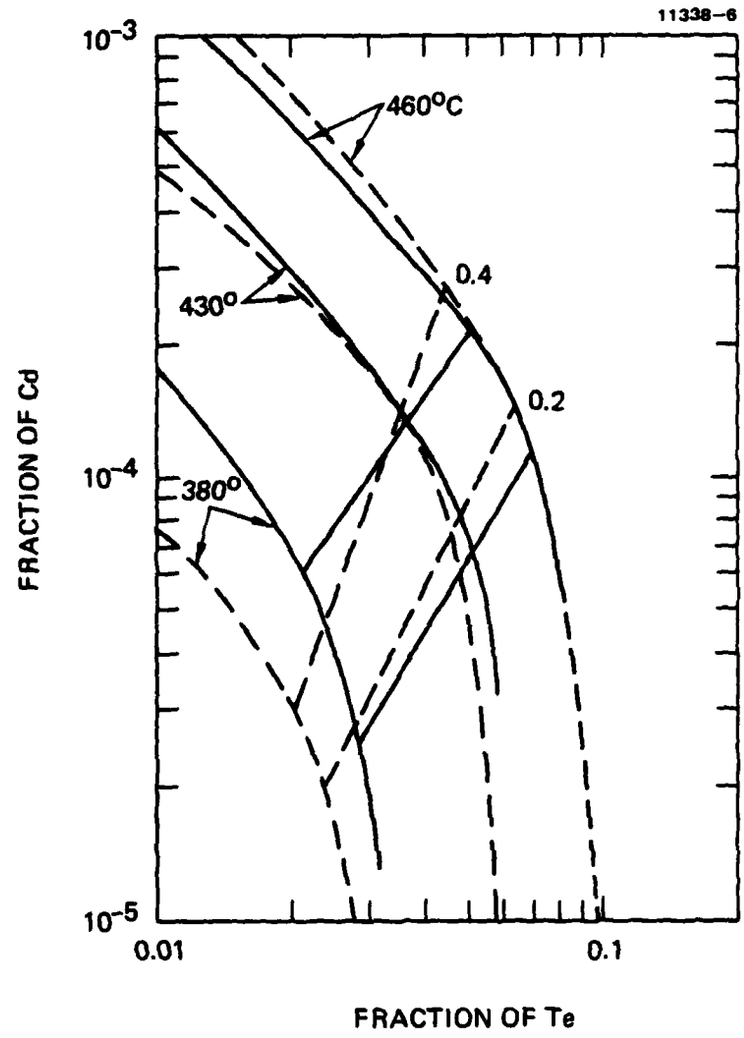

Figure 6. The Hg corner of the ternary Hg-Cd-Te liquidus. The solid curves are the theory, and the broken curves are experiments. The numbers along the curve are the value of x for the solid structure $(HgTe)_{1-x}(CdTe)_x$.

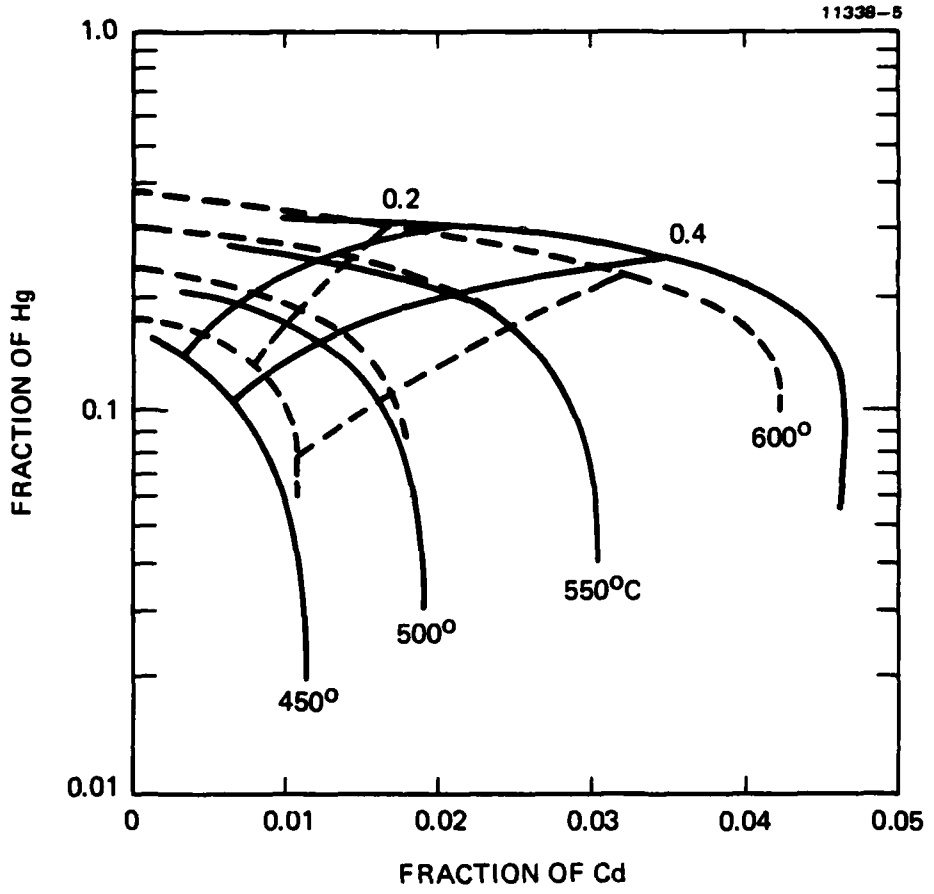

Figure 7. The ternary Hg-Cd-Te liquidus near the Te corner. The solid curves are the theory, and the broken curves are the experiments. The numbers 0.2 and 0.4 have the same meaning as Figure 6.

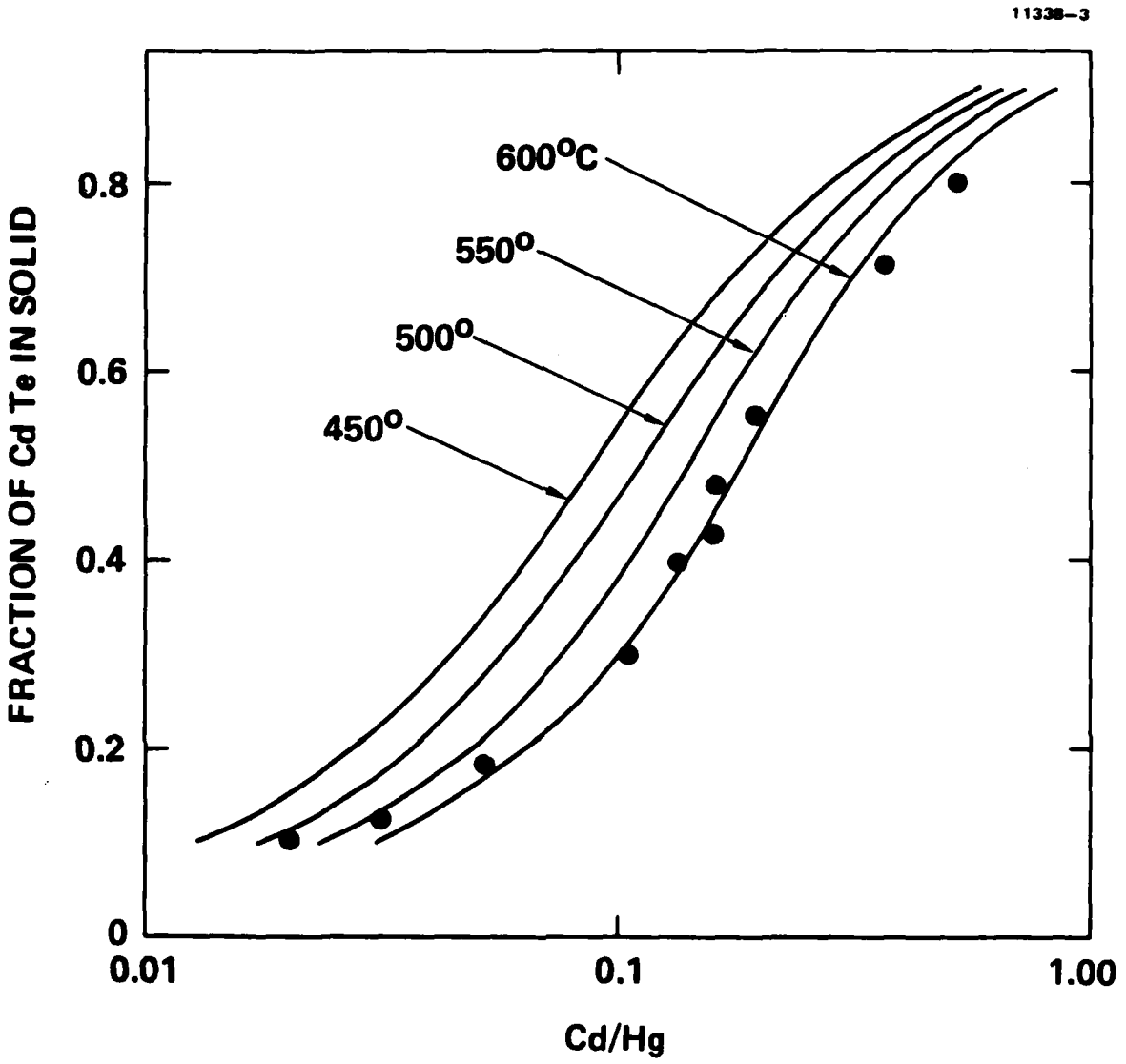

Figure 8. The Hg-Cd-Te liquidus and solidus in the Te-rich side. Curves are theory and dots are experiments for 450-550°C.

SECTION 5

Hg-Cd-Te SOLID PHASE WITH LATTICE DEFECTS

In the treatments of Sections 3 and 4, the solid phase is regarded as perfectly stoichiometric. In actuality, the measured hole concentration is associated with Hg vacancies. It is also known that antiatoms exist, which means that Te atoms may sit on the Hg-Cd sublattice, and Hg or Cd atoms may sit on the Te sublattice.

The structure of such a solid phase with lattice defects has been calculated and is attached as Appendix D. The Gibbs free energy for the solid phase in Appendix A and B is represented by a single point because it is for the perfect stoichiometric state. It is different when lattice defects are included. Figure 9 shows an example of how the Gibbs free energy changes as a function of the vacancy concentration in the Hg-Cd sublattice.

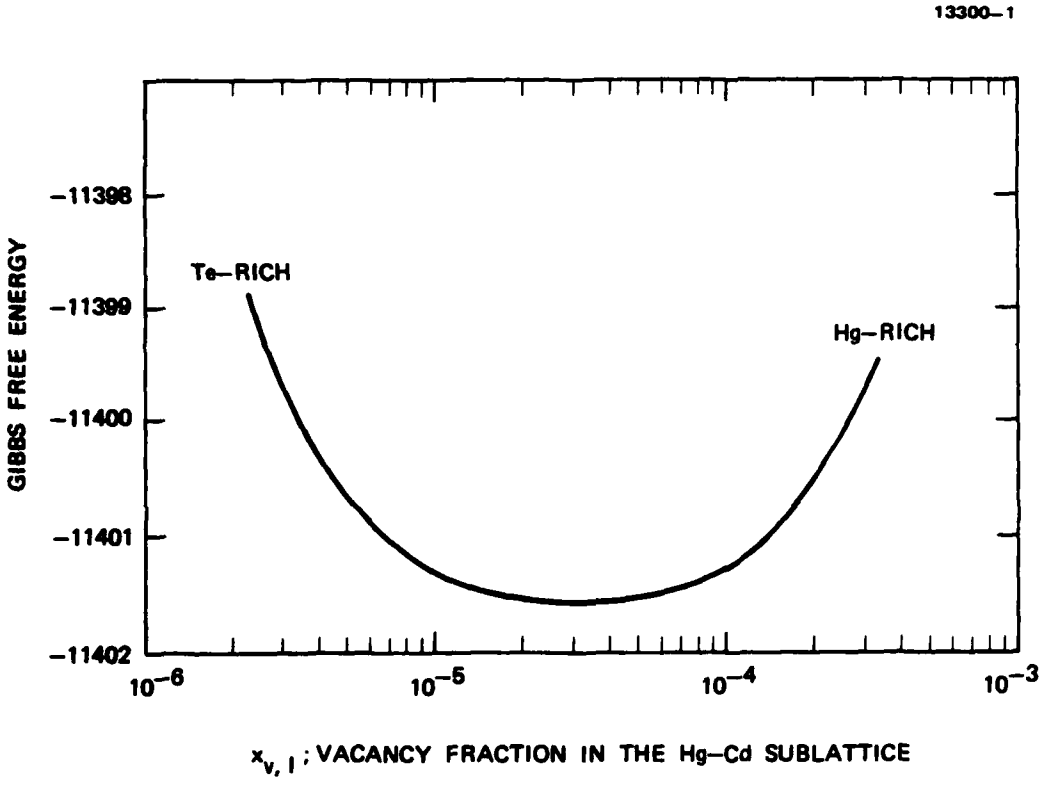

Figure 9. Gibbs free energy of the Hg-Cd-Te solid phase plotted against lattice defects.

SECTION 6

Hg-Cd-Te LIQUIDUS AND SOLIDUS INCLUDING LATTICE DEFECTS IN SOLID

Combining the solid phase theory in Section 5 (and Appendix D) and the liquid phase theory used previously in References 3 and 5, we have formulated the coexistence of the liquid and solid phases. Coexistence is derived by using the conditions in which the chemical potentials of each species in the liquid and solid phases are equal and when the two phases are under the same pressure.

The details of the formulation are described in Appendix E. The main results are shown in Figures 10, 11 and 12. In calculating these figures, the interatomic potentials are adjusted so that we can come to reasonable agreement with experimental data by Vydyanath[6]. These curves are calculated for the $Hg_{0.8}Cd_{0.2}Te$ solid composition.

Figure 10 plots twice the number of vacancies in the Hg-Cd sublattice per cm^3 against 1/T for the liquid-solid coexistence condition. The solid curves are the present theory and the broken curves are the experimental hole concentration due to Vydyanath[6]. The upper curves are when the solid coexists with the Te-rich liquid, and the lower curves are for the Hg-rich liquid. The fair agreement between the theory and the experiments supports the view that a Hg vacancy contributes two holes in the valence bond[6].

In adjusting energy parameters to change the general shape of the curves, we note two properties. Notations are from Appendix E.

[I] As we make ε_{11}, ε_{22} and ε_{12} more negative, keeping $\varepsilon_{12} \equiv \varepsilon_{12} - (\varepsilon_{11}+\varepsilon_{22})/2$ fixed, the 2 v_{Hg} curves in Figure 10 come down parallel to themselves.

[II] As we decrease u_{11} and u_{22} together, the v_{Hg} curve for the Te-rich case does not change, while the v_{Hg} for the Hg-rich case increases.

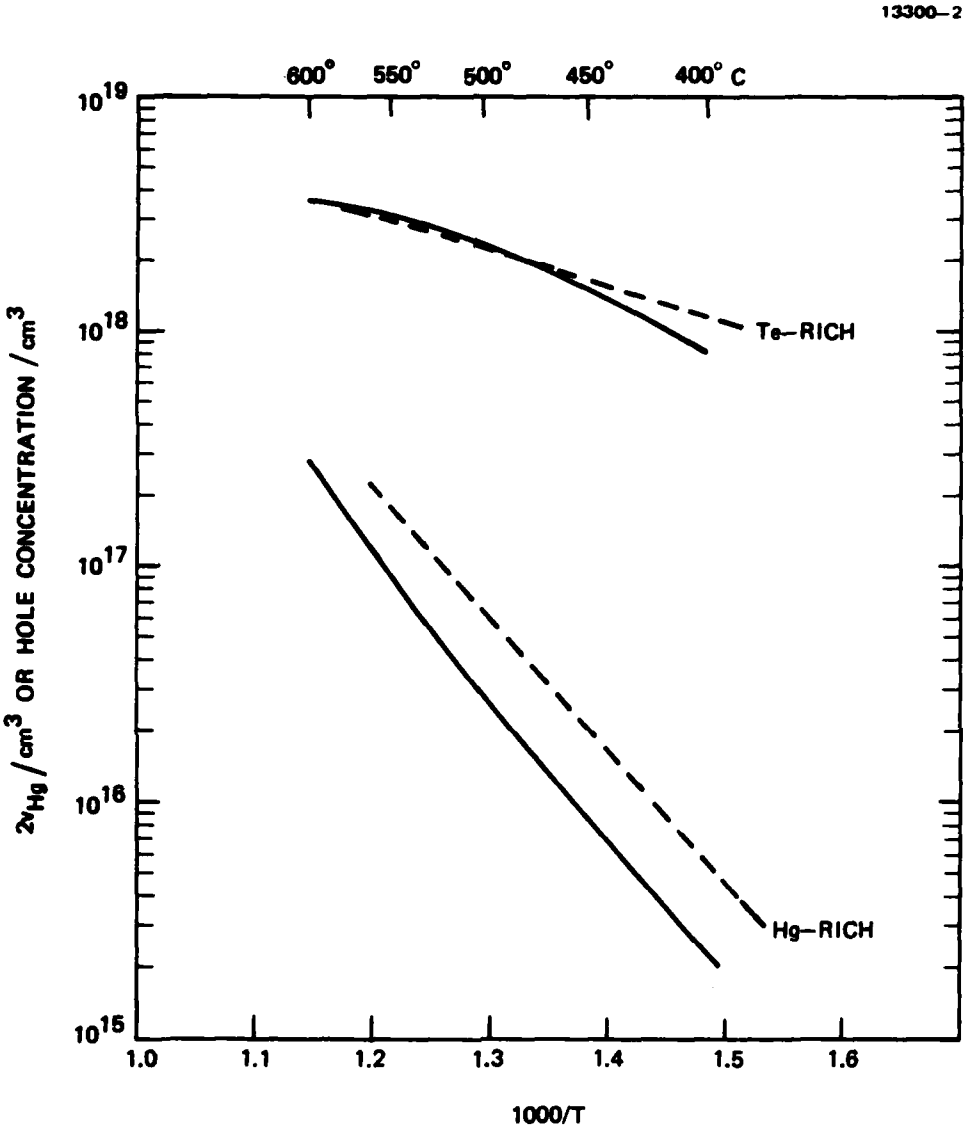

Figure 10. Hg vacancies (times 2) plotted against 1/T. Solid curves are the present theory, and the broken curves are Vydyanath's experiments.[6]

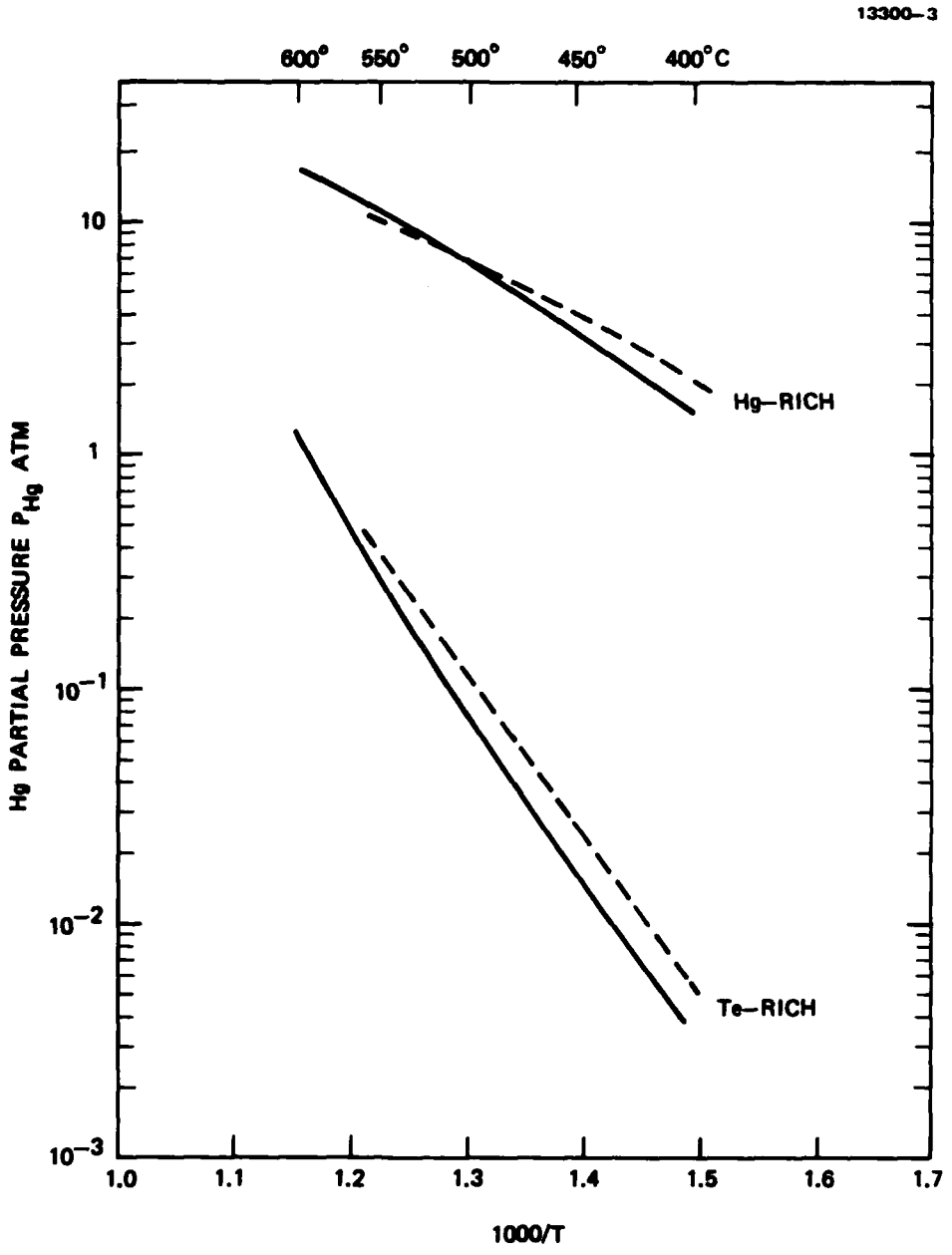

Figure 11. Hg partial pressure plotted against 1/T. Solid curves are the present theory, and the broken curves are Vydyanath's experiments.[6]

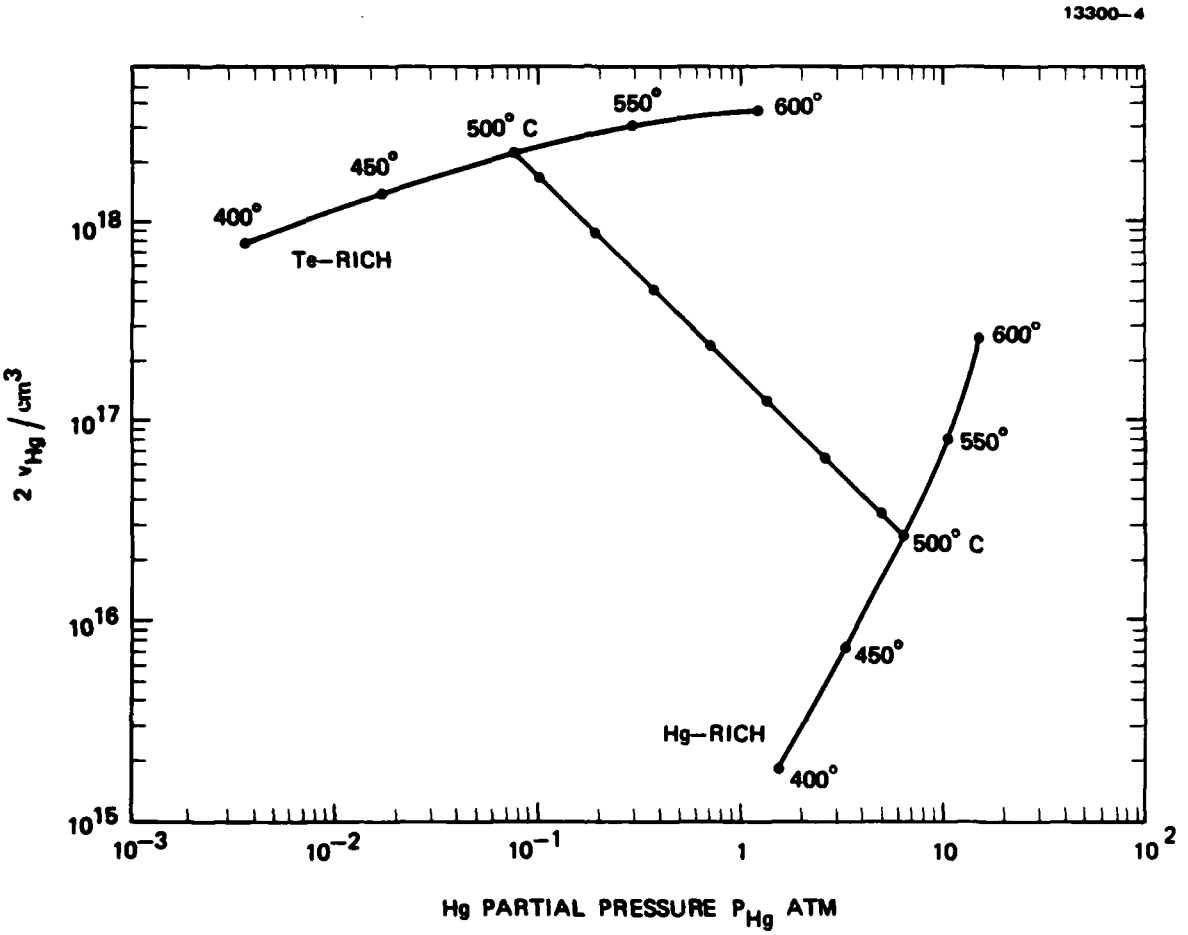

Figure 12. The theoretical relation between Hg vacancies and the partial pressure of Hg. The two outside curves are for liquid-solid coexistence conditions, and the line connecting them is for states of intermediate Hg pressure.

The partial pressure, P_{Hg}, of Hg in the vapor phase can be calculated from the chemical potential of Hg when we assume that Hg in the vapor phase behaves as an ideal gas. Figure 11 plots P_{Hg} against 1/T. The solid curves are the present theory and the broken curves are Vydyanath's experiments[6]. The theory uses the same energy parameters as those for Figure 10. The P_{Hg} value at 500°C for the Hg-rich growth is chosen at the experimental value, 6.5 atom.

In adjusting the theoretical curves, we noted the following property:

[III] The energy parameter, ϵ_{33}, controls the direction of the two P_{Hg} curves. When ϵ_{33} is more negative, the P_{Hg} curves point further upward.

The energy parameter values that we used are in Table 1. The energy, u_{ij}, is for intersublattice pairs. These pairs are predominantly Hg-Te and Cd-Te, and thus the u_{ij} values for these pairs are negative (attractive) while the rest are positive (repulsive). The ϵ_{ij} is for intrasublattice pairs; its sign is opposite to that of u_{ij}. The ϵ_{ij} values for the Hg-Te and Cd-Te pairs were chosen as zero, but they can be positive; since the number of these pairs are very small, the actual values are not important in the phase diagram calculations.

After a crystal is made from a Hg-rich melt or a Te-rich melt, the lattice defect properties can be changed by controlling the Hg partial pressure on the crystal. Figure 12 shows the relation between $2v_{Hg}$ and P_{Hg}. These intermediate points are calculated by changing the chemical potential value in the theory. The intermediate points lie almost on a line in Figure 12, in a manner similar to the experiments reported by Vydyanath[6].

Table 1. Solid State Energy Parameter Values Used in Computing Figures 10 and 11. The Values Are in Units of °K

Intersublattice pair energy, u_{ij}			
i \ j	1 (Hg)	2 (Cd)	3 (Te)
1 (Hg)	1600.	2000.	-1100.
2 (Cd)	2000.	1600.	-1100.
3 (Te)	-1100.	-1100.	1500.
Intrasublattice pair energy, ϵ_{ij}			
i \ j	1 (Hg)	2 (Cd)	3 (Te)
1 (Hg)	-1200.	-1700.	0.
2 (Cd)	-1700.	-1600.	0.
3 (Te)	0.	0.	-1200.

SECTION 7

INTERSTITIAL Hg IN THE Hg-Cd-Te CRYSTAL

In the treatment of Sections 5 and 6, we neglected the possibility of interstitial atoms. Since Hg is volatile, it is worthwhile to consider interstitial Hg atoms.

As is discussed in the Introduction (and Figure 1) of Appendix D, the Hg-Cd-Te crystal is made of two fcc sublattices. We call the white fcc sublattice in Figure 1 of Appendix D as I, and the black sublattice, II. When we shift the fcc I and fcc II by a half of the cube edge, they occupy interstitial positions. We can also call the new fcc sublattices III and IV. The small corner cube shown by dotted lines in Figure 1 of Appendix D now has the structure shown in (a) of Figure 13, and an adjacent small cube becomes (b). There are also small cubes of structures in Figure 13 (c) and (d).

Finally, we can consider whether a Hg atom can easily assume an interstitial position II or IV. In Figure 13, we see that a I site and a III site have the same nearest neighbor configuration, while a II and a IV site have nearest neighbors of their own. Since in the original structure, Hg atoms sit predominantly on I sites, we see that it is quite easy for a Hg atom to come to a III interstitial site. It is therefore reasonable to take into account in the theory the interstitial Hg atoms sitting on the III interstitial sublattice sites. The number of such interstitial Hg atoms will depend on the Hg-Hg and Hg-Cd interactions between I-III sites. Note that the I-III distance is larger than the I-II distance, but smaller than the intrasublattice I-I distance.

Such intersitial atoms have not been treated in the present report, but are to be included in future studies.

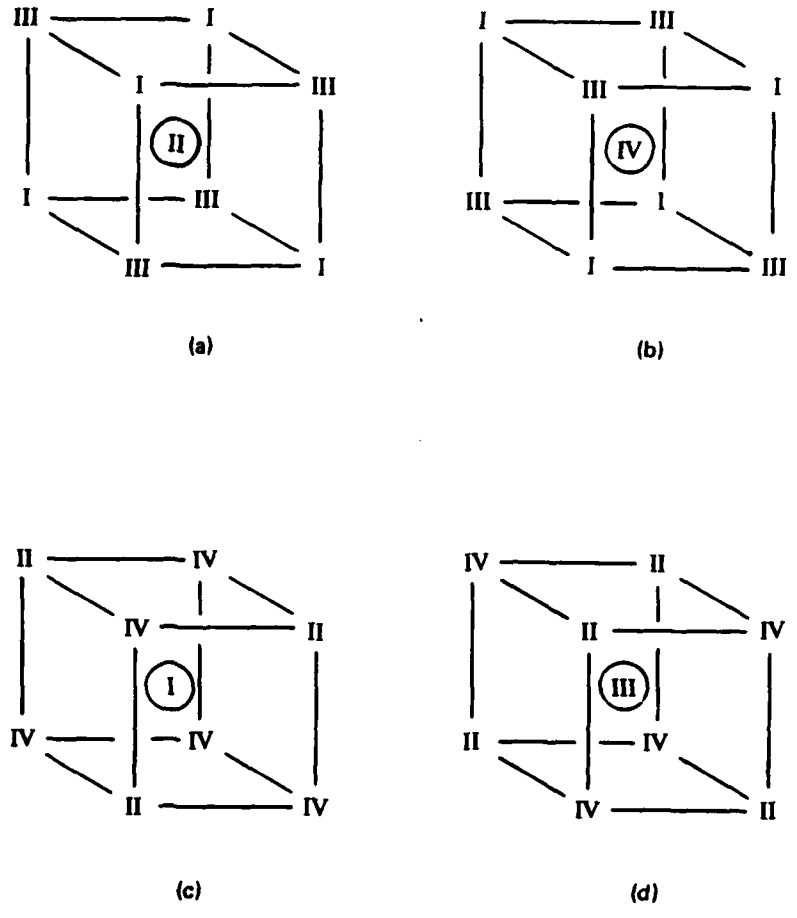

Figure 13. Two fcc sublattices I and II, and the two interstitial positions III and IV.

REFERENCES

1. G.B. Stringfellow and P.E. Greene, J. Phys. Chem. Solids 30, 1779 (19ba)).

2. R. Kikuchi, Physica 103B, 41 (1981).

3. R. Kikuchi, CALPHAD 6, 1 (1982).

4. R. Kikuchi, J. Chem. Phys. 60, 1071 (1974).

5. R. Kikuchi, J. Vac. Sci. Technol. 21, 129 (1982).

6. H.R. Vydyanath, J. Electroch. Soc. 128, 2609 (1981).

APPENDIX A

THEORY OF TERNARY III-V

SEMICONDUCTOR PHASE DIAGRAMS

Physica 103B (1981) 41–56

THEORY OF TERNARY III–V SEMICONDUCTOR PHASE DIAGRAMS

Ryoichi KIKUCHI
Hughes Research Laboratories, Malibu, California 90265, USA

Liquidus–solidus phase diagrams of III–V semiconductors are calculated using the Cluster Variation Method and related techniques developed recently. The liquid phase is treated assuming a lattice model. An equilibrium state is derived by minimizing the grand potential ($\hat{G}$), keeping the chemical potential fixed. The resulting nonlinear equations are solved using the Natural Iteration Method which has a property that the value of $\hat{G}$ always decreases at each iteration cycle.

The phase boundary is derived from an intersection of two $\hat{G}$ curves; the correct forms of $\hat{G}$ values to be used are derived from geometrical considerations. Ternary phase diagrams calculated for In–Ga–As and In–Sb–As agree well with previous calculations of Stringfellow and Greene and with experimental data.

For ternary cases, a tie line connecting coexisting liquid and solid phases are proved to be orthogonal to the phase boundary curve in the chemical potential diagram.

1. Introduction

Some years ago Stringfellow and Greene [1], to be cited as S–G, applied the pair approximation of the quasichemical method (QCM) [2] to calculate liquidus and solidus phase diagrams of III–V binary and ternary semiconductor systems. Their results for In–Ga–As and In–As–Sb agree very well with experiments.

After their work, the present author developed a new method of calculating phase diagrams [3, 4] as an application of the hierarchical cluster variation method (CVM). The new method in refs. 3 and 4 uses the grand potential minimization rather than matching of individual chemical potentials as has been done by S–G and others, and also uses the natural iteration method (NIM) in solving simultaneous nonlinear algebraic equations. The new approach is more compact than other existing methods and thus presents an easier means of generalizing it to more complicated systems.

The present paper reports how the new method is formulated, using the systems treated by S–G as examples. The numerical results are exactly the same as those of S–G, but some of the formulae are interpreted differently and also additional properties of the systems not reported by them are presented.

All existing theoretical treatments of phase diagrams (liquidus and solidus) of III–V and II–VI compounds make use of Vieland's work [5], which establishes the difference between reference levels of the liquid and the solid phases of the same material. We will also use the relation developed by Vieland.

In formulating the liquidus–solidus diagram the free energy of the solid is relatively easy to figure out. However, to treat the liquid phase accurately is a difficult task and one beyond the scope of the present work. Therefore, we follow S–G and use a lattice model for the liquid phase. Since the formulation is done using the pair approximation (which is equivalent to the QCM used in ref. 1) of the CVM, we do not need to specify the lattice structure for the liquid phase except the coordination number z.

2. Sketch of S–G's work of binary liquids

This section reviews those formulations of the S–G paper [1] that are relevant to our development in later sections in order to show the relations between their work and the present one. We do not use their notation, but follow the standard formulation of the pair approximation of the CVM.

In treating the liquid phase, S–G use the lat-

tice model of the coordination number $z = 2\omega$ (since we often use $z/2$, it is written as ω in this paper). Each lattice point is occupied by either an A atom (designated by a subscript $i = 1$) or a B atom ($i = 2$), and we do not allow vacancies in the lattice. The probability of finding an ith species on a lattice point is written as x_i ($i = 1$ or 2). The probability of finding an i–j nearest-neighbour pair is written as y_{ij} ($i, j = 1$ or 2). These variables satisfy the mutual relations

$$x_i = \sum_{j=1}^{2} y_{ij}, \qquad i = 1 \text{ and } 2, \tag{2.1}$$

and the symmetry relation

$$y_{12} = y_{21}. \tag{2.2}$$

The normalization relation is

$$x_1 + x_2 = 1. \tag{2.3}$$

The potential energy of the lattice liquid is written as

$$E = 2\omega N \sum_{i=1}^{2} \sum_{j=1}^{2} \epsilon_{ij} y_{ij}, \tag{2.4a}$$

where $2N$ is the total number of lattice points in the system, and ϵ_{ij} is the potential energy for a nearest-neighbor pair i–j. The energy expression (2.4a) can be rewritten using (2.1) and (2.2) as

$$E = 2\omega N(\epsilon_{11}x_1 + \epsilon_{22}x_2 - 4\epsilon y_{12}), \tag{2.4b}$$

where ϵ is defined as

$$4\epsilon = \epsilon_{11} + \epsilon_{22} - 2\epsilon_{12}. \tag{2.5}$$

The entropy according to the pair approximation of QCM is equivalent to that of CVM and is written as

$$S = 2kN\left[(2\omega - 1)\sum_i x_i \ln x_i - \omega \sum_i \sum_j y_{ij} \ln y_{ij}\right], \tag{2.6}$$

where k is the Boltzmann constant. Using E in (2.4b) and S in (2.6), we can write the free energy

$$F = E - TS \tag{2.7}$$

as a function of x and y values. In (2.7), T is the absolute temperature. Note that S in (2.6) is for $2N$ lattice points.

When the x values are fixed, there is only one independent variable for which we can choose y_{12}. The equilibrium state is derived by minimizing F in (2.7) with respect to y_{12} keeping T and the x values fixed. The differentiation leads to

$$y_{11}y_{22} = e^{-4\beta\epsilon} y_{12}^2, \tag{2.8}$$

where we define

$$\beta = 1/kT. \tag{2.9}$$

Eq. (2.8) corresponds to, for example, (3a) of S–G, and we can derive the identity between S–G's Ω_{AB} and our ϵ as

$$\Omega_{AB} = -4\omega\epsilon. \tag{2.10}$$

Eq. (2.8) can be solved with the aid of (2.1) as

$$y_{12} = y_{21} = 2x_1x_2/(1 + r), \tag{2.11}$$

where r is written as β in S–G and is defined as

$$r = [1 + 4x_1x_2(e^{-4\beta\epsilon} - 1)]^{1/2}. \tag{2.12}$$

In deriving the chemical potentials, it is helpful to use

$$\begin{aligned} N_i &= 2Nx_i, \qquad i = 1 \text{ and } 2, \\ N_{ij} &= 2Ny_{ij}, \qquad i, j = 1 \text{ and } 2. \end{aligned} \tag{2.13}$$

In terms of N values, we can write F in (2.7) explicitly as

$$F = \omega(\epsilon_{11}N_1 + \epsilon_{22}N_2 - 4\epsilon N_{12}) - kT\left[(2\omega - 1)\sum_i \mathcal{L}(N_i) - \omega \sum_i \sum_j \mathcal{L}(N_{ij}) - (\omega - 1)\mathcal{L}(2N)\right], \tag{2.14}$$

where the $\mathcal{L}$ function is defined as

$$\mathcal{L}(x) = x \ln x - x. \tag{2.15}$$

When F is a minimum with respect to $y_{12} = N_{12}/(2N)$ and (2.8) holds, the chemical potentials μ_i are defined from (2.14) by differentiation as

$$\begin{aligned} \mu_1 &= \left(\frac{\partial F}{\partial N_1}\right)_{N_2, N_{12}} = \omega\epsilon_{11} + kT\left[\ln x_1 + \omega \ln \frac{y_{11}}{x_1^2}\right], \\ \mu_2 &= \left(\frac{\partial F}{\partial N_2}\right)_{N_1, N_{12}} = \omega\epsilon_{22} + kT\left[\ln x_2 + \omega \ln \frac{y_{22}}{x_2^2}\right]. \end{aligned} \tag{2.16}$$

S–G calls the last ratio the activity coefficients:

$$\gamma_A \equiv \left[\frac{y_{11}}{x_1^2}\right]^{\omega} \quad \text{and} \quad \gamma_B \equiv \left[\frac{y_{22}}{x_2^2}\right]^{\omega}. \tag{2.17}$$

Using the y_{12} expression in (2.11), we can verify that (2.17) agrees with S–G's eq. (4).

Note that, in eqs. (2.8) and (2.12), the only energy parameter we need for the equilibrium properties of the system is ϵ, defined in (2.5). The individual ϵ_{11} and ϵ_{22} appear in (2.16), but they play the role of only defining the zero levels of the chemical potentials μ_i.

3. Grand potential formulation of the liquid phase

In S–G's formulation (review above) and in most current formulations of phase equilibria, one starts with the free energy and minimizes it keeping the composition fixed in order to obtain the equilibrium state. The grand potential formulation to be presented in this section leads to exactly the same results as those of the previous section, but has several advantages in mathematical convenience.

We start with the grand potential, which is defined as

$$\hat{G} \equiv F - \sum_i \hat{\mu}_i N_i, \tag{3.1}$$

where $\hat{\mu}_i$ are related to the chemical potential but for a moment can be regarded as Lagrange multipliers for adjusting the number of atoms N_i.

To facilitate our further discussions, we write $\hat{G}$ in (3.1) in full using (2.4a) and (2.6):

$$\begin{aligned}\Phi &\equiv \beta\hat{G}/(2N)\\ &= \beta\omega \sum_{ij} \epsilon_{ij} y_{ij} - \tfrac{1}{2}(\omega-1)\left[\sum_i \mathcal{L}(x_i) + \sum_j \mathcal{L}(x_j)\right]\\ &\quad + \omega \sum_{ij} \mathcal{L}(y_{ij}) - (\omega-1)\\ &\quad - \tfrac{1}{2}\beta\left[\sum_i x_i\hat{\mu}_i + \sum_j x_j\hat{\mu}_j\right] + \beta\lambda\left(1 - \sum_{ij} y_{ij}\right),\end{aligned} \tag{3.2}$$

where $\beta\lambda$ is a Lagrange multiplier used for the normalization of y_{ij}:

$$1 = \sum_{ij} y_{ij}. \tag{3.3}$$

The $\mathcal{L}$ function is defined in (2.15). In (3.2), the $\sum \mathcal{L}(x_i)$ sum and $\sum x_i\hat{\mu}_i$ sum are repeated and halved for the sake of later mathematical convenience.

To derive the equilibrium state, we minimize the grand potential $\hat{G}$ in (3.2) with respect to the pair variables y_{ij}, treating all four of them as being independent (in contrast to treating only y_{12} as independent in section 2) and keeping $\hat{\mu}_i$ as fixed (rather than keeping x_i as fixed, as in section 2). In so doing, we regard x_i and x_j in (3.2) as different linear combination of y_{ij}:

$$x_i = \sum_j y_{ij} \quad \text{and} \quad x_j = \sum_i y_{ij}. \tag{3.4}$$

When we minimize Φ in (3.2), keeping β and $\hat{\mu}_i$ fixed, we arrive at

$$\begin{aligned}\frac{\partial\Phi}{\partial y_{ij}} &= \beta\omega\epsilon_{ij} - \tfrac{1}{2}(2\omega-1)\ln(x_i x_j) + \omega \ln y_{ij}\\ &\quad - \tfrac{1}{2}\beta(\hat{\mu}_i + \hat{\mu}_j) - \lambda\beta = 0\end{aligned} \tag{3.5}$$

or

$$\begin{aligned}y_{ij} &= e^{\lambda\beta/\omega}(x_i x_j)^{(2\omega-1)/(2\omega)}\\ &\quad \times \exp\left[-\beta\epsilon_{ij} + \frac{\beta}{2\omega}(\hat{\mu}_i + \hat{\mu}_j)\right].\end{aligned} \tag{3.6}$$

We now see that the normalization (3.3), the reduction relations (3.4), and the "superposition" relations (3.6) form a set of equations to be solved for y_{ij}'s. The NIM solves them systematically as follows.

Note that, for the NIM, we fix the β and $\hat{\mu}_i$'s. We start with the first input values x_1 and x_2. Different from the Newton–Raphson method (NRM), any guess values for the first input lead to a converged solution. The initial guess value is used on the right-hand side of (3.6) without the normalization factor $\exp(\lambda\beta/\omega)$, to derive the first output $y_{ij}\exp(-\lambda\beta/\omega)$. These quantities are used in (3.3) to obtain the normalization factor $\exp(\lambda\beta/\omega)$, and hence the output y_{ij} in (3.6). This set of the first output y_{ij} is used on the right-hand side of (3.4) to derive the second input set x_1 and x_2. The iteration cycle is repeated until the consecutive outputs are sufficiently close to each other.

It was proved previously [6] that the grand potential Φ in (3.2) always decreases step by step

at each iteration cycle. The proof is reviewed in the appendix. This proof guarantees that the iteration always converges to a minimum of Φ. When Φ is a minimum and the set of equations (3.3), (3.4) and (3.5) is satisfied, we can simplify the expression of Φ by forming

$$\frac{\beta\hat{G}}{2N} = \Phi - \sum_{ij} y_{ij} \frac{\partial \Phi}{\partial y_{ij}} = \beta\lambda \tag{3.7a}$$

or

$$\lambda = \frac{\hat{G}}{2N}. \tag{3.7b}$$

Thus, the Lagrange multiplier introduced in (3.2) for the normalization of y_{ij}'s has the meaning of the grand potential per lattice point in the equilibrium state.

One particular case of present interest to us is when $i = j$ in (3.5), which leads to

$$\hat{\mu}_i + \lambda = \omega\epsilon_{ii} + kT\left[\ln x_i + \omega \ln \frac{y_{ii}}{x_i^2}\right]. \tag{3.8}$$

Compared with (2.16) we see that $\hat{\mu}_i$ of the present section is related to the chemical potential μ_i derived in section 2 as

$$\mu_i = \hat{\mu}_i + \lambda. \tag{3.9}$$

Because λ is only an additional constant, we can safely also call $\hat{\mu}_i$, used in (3.1) and (3.2), a chemical potential.

Use of the meaning of λ in (3.7b) and the relation for $\hat{\mu}_i$ in (3.9) leads to a useful relation from the $\hat{G}$ expression (3.1):

$$F = \sum_i \mu_i N_i. \tag{3.10}$$

Note that in this treatment of the liquid phase there is no difference between the Helmholtz free energy and the Gibbs free energy because the volume is kept fixed in the model.

In the previous section it was shown that when the composition x_1 (and x_2) and the temperature T are given, the equilibrium values of y_{11}, y_{12}, and y_{22} can be determined by the parameter ϵ only, as we see in (2.11) and (2.12). Therefore, we expect that the y_{ij}'s in (3.6) should also depend only on ϵ and not ϵ_{11} and ϵ_{22} explicitly, although the latter appear in (3.6). We can derive the formulae for y_{ij}'s which depend only on ϵ as follows.

We write

$$y_{ii} = x_i - \tfrac{1}{2}\sum_{j\neq i} (y_{ij} + y_{ji}) \tag{3.11}$$

and use this in the energy expression in (2.4a):

$$\begin{aligned} E &= 2\omega N \left\{\sum_{i=1}^{2} \epsilon_{ii}\left[x_i - \tfrac{1}{2}\sum_{j\neq i}(y_{ij} + y_{ji})\right] + \sum_{i=1}^{2}\sum_{j\neq i} \epsilon_{ij} y_{ij}\right\} \\ &= 2\omega N \left\{\sum_{i=1}^{2} \epsilon_{ii} x_i + \sum_{i=1}^{2}\sum_{j\neq i} [\epsilon_{ij} - \tfrac{1}{2}(\epsilon_{ii} + \epsilon_{jj})] y_{ij}\right\}. \end{aligned} \tag{3.12}$$

We define

$$\tilde{\epsilon}_{ij} = \epsilon_{ij} - \tfrac{1}{2}(\epsilon_{ii} + \epsilon_{jj}), \tag{3.13a}$$

which can be written explicity as

$$\begin{aligned} &\tilde{\epsilon}_{11} = \tilde{\epsilon}_{22} = 0, \\ &\tilde{\epsilon}_{12} = \tilde{\epsilon}_{21} = -2\epsilon, \end{aligned} \tag{3.13b}$$

where ϵ is defined in (2.5). When (3.13a) is used in (3.12), we can write

$$E = 2\omega N \left[\sum_{i=1}^{2} \epsilon_{ii} x_i + \sum_{i=1}^{2}\sum_{j=1}^{2} \tilde{\epsilon}_{ij} y_{ij}\right]. \tag{3.14}$$

When this expression of energy is used in (3.2), two changes need to be made: ϵ_{ij} should be replaced by $\tilde{\epsilon}_{ij}$, defined in (3.13), and $\hat{\mu}_i$ should be replaced by

$$\tilde{\mu}_i = \hat{\mu}_i - \omega\epsilon_{ii}, \qquad i = 1 \text{ and } 2. \tag{3.15}$$

These two changes appear in the minimization relations in (3.5) and (3.6).

In the NIM, to solve the y_{ij}'s from (3.6), which is now modified, together with the subsidiary conditions (3.3) and (3.4), we fix the value of $\tilde{\mu}_i$, which now replaces $\hat{\mu}_i$ in (3.6), and do the iteration. The $\tilde{\mu}_i$'s are the parameters that control the concentration x_i, and the fact that $\tilde{\mu}_i$ is made up of two terms $\hat{\mu}_i$ and $\omega\epsilon_{ii}$ in (3.15) is immaterial as far as the equilibrium solution is concerned. It is to be noted that, since $\tilde{\epsilon}_{ij}$ in (3.13) depends on ϵ only and not on ϵ_{11} and ϵ_{22} separately, the equilibrium solution for the y_{ij}'s depends on ϵ only in agreement with what we noted at the end of section 2. The relations between the $\tilde{\mu}_i$ and x_i's and λ are also independent of ϵ_{11} and ϵ_{22}. By

using the modified equation (3.5), modified so that ϵ_{ij}, μ_i, and μ_j are replaced by $\tilde{\epsilon}_{ij}$, $\tilde{\mu}_i$, and $\tilde{\mu}_j$, and by comparing with the relations for the μ_i's in (2.16), we can derive

$$\mu_i = \tilde{\mu}_i + \lambda + \omega\epsilon_{ii}, \qquad i = 1 \text{ and } 2, \tag{3.16}$$

which agrees with (3.9) when (3.15) is used. The relations in (3.16) agree with the fact that ϵ_{11} and ϵ_{22} appear explicitly when we write the μ_i values in (2.16).

The actual numerical computation of the equilibrium state is made with $\tilde{\epsilon}_{ij}$ defined in (3.13) replacing ϵ_{ij}, and with $\tilde{\mu}_i$ replacing $\hat{\mu}_i$ in (3.6). Since we assume that there are no vacancies in the system, we have

$$x_1 + x_2 = 1. \tag{3.16}$$

This imposes a mutual relation between $\tilde{\mu}_1$ and $\tilde{\mu}_2$, and thus there is one degree of freedom in choosing them. In calculating binary systems we usually treat the two components symmetrically and use the condition

$$\tilde{\mu}_1 + \tilde{\mu}_2 = 0. \tag{3.17}$$

Sometimes, however, we use the condition

$$\tilde{\mu}_2 = 0, \tag{3.18}$$

as we see in section 9.

When we combine (2.10) with (3.13b) we see that our $\tilde{\epsilon}_{12}$ is related to Ω_{AB} of S–G [1] as

$$\tilde{\epsilon}_{12} = \tilde{\epsilon}_{21} = \Omega_{AB}/z, \tag{3.19}$$

where z is the coordination number used for the liquid phase.

4. Derivation of the binary liquidus

The liquidus of a III–V system like Ga–As, In–As, Ga–Sb, and In–Sb schematically looks like fig. 1a. The point P is in the liquid phase, and Q is on the solid phase of the composition AB. The width of the solid phase can be neglected in this study and thus we assume that the solid phase has the fixed composition $x_1 = x_2 = \frac{1}{2}$.

Since the two points P and Q coexist, the tangent of the F curve at P in fig. 1b passes through Q, which is the value of the free energy in the solid phase. This condition is now expressed in mathematical form. First, the equation of a tangent of the F curve at P can be written as

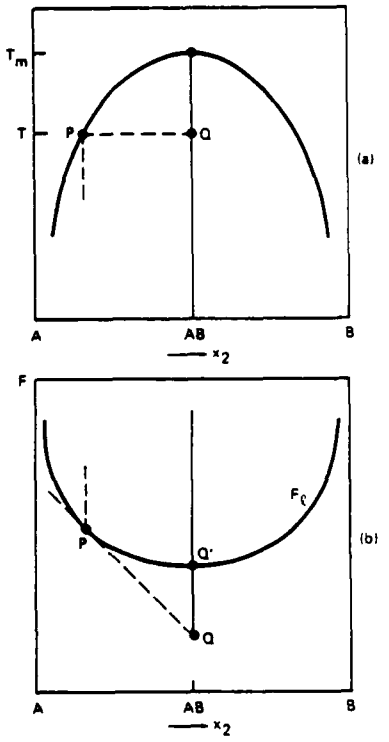

Fig. 1. Schematics of the liquidus curve (a) and the free energy F (b) for a binary semiconductor. Points P and Q coexist.

$$F - F^{(P)} = \left(\frac{dF}{dx_2}\right)^{(P)}(x_2 - x_2^{(P)}). \tag{4.1}$$

Using the normalization of x_i in (2.3) and the definition of μ_i in (2.16), we can write

$$\left(\frac{dF}{dx_2}\right)^{(P)} = \left[\left(\frac{\partial F}{\partial x_2}\right)_{x_1} - \left(\frac{\partial F}{\partial x_1}\right)_{x_2}\right]^{(P)}$$
$$= [\mu_2^{(P)} - \mu_1^{(P)}]2N. \tag{4.2}$$

When (4.2) and (3.10) are substituted into (4.1), we obtain

$$F = [\mu_1^{(P)}x_1 + \mu_2^{(P)}x_2]2N. \tag{4.3}$$

This is the equation for the tangent to the F curve in fig. 1b going through the point P. Eq. (4.3) looks similar to the general expression of F

in (3.10), but is different in the sense that x_1 and x_2 are variables independent of the point P.

The next important step is to estimate the value of the free energy of the solid phase at the point Q. For this purpose we follow S–G [1] and use the relation originally derived by Vieland [5]. Vieland's relation says that the free energy of one mole of molecular AB in the solid phase is written as

$$F_{\text{solid}}^{(Q)} = F^{(Q')} - (T_m - T)\Delta S_m, \tag{4.4}$$

where $F^{(Q')}$ is the free energy of the supercooled liquid system at Q' in fig. 1b. This state is "supercooled" because it is not stable compared with the solid phase. In (4.4) T_m is the melting temperature of the solid AB, as indicated in fig. 1a, and ΔS_m is the entropy of melting of one mole of the solid. Eq. (4.4) is important in fixing the relative zero points of the solid and liquid phases.

We can use (3.10) in writing $F^{(Q')}$,

$$F^{(Q')} = (\mu_1^{(Q')} + \mu_2^{(Q')})N, \tag{4.5}$$

where $2N$ is the total number of atoms in the liquid phase, and $N_1 = N_2 = N$.

In the (F, x_2) plane, a line passing through the solid point $(F^{(Q)}, x^{(Q)})$ is written as

$$F - F^{(Q)} = \alpha(x_2 - x_2^{(Q)}), \tag{4.6}$$

where α can be any value and, as shown in fig. 1b,

$$x_2^{(Q)} = \tfrac{1}{2}. \tag{4.7}$$

Eq. (4.6) is to be compared with the liquid counterpart (4.1).

The condition that the solid at Q in fig. 1b is in equilibrium with the liquid at P is that the tangent lines (4.1) and (4.6) become identical.

To put this in mathematical form, it is convenient to introduce the following two expressions:

$$\tilde{G}_l = F^{(P)} - \left(\frac{dF}{dx_2}\right)^{(P)} x_2^{(P)}, \tag{4.8}$$

$$\tilde{G}_s = F_s^{(Q)} - \alpha x_2^{(Q)}. \tag{4.9}$$

Since no confusion is expected with the analysis in section 3, we may call $\tilde{G}_l$ and $\tilde{G}_s$ grand potentials also. In (4.9), $x_2^{(Q)}$ actually is $\frac{1}{2}$, as we see in (4.7). Since α in (4.6) and hence in (4.9) can be any value, and since we require that the lines in (4.1) and (4.6) coincide, we require

$$\alpha = \left(\frac{dF}{dx_2}\right)^{(P)}. \tag{4.10}$$

When

$$\tilde{G}_l = \tilde{G}_s, \tag{4.11}$$

we can prove that the tangent to F_l at P goes through the solid point Q as follows. Using $\tilde{G}_l$ in (4.8), we can write eq. (4.1) for the tangent to the F curve at P as

$$F - \left(\frac{dF}{dx_2}\right)^{(P)} x_2 = \tilde{G}_l. \tag{4.12}$$

We can show using (4.10) that the point $(F^{(Q)}, x_2^{(Q)})$ lies on this line when (4.11) holds, because

$$F^{(Q)} - \alpha x_2^{(Q)} = \tilde{G}_s = \tilde{G}_l. \tag{4.13}$$

For numerical computation, (4.11) can be further simplified. We use relations (4.2), (4.3), (4.4), and (4.5) to obtain

$$\tilde{G}_l = 2N\mu_1^{(P)} \tag{4.14a}$$

$$\tilde{G}_s = N(\mu_1^{(Q')} + \mu_2^{(Q')}) - (T_m - T)\Delta S_m - N(\mu_2^{(P)} - \mu_1^{(P)}). \tag{4.14b}$$

Substituting thes two expressions into (4.11) yields

$$N(\mu_1^{(P)} + \mu_2^{(P)}) = N(\mu_1^{(Q')} + \mu_2^{(Q')}) + (T_m - T)\Delta S_m. \tag{4.15}$$

In reducing the equation in the next step, we have to be careful about the mole number. When one mole of GaAs melts, it produces one mole of Ga and one mole of As. Thus, the total number of atoms in the liquid phase is two moles. If ΔS_m in (4.15) is measured for one mole of GaAs, N in (4.15) is the Avogadro number N_{Avg}. Thus, by dividing both sides by N_{Avg} we obtain

$$\mu_1^{(P)} + \mu_2^{(P)} = \mu_1^{(Q')} + \mu_2^{(Q')} - (T_m - T)\frac{\Delta S_m}{N_{Avg}}. \tag{4.16}$$

We can further simplify this by using (3.16) and

Table I
Parameters used in the calculation of Ga–As, In–As and In–Sb binary liquidus.

	T_m (K)	ΔS_m (cal deg^{-1} mole^{-1})[a]	$\tilde{\epsilon}_{12}$ (cal/mole)
GaAs	1511	14.7	−4380/6
InAs	1215	14.7	−6070/6
InSb	803	13.3	−3980/6

[a] In table 1 of S–G [1] the unit of ΔS_m is written as eu. Usually eu means entropy unit and represents the number in units of the gas constant R. Their eu should read cal deg^{-1} mole^{-1}. T_m is the melting temperature of the compound, ΔS_m is the entropy of melting of the compound, and ϵ is the energy parameter of the pair in the liquid phase in eq. (2.5a).

adopting the condition (3.17) as

$$\lambda^{(P)} = \lambda^{(Q')} - (T_m - T)\frac{\Delta S_m}{2N_{Avg}}. \tag{4.17}$$

The numerical calculation of finding the liquidus at a temperature T is done in the following way. We use the values of ΔS_m and T_m given in table I, which shows the values used by S–G [1]. First, we solve the supercooled liquid state for the temperature and determine the value $\lambda^{(Q')}$ for the point Q' in fig. 1b; for that purpose, we use the NIM of section 3.

Next we vary $\tilde{\mu}_i^{(P)}$ in the liquid phase and find the value $\lambda^{(P)}$ which satisfies (4.17). Then the point P is on the liquidus. We have used this formulation and calculated the liquidus curves for GaAs, InAs, and InSb. The results agree exactly with those of fig. 3 in S–G [1] and thus fit nicely with experiments. To make the presentation complete, we plot the curves in fig. 2.

The $\tilde{\epsilon}_{12}$ values in table I are negative. This shows from the definition of $\tilde{\epsilon}_{12}$ in (3.13) that the different species of the pair in the table have the tendency to attract in the liquid phase.

5. Ternary liquid phase

In section 3 we worked out the binary liquid phase using the grand potential and NIM formulation. The advantage of the formulation is that it is applicable to the ternary liquid system almost without change except for the subscript i or j taking values 1, 2, and 3, corresponding to the A, B, and C components.

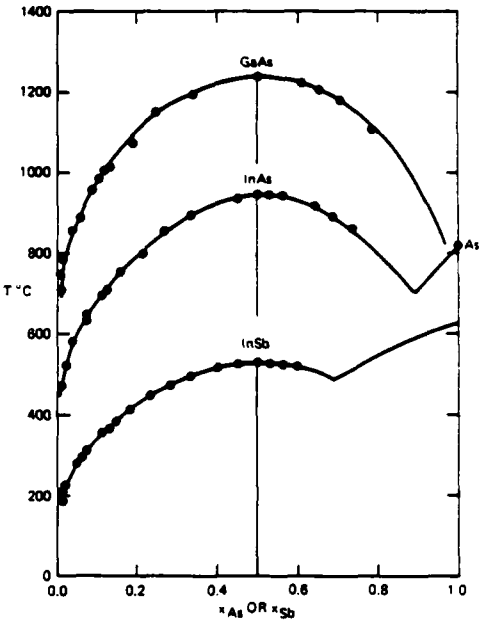

Fig. 2. Liquidus curves of III–V semiconductors. Solid curves are theory, calculated independently by Stringfellow and Greene [1] and Kikuchi in this paper. Circles are experiments.

To make sure of the relations, and also to rewrite equations using $\tilde{\epsilon}_{ij}$ and $\tilde{\mu}_i$, we now reexamine the equations in section 3 one by one. Eq. (3.1) for the grand potential $\hat{G}$ holds without change when Σ_i is for $i = 1$, 2, and 3 and as before $\tilde{\mu}_i$ is a parameter related to the chemical potential. We then use the pair approximation expression of the CVM and write $\hat{G}$ as in (3.2). At this point, however, we use $\tilde{\epsilon}_{ij}$ introduced in (3.13a) and $\tilde{\mu}_i$ in (3.15) and write $\hat{G}$ as

$$\begin{aligned}\Phi = \frac{\beta\hat{G}}{2N} &= \beta\omega \sum_{ij} \tilde{\epsilon}_{ij} y_{ij} - \tfrac{1}{2}(\omega - 1) \\ &\times \left[\sum_i \mathcal{L}(x_i) + \sum_j \mathcal{L}(x_j)\right] \\ &+ \omega \sum_{ij} \mathcal{L}(y_{ij}) - (\omega - 1) - \tfrac{1}{2}\beta \\ &\times \left[\sum_i x_i\tilde{\mu}_i + \sum_j x_j\tilde{\mu}_j\right] \\ &+ \beta\lambda\left[1 - \sum_{ij} y_{ij}\right].\end{aligned} \tag{5.1}$$

Different from (3.13b), we need three energy parameters $\tilde{\epsilon}_{12}$, $\tilde{\epsilon}_{23}$ and $\tilde{\epsilon}_{31}$.

The normalization of y_{ij} is written as in (3.3), and the geometrical relations in (3.4) hold. When the grand potential is minimized with respect to y_{ij}, using (3.4), we arrive at

$$\frac{\partial \Phi}{\partial y_{ij}} = \beta\omega\tilde{\epsilon}_{ij} - \tfrac{1}{2}(2\omega - 1)\ln(x_i x_j) + \omega \ln y_{ij} - \tfrac{1}{2}\beta(\tilde{\mu}_i + \tilde{\mu}_j) - \lambda\beta = 0 \tag{5.2a}$$

or

$$y_{ij} = e^{\lambda\beta/\omega}(x_i x_j)^{(2\omega-1)/(2\omega)} \exp\left[-\beta\tilde{\epsilon}_{ij} + \frac{\beta}{2\omega}(\tilde{\mu}_i + \tilde{\mu}_j)\right]. \tag{5.2b}$$

The set of equations for nine y_{ij} values is solved with ease using the NIM. The NIM is particularly useful when the number of variables is large.

The chemical potential μ_i can be written in the same way as in (2.16). Comparing (5.2) with (2.16) we see

$$\tilde{\mu}_i + \lambda = \mu_i - \omega\epsilon_{ii}, \qquad i = 1, 2 \text{ and } 3, \tag{5.3}$$

which are similar to the binary case (3.16).

When the grand potential $\hat{G}$ in (5.1) is a minimum and (5.2) holds, the same transformation as (3.7a) leads to the identity

$$\lambda = \hat{G}/(2N). \tag{5.4}$$

Using this and using the relation between $\hat{G}$ and F in (3.1), we can derive

$$F = \hat{G} + \sum(\tilde{\mu}_i + \omega\epsilon_{ii})N_i = \sum_{i=1}^{3} \mu_i N_i, \tag{5.5}$$

where we used (5.3), (5.4), and the relation between $\tilde{\mu}_i$ and $\tilde{\mu}_i$ in (3.15).

Similar to the last comment in section 3, we can impose one condition among three $\tilde{\mu}_i$ values because of the normalization relation

$$\sum_{i=1}^{3} x_i = 1. \tag{5.6}$$

It is convenient to impose the condition

$$\sum_{i=1}^{3} \tilde{\mu}_i = 0, \tag{5.7}$$

or

$$\tilde{\mu}_3 = 0. \tag{5.8}$$

6. Ternary solid phase

As an example, consider a ternary solid of composition $(GaAs)_{1-x}(InAs)_x$. This possesses a structure modified from a zinc-blende structure, shown in fig. 3. It is made up of two f.c.c. sublattice: As occupies the white f.c.c. sublattice in fig. 3, and Ga and In share the black f.c.c. sublattice. Let us write the three species Ga, In, and As by subscripts $i = 1$, 2, and 3 in this order.

First, we examine the energy of this system. Since each Ga and each In are individually surrounded by four As atoms, the nearest neighbor interactions contribute the energy

$$E = N(4\epsilon_{13}x_1 + 4\epsilon_{23}x_2), \tag{6.1}$$

where N is the number of black sublattice points in fig. 3, x_i is the fraction of Ga and In atoms on this sublattice, and ϵ_{i3} is the interaction potential between the ith and the 3rd (As) species.

Our first calculation, based on the energy expression (6.1), was not in good agreement with experiment. Therefore, as the next step, we have introduced the second-neighbor interactions: interactions among Ga–Ga, Ga–In, and In–In on the black sublattice of fig. 3. We write the fraction of i–j ($i, j = 1$ and 2) second-neighbor pairs as y_{ij} and the interaction potential for this pair as ϵ_{ij}. Then we can write the total potential energy as

$$E = 4N\sum_{i=1}^{2}\epsilon_{i3}x_i + 6N\sum_{i=1}^{2}\sum_{j=1}^{2}\epsilon_{ij}y_{ij}, \tag{6.2}$$

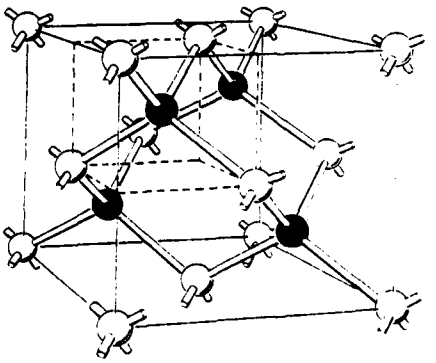

Fig. 3. Structure of III–V semiconductor solid phase. If all black balls were the same, the structure is the zinc-blende type.

where $6N$ is the number of second-neighbor bonds in the black sublattice of fig. 3. Using a procedure similar to (2.4), eq. (6.2) can be rewritten as

$$E = N[4\epsilon_{13} + 6\epsilon_{11})x_1 + (4\epsilon_{23} + 6\epsilon_{22})x_2 + 24\epsilon_s y_{12}], \tag{6.3}$$

where, analogous to (2.5), we define,

$$4\epsilon_s = 2\epsilon_{12} - \epsilon_{11} - \epsilon_{22}. \tag{6.4}$$

Since we assume in this paper that no vacancies occur in the lattice and thus that the white lattice points in fig. 3 are all occupied by As atoms, we can take the statistics of the black sublattice only. The entropy for this sublattice can be written exactly as in (2.6) with the coordination number $2\omega = 12$. When $F = E - TS$ is minimized with respect to y_{12}, keeping x_1 and x_2 fixed, we obtain an equation with the form of (2.8):

$$y_{11}y_{12} = y_{12}^2 \exp(4\beta\epsilon_s), \tag{6.5}$$

the only difference being that the $-\epsilon$ in (2.8) is replaced by ϵ_s in (6.5). The definition of ϵ_s in (6.4) has a sign different from (2.5). Eq. (6.5) can be solved as in (2.11) and (2.12) as

$$y_{12} = \frac{2x_1x_2}{1+r}, \tag{6.6a}$$

$$r \equiv \{1 + 4x_1x_2[\exp(4\beta\epsilon_s) - 1]\}^{1/2}. \tag{6.6b}$$

When the free energy is minimized with respect to y_{12} and (6.6) holds, the chemical potentials of the species $i = 1$ and 2 in the solid phase are written in exactly the same way as in (2.16). Comparing the energy expressions (2.4b) and (6.3), and remembering that the number of lattice points in the liquid phase in section 2 was written as $2N$ and that the number of points on the black sublattice in fig. 3 is N, we see that

$$\mu_{s,i} = 4\epsilon_{i3} + 6\epsilon_{ii} + kT(6\ln y_{ii} - 11\ln x_i), \quad \text{for } i = 1 \text{ and } 2, \tag{6.7}$$

where the subscript s stands for the solid phase. At this point note that the free energy of the black sublattice for the composition $x_1 = 1 - x_2$ is written in the same way as (3.10):

$$F_s = \sum_i \mu_{s,i}x_iN. \tag{6.8}$$

In the special case where $x_1 \to 1$, y_{11} also approaches unity so that (6.7) and (6.8) reduce to

$$F_{s,1}^{(0)}/N = \mu_{s,1}^{(0)} = 4\epsilon_{13} + 6\epsilon_{11}, \qquad \text{when } x_1 \to 1, \tag{6.9a}$$

and similarly

$$F_{s,2}^{(0)}/N = \mu_{s,2}^{(0)} = 4\epsilon_{23} + 6\epsilon_{22}, \quad \text{when } x_2 \to 1. \tag{6.9b}$$

When we examine the meaning of $F_{s,1}^{(0)}$, we see that it is the free energy of the GaAs solid phase at the temperature of interest to us. Recall that it was already calculated in (4.4) as $F_{\text{solid}}^{(0)}$. Therefore, when we have the data for the entropy of melting ΔS_m and the temperature of melting T_m for the solid-phase GaAs, we can calculate $F_{s,1}^{(0)}/N = \mu_{s,1}^{(0)}$. The corresponding data for InAs leads to the value $F_{s,2}^{(0)}/N = \mu_{s,2}^{(0)}$. Using (4.4) and (4.5), we can write them explicitly as

$$\mu_{s,i}^{(0)} = \mu_{l,i}^{(i3)} + \mu_{l3}^{(i3)} - (T_m^{(i3)} - T)\frac{\Delta S_m^{(i3)}}{N_{\text{Avg}}}, \tag{6.10}$$

where the subscript l indicates that the quantity is in the liquid phase, and $\mu_{l,i}^{(i3)}$ is the chemical potential of the ith species ($i = 1$ and 2) in the supercooled liquid state in which As composition is 50% and the other 50% is the ith species.

When we compare our (6.5) with eq. (3a) of S–G [1], we see that our $4\epsilon_s$ in (6.4) corresponds to S–G's $\Omega_{\text{AC-BC}}$ in the solid phase by

$$4\epsilon_s = 2\Omega_{\text{AC-BC}}/z, \tag{6.11}$$

where $z = 12$ is the coordination number of the f.c.c.

7. Geometry of the ternary coexistence condition

We now consider the condition that the solid phase of section 6 and the liquid phase of section 5 can coexist. As in section 5, we write Ga, In, and As by the subscript $i = 1$, 2, and 3. When the number of these atoms are written as N_i ($i = 1$, 2, and 3), the condition in the solid phase is

$$N_1 + N_2 = N_3 = N, \tag{7.1}$$

where N is the number of lattice sites in one f.c.c. sublattice. The total number of atoms in the solid phase is $2N$. Thus, for the liquid phase we require

$$\sum_{i=1}^{3} N_i = 2N \tag{7.2}$$

so that the number of atoms does not change when the solid melts. However, relation (7.1) does not hold in general in the liquid phase because the composition in the liquid phase can be different from that in the solid phase.

Because N in (7.2) is fixed in our paper, the number of independent variables for the components is equal to two in the liquid phase: N_1 and N_2. The allowed range of N_1 and N_2 is the rectangular triangle $(0, 0)$, $(2N, 0)$, and $(0, 2N)$, shown in fig. 4. For the purpose of our analysis it is convenient to introduce the following variables:

$$U = N_1 + N_2; \qquad V = N_1 - N_2, \tag{7.3}$$

or

$$N_1 = \tfrac{1}{2}(U + V); \qquad N_2 = \tfrac{1}{2}(U - V). \tag{7.4}$$

In the solid phase, $U = N$ is constant, as is shown in (7.1) and also in fig. 4, and thus V is the only composition variable. When we consider the free-energy axis perpendicular to the plane of N_1 and N_2 in fig. 4, the free energy F_s for the solid phase is a planar curve which lies within the vertical plane $U = N_1 + N_2 = N$. The derivative of F_s with respect to V is

$$\frac{dF_s}{dV} = \frac{1}{2}\left[\left(\frac{\partial F_s}{\partial N_2}\right)_{N_1} - \left(\frac{\partial F_s}{\partial N_2}\right)_{N_1}\right] = \tfrac{1}{2}(\mu_{s,1} - \mu_{s,2}), \tag{7.5}$$

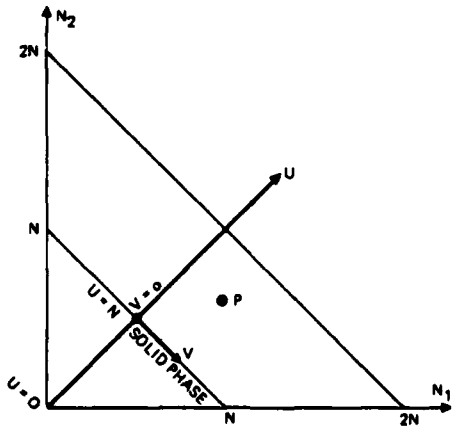

Fig. 4. Relation between the (N_1, N_2) coordinate system and the (U, V) coordinate system.

where we have used the $\mu_{s,i}$ for the solid defined in (6.7).

At the composition $V^{(Q)}$, the free energy value is written as $F_s^{(Q)}$. When we consider a plane which contains the tangent dF_s/dV at this point, the equation of the tangent plane is written using an arbitrary constant α as

$$F - F_s^{(Q)} = \alpha(U - N) + \left(\frac{dF_s}{dV}\right)^{(Q)}(V - V^{(Q)}). \tag{7.6}$$

This arbitrary coefficient α has an origin similar to that of the α used in (4.6) for the binary case.

Now we consider the free energy F_l surface for the liquid phase in the same three-dimensional F–N_1–N_2 space based on fig. 4. We consider a certain composition P in the liquid phase as in fig. 4 and form a plane tangent to the F_l surface at P:

$$F - F^{(P)} = \left(\frac{\partial F_l}{\partial U}\right)_V^{(P)}(U - U^{(P)}) + \left(\frac{\partial F_l}{\partial V}\right)_U^{(P)}(V - V(P)). \tag{7.7}$$

Note that in this equation F is a function of the variables U and V and represents a plane in F–U–V space. The same comment holds for (7.6).

The condition that the solid state at $(N, V^{(Q)})$ and the liquid state at $(U^{(P)}, V^{(P)})$ coexist is that the tangent planes in (7.6) and (7.7) become identical. For the purpose, two sets of mathematical equations need to be satisfied. One is that the coefficients of U and those of V be equal, respectively:

$$\alpha = \left(\frac{\partial F_l}{\partial U}\right)_V^{(P)}, \tag{7.8a}$$

$$\left(\frac{dF_s}{dV}\right)^{(Q)} = \left(\frac{\partial F_l}{\partial V}\right)_U^{(P)}. \tag{7.8b}$$

The other requirement is that (7.6) pass through the point $(F^{(P)}, U^{(P)}, V^{(P)})$ or, equivalently, that (7.7) pass through $(F_s^{(Q)}, N, V^{(Q)})$.

For the purpose of satisfying these two conditions, it is convenient to introduce the follow-

ing two functions:

$$\tilde{G}_s^{(O)} \equiv F_s^{(O)} - \alpha N - \left(\frac{dF_s}{dV}\right)^{(O)} V^{(O)}, \tag{7.9a}$$

$$\tilde{G}^{(P)} \equiv F^{(P)} - \left(\frac{\partial F_l}{\partial U}\right)_V^{(P)} U^{(P)} - \left(\frac{\partial F_l}{\partial V}\right)_U^{(P)} V^{(P)}. \tag{7.9b}$$

Then we can prove that when (7.8a) and (7.8b) are satisfied,

$$\tilde{G}_s^{(O)} = \tilde{G}^{(P)} \tag{7.10}$$

satisfies the second requirement. The proof is similar to what we did in section 4. Using (7.9a), we can rewrite (7.6) as

$$\tilde{G}_s^{(O)} = F - \alpha U - \left(\frac{dF_s}{dV}\right)^{(O)} V. \tag{7.11a}$$

When we use (7.8), we can rewrite this further as

$$\tilde{G}_s^{(O)} = F - \left(\frac{\partial F_l}{\partial U}\right)_V^{(P)} U - \left(\frac{\partial F_l}{\partial V}\right)_U^{(P)} V. \tag{7.11b}$$

On the other hand, (7.10) requires that (7.11b) be equal to (7.9b). Then, when

$$U = U^{(P)} \quad \text{and} \quad V = V^{(P)}, \tag{7.12a}$$

it follows that

$$F = F^{(P)}. \tag{7.12b}$$

This means that (7.6) passes through the point $(F^{(P)}, U^{(P)}, V^{(P)})$, and the proof is finished.

Thus, what we need when calculating the coexisting solid and liquid phases is to evaluate $\tilde{G}_s^{(O)}$ and $\tilde{G}^{(P)}$ in (7.9). The derivative dF_s/dV in (7.9a) has already been derived in (7.5). The derivatives in (7.9b) are derived using

$$\left(\frac{\partial F_l}{\partial N_1}\right) N_2 = \mu_1 - \mu_3 \quad \text{and} \quad \left(\frac{\partial F_l}{\partial N_2}\right) N_1 = \mu_2 - \mu_3, \tag{7.13}$$

and referring to (7.4) as

$$\left(\frac{\partial F_l}{\partial U}\right)_V = \frac{1}{2}\left[\left(\frac{\partial F_l}{\partial N_1}\right)_{N_2} + \left(\frac{\partial F_l}{\partial N_2}\right)_{N_1}\right] = \tfrac{1}{2}(\mu_1 + \mu_2 - 2\mu_3), \tag{7.14a}$$

$$\left(\frac{\partial F_l}{\partial V}\right)_U = \frac{1}{2}\left[\left(\frac{\partial F_l}{\partial N_1}\right)_{N_2} - \left(\frac{\partial F_l}{\partial N_2}\right)_{N_1}\right] = \tfrac{1}{2}(\mu_1 - \mu_2). \tag{7.14b}$$

Before substituting these derivatives in $\tilde{G}_s^{(O)}$ and $\tilde{G}^{(P)}$ of (7.9) we first examine α. We use (7.14) and (7.5) in (7.8) to derive

$$\alpha = \tfrac{1}{2}(\mu_1^{(P)} + \mu_2^{(P)} - 2\mu_3^{(P)}), \tag{7.15a}$$

$$\tfrac{1}{2}(\mu_{s1}^{(Q)} - \mu_{s2}^{(Q)}) = \tfrac{1}{2}(\mu_1^{(P)} - \mu_2^{(P)}). \tag{7.15b}$$

It is convenient to define $\hat{\alpha}$ in place of α as

$$\hat{\alpha} \equiv \alpha - \tfrac{1}{2}(\mu_{s1}^{(Q)} + \mu_{s2}^{(Q)}). \tag{7.16}$$

By replacing α in (7.15a) by $\hat{\alpha}$ and adding and subtracting (7.15a) and (7.15b), we obtain

$$\hat{\alpha} + \mu_{s1}^{(Q)} = \mu_1^{(P)} - \mu_3^{(P)}, \tag{7.17a}$$

$$\hat{\alpha} + \mu_{s2}^{(Q)} = \mu_2^{(P)} - \mu_3^{(P)}. \tag{7.17b}$$

These relations are helpful when we examine the limit of either N_1 or N_2 approaching zero. For this purpose, we first rewrite the $\mu_{s,i}$ in (6.7) for the solid phase as

$$\mu_{s,i} = 4\epsilon_{i3} + 6\epsilon_{ii} + kT[\ln x_i + 6 \ln (y_{ii}/x_i^2)], \quad i = 1 \text{ or } 2. \tag{7.18}$$

When the solid composition x_i goes to zero, we know that

$$\lim_{x_i \to 0} \frac{y_{ii}}{x_i^2} = 1, \tag{7.19}$$

and therefore that when N_i approaches zero, $\mu_{s,i}$ becomes negative and its absolute value becomes large as

$$\mu_{s,i} \to kT \ln x_i. \tag{7.20}$$

Since we expect $\hat{\alpha}$ and $\mu_3^{(P)}$ in (7.17) to remain finite, we see

$$\mu_1^{(P)} \to kT \ln x_1^{(O)} \quad \text{as} \quad x_1^{(O)} \to 0. \tag{7.21}$$

The relations in (7.20) and (7.21) guarantees that the ternary system results reduce smoothly to those of the binary system.

We now rewrite $\tilde{G}_s^{(O)}$ in (7.9a). We use $\hat{\alpha}$ of (7.16) and dF_s/dV of (7.5) in (7.9a) to derive

$$\tilde{G}_s^{(O)} = F_s^{(O)} - [\hat{\alpha} + \tfrac{1}{2}(\mu_{s1}^{(Q)} + \mu_{s2}^{(Q)})]N - \tfrac{1}{2}(\mu_{s1}^{(Q)} - \mu_{s2}^{(Q)})V^{(O)}. \tag{7.22a}$$

We further use (7.1) for N and (7.3) for $V^{(O)}$ to transform

$$\tilde{G}_s^{(O)} = F_s^{(O)} - \hat{\alpha}N - (\mu_{s1}^{(Q)} N^{(O)} + \mu_{s2}^{(Q)} N_2^{(O)}). \tag{7.22b}$$

Since we see from (6.8) that the terms in parentheses are equal to $F_s^{(Q)}$, we arrive at the simple result

$$\tilde{G}_s^{(Q)} = -\hat{\alpha}N. \tag{7.22c}$$

The $\tilde{G}^{(P)}$ in (7.9b) is transformed as follows. We use (7.14) for the derivatives and use (7.3) for U and V to derive

$$\tilde{G}^{(P)} = F^{(P)} - (\mu_1^{(P)} - \mu_3^{(P)})N_1^{(P)} - (\mu_2^{(P)} - \mu_3^{(P)})N_2^{(P)}. \tag{7.23a}$$

Then, using the expression for $F^{(P)}$ in (5.5), we arrive at the result

$$\tilde{G}^{(P)} = 2\mu_3^{(P)}N. \tag{7.23b}$$

Remember that $2N$ is the number of lattice points in the lattice model of the liquid phase.

When we substitute $\tilde{G}_s^{(Q)}$ of (7.22c) and $\tilde{G}^{(P)}$ of (7.23b) in (7.10), we obtain the relation to be satisfied for coexistence:

$$-\hat{\alpha} = 2\mu_3^{(P)}. \tag{7.24}$$

This relation further leads to an important consequence. When we use this in (7.17), we obtain

$$\mu_{s1}^{(Q)} = \mu_1^{(P)} + \mu_3^{(P)},$$
$$\mu_{s2}^{(Q)} = \mu_2^{(P)} + \mu_3^{(P)}. \tag{7.25}$$

These are exactly the thermodynamic conditions that show the chemical potential of the AC molecule ($\mu_{s1}^{(Q)}$) in the solid phase is equal to the sum of the chemical potentials of the A atom and C atom in the liquid phase. The fact that the coexistence condition (7.24) leads to the established thermodynamic relations (7.25) supports the correctness of the analysis in these sections.

8. Derivation of ternary liquidus and solidus

In the previous section we formulated using μ's. As discussed in section 3, in the actual computation we use $\tilde{\mu}$'s, which differ from μ's by $\lambda + \omega\epsilon_{ii}$, as was shown in (3.16) and (5.3). Therefore, the next step is to rewrite the key equations in terms of $\tilde{\mu}$'s.

Using (5.3) we rewrite (7.17) as

$$\hat{\alpha} + \mu_{s,i}^{(Q)} = \tilde{\mu}_i^{(P)} - \tilde{\mu}_3^{(P)} + \omega(\epsilon_{ii} - \epsilon_{33}), \quad \text{for } i = 1 \text{ and } 2. \tag{8.1}$$

We can let $\tilde{\mu}_i$ satisfy either (5.7) or (5.8). In this section we chose the latter. Then, (8.1) can be written as

$$\tilde{\mu}_i^{(P)} = \hat{\alpha} + \mu_{s,i}^{(Q)} - \omega(\epsilon_{ii} - \epsilon_{33}), \quad \text{for } i = 1 \text{ and } 2.$$
$$\tilde{\mu}_3^{(P)} = 0. \tag{8.2}$$

From (6.7) and (6.9), we can write

$$\mu_{s,i} = \mu_{s,i}^{(0)} + kT(6 \ln y_{ii} - 11 \ln x_i), \quad \text{for } i = 1 \text{ and } 2. \tag{8.3}$$

The constant term $\mu_{s,i}^{(0)}$ is obtained by using Vieland's formula [5] from the liquid phase of the 50–50 composition as in (6.10). The quantity $\mu_{l,i}^{(i3)}$ on the right-hand side of (6.10) is the chemical potential in a binary liquid phase, so that it is rewritten using (3.16) as

$$\mu_{l,i}^{(i3)} + \mu_{l3}^{(i3)} = \tilde{\mu}_{l,i}^{(i3)} + \lambda + \omega\epsilon_{ii} + \tilde{\mu}_{l3}^{(i3)} + \lambda + \omega\epsilon_{33}. \tag{8.4a}$$

Since we use (3.17) to calculate $\mu_{s,i}^{(0)}$, we can simplify (8.4a) as

$$\mu_{l,i}^{(i3)} + \mu_{l3}^{(i3)} = 2\lambda + \omega(\epsilon_{ii} + \epsilon_{33}). \tag{8.4b}$$

This is a part of $\mu_{s,i}^{(0)}$ in (6.10). Suppose we define $\tilde{\mu}_{s,i}^{(0)}$ as

$$\tilde{\mu}_{s,i}^{(0)} = \mu_{s,i}^{(0)} - \omega(\epsilon_{ii} + \epsilon_{33}), \qquad i = 1 \text{ and } 2. \tag{8.5}$$

Then $\tilde{\mu}_{s,i}^{(0)}$ can, without knowing $\epsilon_{ii} + \epsilon_{33}$, be evaluated as

$$\tilde{\mu}_{s,i}^{(0)} = 2\lambda - (T_m^{(i3)} - T)\frac{\Delta S_m^{(i3)}}{N_{Avg}}, \tag{8.6}$$

where λ is calculated for the liquid phase of the 50–50 composition. This relation replaces (6.10). Corresponding to (8.5), we define

$$\tilde{\mu}_{s,i} = \mu_{s,i} - \omega(\epsilon_{ii} + \epsilon_{33}), \qquad i = 1 \text{ and } 2. \tag{8.7}$$

Then the relation (8.3) changes into

$$\tilde{\mu}_{s,i} = \tilde{\mu}_{s,i}^{(0)} + kT(6 \ln y_{ii} - 11 \ln x_i), \qquad i = 1 \text{ and } 2. \tag{8.8}$$

We then use (8.7) and rewrite (8.2) in terms of $\tilde{\mu}_{s,i}^{(Q)}$:

$$\tilde{\mu}_1^{(P)} = \tilde{\mu}_{s1}^{(Q)} + \tilde{\alpha},$$
$$\tilde{\mu}_2^{(P)} = \mu_{s2}^{(Q)} + \tilde{\alpha}, \tag{8.9}$$
$$\tilde{\mu}_3^{(P)} = 0,$$

where

$$\tilde{\alpha} \equiv \hat{\alpha} + 2\omega\epsilon_{33}. \tag{8.10}$$

The coexistence condition (7.24) can be rewritten, using $\tilde{\alpha}$ in (8.10) and $\tilde{\mu}_3$ in (3.16), as

$$-\tilde{\alpha} = 2\lambda. \tag{8.11}$$

Note that $2\omega\epsilon_{33}$ cancels out, and $\tilde{\mu}_3^{(P)} = 0$ in (8.9) is used here.

The long transformations done so far in this section simply mean that, for the phase diagram calculation, we can treat the liquid phase as though the A–A, B–B, and C–C pair interactions vanished.

Thus, the actual computational steps are as follows.

(a) We first solve 1–3 and 2–3 binary liquid equilibrium states for 50–50 composition and then estimate (8.6):

$$\tilde{\mu}_{i3}^{(0)} = 2\lambda - (T_m^{(i3)} - T)\frac{\Delta S_m^{(i3)}}{N_{Avg}}, \qquad i = 1 \text{ and } 2, \tag{8.12}$$

where λ is the Lagrange multiplier used in (3.6). As was the case in section 4, $T_m^{(i3)}$ is the melting temperature of the AC solid, and $\Delta S_m^{(i3)}$ is the entropy of melting of one mole of the solid.

(b) Choose a composition $x_1^{(Q)} = 1 - x_2^{(Q)}$ in the solid phase and calculate (8.8):

$$\tilde{\mu}_{i3}^{(Q)} = \tilde{\mu}_{i3}^{(0)} + kT(6 \ln y_{ii}^{(Q)} - 11 \ln x_i^{(Q)}), \qquad i = 1 \text{ and } 2, \tag{8.13}$$

where $y_{ii}^{(Q)}$ is calculated analytically using $x_i^{(Q)}$ as in (6.6) when the second-neighbor interaction energy ϵ_s is given.

(c) Assume a value $\tilde{\alpha}$ and calculate $\tilde{\mu}_i^{(P)}$ from (8.9):

$$\tilde{\mu}_i^{(P)} = \tilde{\mu}_{i3}^{(Q)} + \tilde{\alpha}, \quad \text{for } i = 1 \text{ and } 2, \qquad \tilde{\mu}_3^{(P)} = 0. \tag{8.14}$$

(d) When $\tilde{\mu}_i^{(P)}$ ($i = 1$, 2 and 3) are thus given, we can calculate the ternary liquid phase using the NIM of section 5. The normalization parameter λ is then derived and used to see that the coexistence relation (8.11) holds:

$$-\tilde{\alpha} = 2\lambda. \tag{8.15}$$

Note that this λ is different from λ in (8.12).

If the relation does not hold, we change $\tilde{\alpha}$ and repeat the procedure from (c). When (8.15) holds, then the liquid phase for this $\tilde{\alpha}$ is the phase which coexists with the solid phase chosen in (b).

As an example, we calculate the phase diagram for Ga–In–As. The calculation is based on the binary phase diagrams in fig. 2, which were calculated using the parameters in table I. The additional parameter we need for the ternary case is ϵ_s in (6.4) for the second-neighbor interaction in the solid phase. In view of (6.11), we used the value

$$4\epsilon_s = 2800/6 \text{ cal/mole} \tag{8.16}$$

which is consistent with the value used by S–G, Ω(GaAs–InAs) = 2800 cal/mole. Our ϵ_s corresponds to S–G's Ω divided by 24. The positive value of ϵ_s in (8.16) shows from (6.4) that Ga and In in the solid have a tendency to repel each other. A liquidus isotherm at 1250 K and a few tie lines are plotted in fig. 5. The solid phase is always on the pseudobinary line $(GaAs)_{1-x}(InAs)_x$.

The liquidus and solidus on the pseudobinary line are plotted in fig. 6a. The calculated curves are exactly the same as those calculated by S–G

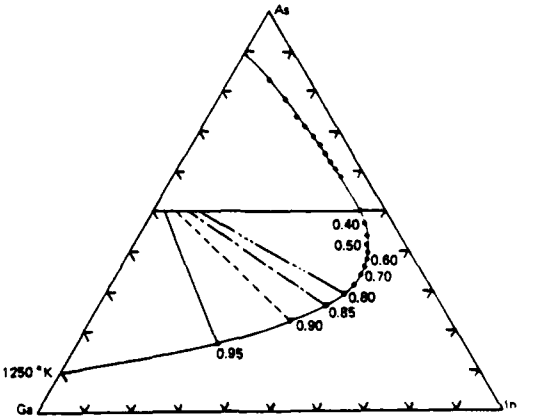

Fig. 5. The isothermal liquidus of Ga–In–As ternary system at 1250 K, calculated independently by Stringfellow–Greene [1] and Kikuchi in this paper. The numbers along the curve are x in the solid composition $(GaAs)_{1-x}(InAs)_x$. Four tie lines are shown.

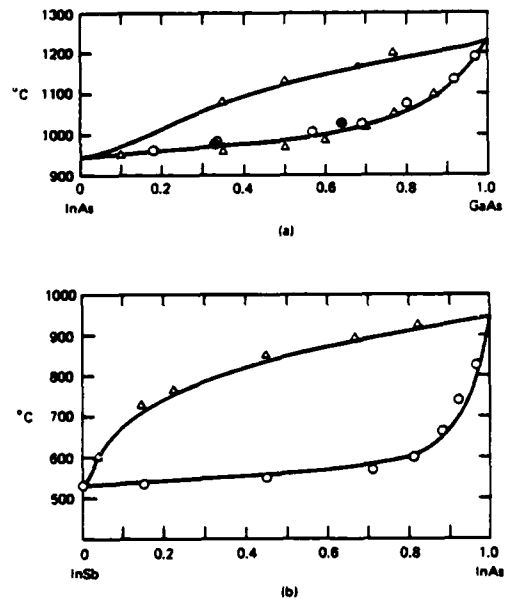

Fig. 6. Pseudobinary liquidus and solidus curves of InAs–GaAs (a) and InSb–InAs (b). The solid curves were calculated independently by Stringfellow–Greene [1] and Kikuchi in this paper, and the circles and triangles represent experimental results.

and agree well with the experimental points marked in the figure.

Although the computed results are the same, a slight difference in the identification of the energy parameter ϵ_s between this paper and S–G may be worth pointing out. We identified ϵ_s as the parameter for the second-neighbor interaction (in the zinc-blende-type lattice) between Ga and In in the solid phase, as introduced in section 6 and illustrated in fig. 3. On the other hand, S–G regarded Ω(GaAs–InAs) as the parameter for the GaAs–InAs interaction.

The calculation was also done for the In–As–Sb system. The energy parameters are those in table I together with the solid phase value

$$4\epsilon_s = 2900/6 \text{ cal/mole}. \qquad (8.17)$$

The liquidus and solidus on the pseudobinary line are plotted in fig. 6b; they are in good agreement with S–G's curves and with experimental data.

9. The orthogonality relation

At the end of section 5 we commented that either (5.7) or (5.8) could be used as the condition for the $\tilde{\mu}$. In section 5, we used $\tilde{\mu}_3 = 0$ in (5.8). We now form linear combination of $\tilde{\mu}_i$ and define

$$\tilde{\mu}_i^* \equiv \tilde{\mu}_i - (\tilde{\mu}_1 + \tilde{\mu}_2)/3, \qquad i = 1, 2 \text{ and } 3, \qquad (9.1)$$

so that

$$\sum_{i=1}^{3} \tilde{\mu}_i^* = 0, \qquad (9.2)$$

which is of the form of (5.7). Solving (9.1) for $\tilde{\mu}_i$'s we can write

$$\tilde{\mu}_i = \tilde{\mu}_i^* - \tilde{\mu}_3^*, \qquad i = 1, 2 \text{ and } 3. \qquad (9.3)$$

Since the $\tilde{\mu}_i^*$ satisfy condition (9.2), we can plot them on a star-shaped graph. An example is shown in fig. 7. Each $\tilde{\mu}_i^*$ ($i = 1$, 2 or 3) point corresponds to a coexisting liquid state P and a solid state Q and thus to the tie line PQ. We can

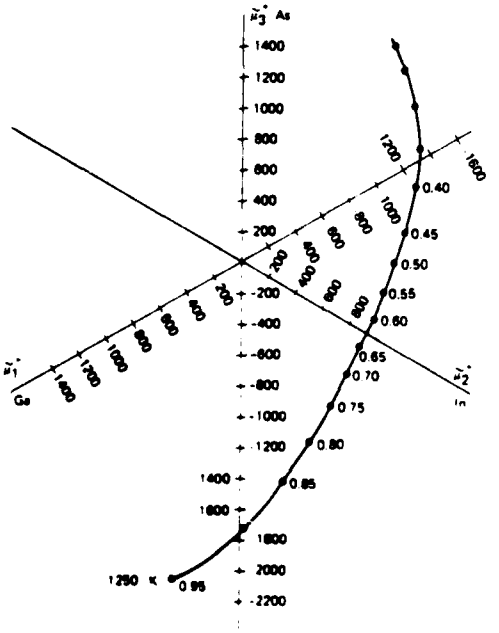

Fig. 7. The chemical potential diagram corresponding to fig. 5. The numbers along the curve are the x values corresponding to those in fig. 5. The $\tilde{\mu}$ curve at x is perpendicular to the tie line at x in fig. 5.

now prove that the tie line PQ is perpendicular to the tangent of the $\tilde{\mu}_i^*$ curve.

From (5.3) the chemical potential $\mu_i^{(P)}$ at the liquid point P can be written as

$$\mu_i^{(P)} = \tilde{\mu}_i + \lambda + \omega\epsilon_{ii} = \tilde{\mu}_i^* - \tilde{\mu}_3^* + \lambda + \omega\epsilon_{ii}, \quad i = 1\ 2 \text{ and } 3. \tag{9.4}$$

where we used (9.3). The chemical potential for an AC unit and a BC unit in the solid phase can be written as $\mu_{s,1}^{(Q)}$ and $\mu_{s,2}^{(Q)}$ in (7.25). Furthermore, using (9.4) we can write them as

$$\mu_{s,i}^{(Q)} = \tilde{\mu}_i^* - \tilde{\mu}_3^* + 2\lambda + \omega(\epsilon_{ii} + \epsilon_{33}), \qquad i = 1 \text{ and } 2. \tag{9.5}$$

Along a liquidus isotherm for T, the change of the grand potential $\hat{G}$ due to the change in the chemical potential is written for the liquid phase as

$$\Delta\hat{G}^{(P)} = 2N \sum_{i=1}^{3} x_i^{(P)} \Delta\mu_i^{(P)}, \tag{9.6a}$$

where $2N$ is the total number of atoms in the liquid phase. Using (9.4), we can rewrite this as

$$\Delta\hat{G}^{(P)} = 2N \left[\sum_{i=1}^{3} x_i^{(P)} \Delta\tilde{\mu}_i^* - \Delta\tilde{\mu}_3^* + \Delta\lambda \right]. \tag{9.6b}$$

At the other end of the tie line the solid phase is made up of $Nx_{s,1}$ AC units and $Nx_{s,2}$ BC units; these have chemical potentials $\mu_{s,1}^{(Q)}$ and $\mu_{s,2}^{(Q)}$, respectively, as shown in (9.5). Thus, the change of the grand potential along the solid phase isotherm is

$$\Delta\hat{G}_s^{(Q)} = N \sum_{i=1}^{2} x_{s,i} \Delta\mu_{s,i}^{(Q)}. \tag{9.7a}$$

In rewriting this expression, note that the coordinate $x_i^{(Q)}$ for the solid state in the Gibbs triangle plot is:

$$x_i^{(Q)} = \tfrac{1}{2}x_{s,i}, \qquad i = 1 \text{ and } 2,$$
$$x_3^{(Q)} = \tfrac{1}{2}. \tag{9.7b}$$

Combining these relations with (9.5), we can rewrite (9.7a) as

$$\Delta\hat{G}_s^{(Q)} = 2N[x_i^{(Q)} \Delta\tilde{\mu}_i^* - \Delta\tilde{\mu}_3^* + \Delta\lambda]. \tag{9.7c}$$

The grand potentials $\hat{G}^{(P)}$ and $\hat{G}_s^{(Q)}$ are equal when P and Q are connected by a tie line. Thus, $\Delta\hat{G}^{(P)}$ and $\Delta\hat{G}_s^{(P)}$ are also equal. Then, by equating (9.6b) and (9.7c), we obtain

$$\sum_{i=1}^{3} (x_i^{(P)} - x_i^{(Q)}) \Delta\tilde{\mu}_i^* = 0. \tag{9.8}$$

Note that $x_i^{(P)} - x_i^{(Q)}$ and $\Delta\tilde{\mu}_i^*$ are components on three coplanar axes. It was proved in the appendix of ref. 4 by simple geometry that the components of these vectors on Cartesian coordinate systems obey an equation similar to (9.8). Therefore, we can conclude that the tie line represented by $x_i^{(P)} - x_i^{(Q)}$ ($i = 1$, 2, and 3) is perpendicular to the tangent of the $\tilde{\mu}_i^*$ curve.

Appendix

Proof that the grand potential decreases as the interaction proceeds in the NIM

In this appendix we prove that the grand potential $\hat{G}$ or Φ in (3.2) decreases in one iteration step of the NIM. We rewrite (3.5) as

$$\psi_{ij} \equiv \beta\omega\epsilon_{ij} - \tfrac{1}{2}(2\omega - 1)\ln(x_i x_j) + \omega \ln \hat{y}_{ij} - \tfrac{1}{2}\beta(\hat{\mu}_i + \hat{\mu}_j) - \lambda\beta = 0, \tag{A.1}$$

where x_i and x_j are the input to the iteration cycle, $\hat{y}_{ij}$ is the output, and other quantities are constants. We can rewrite the grand potential Φ in (3.2) as

$$\Phi\{y_{ij}\} = \beta\omega \sum_{ij} \epsilon_{ij} y_{ij} - \tfrac{1}{2}(\omega - 1) \times \left[\sum_i x_i \ln x_i + \sum_j x_j \ln x_j \right] + \omega_i \sum_{ij} y_{ij} \ln y_{ij} - \tfrac{1}{2}\beta \left[\sum_i x_i \hat{\mu}_i + \sum_j x_j \hat{\mu}_j \right]. \tag{A.2}$$

This is a function of the input x_i and y_{ij} values, as indicated by $\{y_{ij}\}$. Note that in (A.2) x_i and x_j represent

$$x_i = \sum_j y_{ij} \quad \text{and} \quad x_j = \sum_i y_{ij}. \tag{A.3}$$

In later transformations we use $\Phi\{\hat{y}_{ij}\}$, which is derived by replacing the x_i and y_{ij} values by $\hat{x}_i$ and $\hat{y}_{ij}$ values. The relations (A.3) hold for quantities with carets also.

Next, we use (A.1) and form

$$\sum_{ij} y_{ij}\psi_{ij} = \beta\omega \sum_{ij} [_{ij}y_{ij} - \tfrac{1}{2}(2\omega - 1) \times \left[\sum_i x_i \ln x_i + \sum_j x_i \ln x_i\right] + \omega \sum_{ij} y_{ij} \ln \hat{y}_{ij} - \tfrac{1}{2}\beta \left[\sum_i x_{i\mu}\hat{\mu}_i + \sum_j x_{j\mu}\hat{\mu}_j\right] - \lambda\beta = 0. \quad (A.4)$$

Since this vanishes, we can simplify $\Phi\{y_{ij}\}$ in (A.2) by subtracting (A.4) from (A.2) as

$$\Phi\{y_{ij}\} = \omega \sum_{ij} y_{ij}(\ln y_{ij} - \ln \hat{y}_{ij}) + \lambda\beta. \quad (A.5)$$

Then from (A.1) we form

$$\sum_{ij} \hat{y}_{ij}\psi_{ij} = \beta\omega \sum_{ij} \epsilon_{ij}\hat{y}_{ij} - \tfrac{1}{2}(2\omega - 1) \times \left[\sum_i \hat{x}_i \ln x_i + \sum_j \hat{x}_j \ln x_j\right] + \omega \sum_{ij} \hat{y}_{ij} \ln \hat{y}_{ij} - \tfrac{1}{2}\beta \left[\sum_i \hat{x}_{i\mu}\hat{\mu}_i + \sum_j \hat{x}_{j\mu}\hat{\mu}_j\right] - \lambda\beta = 0 \quad (A.6)$$

and subtract this from $\Phi\{\hat{y}_{ij}\}$, which is derived from (A.2):

$$\Phi\{\hat{y}_{ij}\} = -\tfrac{1}{2}(2\omega - 1) \times \left[\sum_i \hat{x}_i(\ln \hat{x}_i - \ln x_i) + \sum_j \hat{x}_j(\ln \hat{x}_j - \ln x_j)\right] + \lambda\beta. \quad (A.7)$$

We note that $\Phi\{y_{ij}\}$ in (A.5) is the input value of the grand potential, and $\Phi\{\hat{y}_{ij}\}$ in (A.7) is the output value. We are interested in the difference between the two:

$$\Phi\{y_{ij}\} - \{\hat{y}_{ij}\} = (2\omega - 1) \sum_i \hat{x}_i \ln(\hat{x}_i - x_i) + \omega \sum_{ij} y_{ij} \ln(y_{ij}/\hat{y}_{ij}). \quad (A.8)$$

In transforming this expression, we use Gibbs's lemma [7]:

$$\Delta\eta\, e^{\Delta\eta} + 1 - e^{\Delta\eta} \geq 0, \quad (A.9)$$

which holds for any real number $\Delta\eta$. The left-hand side is a decreasing function of $\Delta\eta$ for negative values of $\Delta\eta$ and an increasing function of $\Delta\eta$ for positive values of $\Delta\eta$; it vanishes for $\Delta\eta = 0$. We rewrite (A.8) as

$$\Phi\{y_{ij}\} - \Phi\{\hat{y}_{ij}\} = (2\omega - 1) \sum_i [\hat{x}_i \ln(\hat{x}_i/x_i) + x_i - \hat{x}_i] + \omega \sum_{ij} [y_{ij} \ln(y_{ij}/\hat{y}_{ij}) + \hat{y}_{ij} - y_{ij}]. \quad (A.10)$$

Since the summand of each term is non-negative because of (A.9), we therefore have proved that

$$\Phi\{y_{ij}\} - \Phi\{\hat{y}_{ij}\} \geq 0. \quad (A.11)$$

References

[1] G.B. Stringfellow and P.E. Greene, J. Phys. Chem. Solids 30 (1969) 1779.
[2] E.A. Guggenheim, "Mixtures" (Oxford Univ. Press, Oxford, 1952).
[3] R. Kikuchi, Acta Met. 25 (1977) 195.
[4] R. Kikuchi, D. de Fontaine, M. Murakami and T. Nakamura, Acta Met. 25 (1977) 207.
[5] L.J. Vieland, Acta Met. 11 (1963) 137.
[6] R. Kikuchi, J. Chem. Phys. 60 (1974) 1071.
[7] J.W. Gibbs, Elementary Principles in Statistical Mechanics in: The Collected Works of J. Willard Gibbs, vol. II (Yale Univ. Press, New Haven, Conn., 1957) p. 130.

APPENDIX B

LIQUIDUS CALCULATION OF

II-VI COMPOUND SEMICONDUCTORS

CALPHAD Vol.6, No.1, pp. 1-10, 1982
Printed in the USA.

0364-5916/82/010001-10$03.00/0

LIQUIDUS CALCULATION OF II-VI COMPOUND SEMICONDUCTORS*

Ryoichi Kikuchi
Hughes Research Laboratories
Malibu, CA 90265 U.S.A.

(This paper was presented at CALPHAD X Vienna, Austria July 1981)

ABSTRACT. The pair approximation (which is equivalent to the quasi-chemical method) is used to calculate liquidus of II-VI compound semiconductors. For the liquid phase, a quasi-lattice structure is assumed, and the pressure and the association property are taken into account. Vieland's formula is used for the free energy difference between liquid and solid. Numerical calculation was made with the Hg-Te and Cd-Te systems. For each system, one set of parameters is found which computes the liquidus in good agreement with experiments for the entire composition and temperature ranges.

A particular attention is paid to the shape of the liquidus curve near its top. Experimentally it looks pointed, although thermodynamics requires it to be rounded. Our calculation shows that when the AB-A and AB-B interactions are repulsive, the theoretical curve looks pointed and the top region has a very small radius of curvature.

1. Introduction

A theory of liquidus of III-V semiconductors was formulated using the quasi-chemical method by Stringfellow and Greene (1), and later by the present author (2). In the latter, the cluster variation method (CVM) approach (3,4) was used; the pair approximation of CVM is equivalent to the method commonly known as the quasi-chemical method (5).

In the present paper, we extend the previous treatment (2) to the II-VI semiconductor liquidus calculations. The main difference is the association property, that means inclusion of molecular species in the liquid phase in the II-VI case.

The liquid phase is represented by a lattice structure. In the pair approximation we are using in the paper, the information on the structure of the lattice appears only in the coordination number which is written as $2w$.

2. Chemical Potentials of the Liquid Phase

The two atomic species in the system are written as A and B. They are, for example, Hg and Te. We assume that in the liquid phase the molecular species AB also exists. We use a lattice model for the liquid phase, and these species can sit only on lattice points. Although in reality obviously the liquid does not have a lattice structure, the approximation is considered acceptable because the local correlation among atoms and molecules in the real liquid system can be simulated adequately using the lattice structure, as far as no superlattice structure is introduced.

The three species A, B, and AB are designated by i=1, 2, and 3. We also include vacancies (i=4) in the lattice in order to take into account the pressure effect. The probability of finding an ith species on a lattice point is written as x_i and the probability of finding an i-j nearest-neighbor pair is written as y_{ij}. These variables satisfy the geometrical relation or the reduction relation:

---

*Supported by U.S. Army Research Office

Received 6 November 1981

$$x_i = \sum_{j=1}^{4} y_{ij} \qquad i=1,\ldots,4 \tag{2.1}$$

Since there is no superlattice structure in the lattice, the symmetry relation holds:

$$y_{ij} = y_{ji} \tag{2.2}$$

The normalization relation is

$$\sum_{i=1}^{4} x_i = 1. \tag{2.3}$$

Before going into the main treatment of the liquid phase, in this section we discuss the chemical potentials of species in the liquid phase. For this purpose we write the Helmholtz free energy F=E-TS. The energy E is written as

$$E = \omega N \sum_{i=1}^{4}\sum_{j=1}^{4} \varepsilon_{ij} y_{ij} - N\varepsilon_3 x_3 \tag{2.4}$$

where N is the number of lattice points in the liquid system, ε_{ij} is the interaction potential for the nearest-neighbor i-j pair, and ε_3 is the formation energy of the AB molecular species. Since we assume no interaction energy with vacancies, we require

$$\varepsilon_{14} = \varepsilon_{41} = 0 \qquad \text{for } i=1,\ldots,4 \tag{2.5}$$

The entropy formula is the same as Equation 2.6 in Reference 2:

$$S = kN\,(2\omega-1) \sum_{i} L(x_i) - \omega \sum_{i,j} L(y_{ij}) \tag{2.6}$$

where the L(x) function originates in the logarithm of a factorial and is defined as

$$L(x) \equiv x \ln x - x \quad . \tag{2.7}$$

The S expression in Equation 2.6 is for the pair approximation of the CVM and is the same as the expression used in the quasi-chemicaL method (5).

When we use E in Equation 2.4 and S in Equation 2.6, we can write the Helmholtz free energy F as

$$F = Nf \tag{2.8a}$$

where

$$f = \omega \sum_{i,j} \varepsilon_{ij} y_{ij} - \varepsilon_3 x_3 - kT\,(2\omega-1) \sum_{i} L(x_i) - \omega \sum_{i,j} L(y_{ij}) \tag{2.8b}$$

For the discussion of chemical potentials, it is convenient to use the relation of Equation 2.1 and write

$$y_{ii} = x_i - \sum_{j \neq i} y_{ij} \tag{2.9}$$

Based on this relation, we treat f as a function of x_i (i=1,...,4) and y_{ij} (i≠j).

The number of the ith species in a lattice is written as N_i, which satisfies

$$N_i = x_i N \ , \quad i=1,\ldots,4 \tag{2.10}$$

Note N_4 is the number of vacancies. When we use the Helmholtz free energy F as the thermodynamic potential, the total volume of the system is fixed. In the lattice model, this means that the total number of lattice points N is fixed. We can choose N_1, N_2, and N_3 as independent and write N_4 as

$$N_4 = N - N_1 - N_2 - N_3 \ . \tag{2.11}$$

We then calculate chemical potentials as follows:

$$\mu_1 \equiv \left(\frac{\partial F}{\partial N_1}\right)_{N_2,N_3} = \left(\frac{\partial F}{\partial N_1}\right)_{N_2,N_3,N_4} - \left(\frac{\partial F}{\partial N_4}\right)_{N_1,N_2,N_3} \tag{2.12}$$

When we use the free energy expression in Equation 2.8, we can obtain explicitly,

$$\mu_1 = \omega\epsilon_{11} + kT\left[\ln x_1 + \omega \ln\left(y_{11}/x_1^2\right)\right] - \mu_v \tag{2.13}$$

where

$$\mu_v \equiv \frac{\partial F}{\partial x_4} = kT\left[\ln x_4 + \omega \ln\left(y_{44}/x_4^2\right)\right] \ . \tag{2.14}$$

We can perform the same differentiation as Equation 2.12 for i=2 and 3 and obtain

$$\mu_i = \omega\epsilon_{ii} - \epsilon_i + kT\left[\ln x_i + \omega \ln(y_{ii}/x_i^2)\right] - \mu_v \text{ for } i=1,\ 2 \text{ and } 3 \tag{2.15}$$

where we wrote ϵ_i as a general term but it is defined as

$$\epsilon_i = 0 \qquad \text{for } i \neq 3 \tag{2.16}$$

and ϵ_3 is the energy parameter in Equation 2.4 and 2.8b.

The total number of A atoms including those in molecules AB is written as N_A. We define the corresponding quantity N_B for the B atoms. Then

$$N_A = N_1 + N_3 \ ,$$

$$N_B = N_2 + N_3 \ . \tag{2.17}$$

When the compositions N_A and N_B are given, the system adjusts itself to come to the value of N_3 such that the free energy is a minimum with respect to N_3. In order to see this relation, we can use N_A, N_B, and N_3 as independent and write N_1, N_2, and N_4 as

$$N_1 = N_A - N_3 \ ,$$

$$N_2 = N_B - N_3 \ ,$$

$$N_4 = N - N_A - N_B + N_3 \ . \tag{2.18}$$

When we minimize F with respect to N_3 keeping N_A and N_B fixed, we can use Equation 2.12 and corresponding relations for i=2 and 3 to obtain

$$\mu_3 = \mu_1 + \mu_2 \quad . \tag{2.19}$$

This is the equilibrium condition among atoms A and B and the molecular species AB.

We can use Equation 2.18 again and derive that μ_1 in Equation 2.12 is identical to the following differentiation:

$$\mu_1 = \left(\frac{\partial F}{\partial N_A}\right)_{N_B} \tag{2.20}$$

This says that the chemical potential μ_1 can be calculated by either Equations 2.12 or Equation 2.20.

3. Grand Potential

In numerically solving the liquid state, it is convenient not to fix the composition N_i but to let it vary by using Lagrange multipliers. We define the grand potential G as

$$\hat{G} = E - TS - \sum_{i=1}^{4} \mu_i' N_i \tag{3.1}$$

where, at this stage, μ_i' is regarded as Lagrange multipliers. Since N is fixed and we treat N_4 as dependent as in Equation 2.11, we actually do not need μ_4' in Equation 3.1. So we require

$$\mu_4' = 0 \quad . \tag{3.2}$$

We use Equation 2.9 and rewrite the energy E in Equation 2.4 as

$$E = \omega N \left(\sum_{i=1}^{4} \varepsilon_{ii} x_i + \sum_{i \neq j} \hat{\varepsilon}_{ij} y_{ij} \right) - N \sum_{i=1}^{4} \varepsilon_i x_i \tag{3.3}$$

where we define

$$\hat{\varepsilon}_{ij} \equiv \varepsilon_{ij} - \tfrac{1}{2} \left(\varepsilon_{ii} + \varepsilon_{jj} \right) \tag{3.4a}$$

Special cases are

$$\hat{\varepsilon}_{ii} = 0 \qquad i=1,\ldots,4 \tag{3.4b}$$

and

$$\hat{\varepsilon}_{i4} = \hat{\varepsilon}_{4i} = -\tfrac{1}{2} \varepsilon_{ii} \quad . \tag{3.4c}$$

When we combine E in Equation 3.3 and the chemical potential terms in Equation 3.1, we can write

$$E - \sum_{i=1}^{4} \mu_i' N_i = \omega N \sum_{i,j} \hat{\varepsilon}_{ij} y_{ij} + N \sum_{i=1}^{4} \left(\omega \varepsilon_{ii} - \varepsilon_i - \mu_i' \right) x_i \quad . \tag{3.5}$$

We can simplify this when we write

$$\hat{\mu}_i \equiv \mu_i' - \omega\varepsilon_{ii} + \varepsilon_i \quad , \quad i=1,2,3 \quad . \tag{3.6}$$

Because of Equations 3.2, 2.5, and 2.16, we see

$$\hat{\mu}_4 = 0 \quad . \tag{3.7}$$

When we combine Equations 3.5 and 2.6, we can write the grand potential $\hat{G}$ in Equation 3.1 explicitly as

$$\phi \equiv \frac{\beta\hat{G}}{N} = \beta\omega\sum_{ij}\hat{\varepsilon}_{ij}y_{ij} - \beta\sum_i \hat{\mu}_i x_i$$

$$- (2\omega - 1)\sum_i L(x_i) + \omega\sum_{i,j} L(y_{ij}) + \beta\lambda\left(1 - \sum_{i,j} y_{ij}\right) \tag{3.8}$$

where

$$\beta = \frac{1}{kT} \tag{3.9}$$

and λ is a Lagrange multiplier. The λ terms are added in Equation 3.8 in order to take into account the normalization of y_{ij}.

The equilibrium state is obtained by minimizing G in Equation 3.8 with T and $\hat{\mu}_i$ fixed:

$$\frac{\partial\phi}{\partial y_{ij}} \equiv \beta\omega\,\hat{\varepsilon}_{ij} - \frac{2\omega - 1}{2}\ln(x_i x_j) + \omega\ln y_{ij} - \frac{1}{2}\beta(\hat{\mu}_i + \hat{\mu}_j) - \lambda\beta = 0 \tag{3.10}$$

At this point we digress and examine the i=j case. Using Equation 3.4 we can derive

$$\hat{\mu}_i + \lambda = kT\left[\ln x_i + \omega\ln\left(y_{ii}/x_i^2\right)\right] \qquad \text{for } i = 1,2,3 \quad . \tag{3.11}$$

The fourth equation can be simplified by using Equations 3.7 and 3.4 as

$$\lambda = kT\left[\ln x_4 + \omega\ln\left(y_{44}/x_4^2\right)\right] \quad . \tag{3.12}$$

When we compare this with Equation 2.14, we identify μ_v used in Section 2 as

$$\mu_v = \lambda \tag{3.13}$$

Use of this in Equation 2.15 and comparison with Equation 3.11 allow us to derive

$$\hat{\mu}_i = \mu_i - \omega\varepsilon_{ii} + \varepsilon_i \quad , \quad i = 1,2,3 \quad . \tag{3.14}$$

Further, when we compare this with Equation 3.6, we can identify

$$\mu_i' = \mu_i \quad , \quad i = 1,2,3 \quad . \tag{3.15}$$

which means that μ_i' used in the expression of $\hat{G}$ in Equation 3.1 is actually the chemical potential itself. Therefore, from now on we can drop the prime from μ_i'.

When this relation is used, $\sum_i \mu_i N_i$ becomes the Gibbs free energy G itself. Thus $\hat{G}$ in Equation 3.1 is

$$\hat{G} = F - G = -pvN \tag{3.16}$$

where v is the volume per lattice point in the lattice model of the liquid phase.

The identity in Equation 3.15 leads to another important relation. We can write the association equilibrium relation in Equation 2.19 in terms of μ_i using Equations 3.15 and 3.14:

$$\hat{\mu}_1 + \hat{\mu}_2 - \hat{\mu}_3 = \omega(\epsilon_{33} - \epsilon_{11} - \epsilon_{22}) - \epsilon_3 \equiv u \quad . \tag{3.17}$$

We can interpret the meaning of the energy constant u as follows. When $\hat{\mu}_i$ in Equation 3.11 is written as

$$\hat{\mu}_i \equiv kT \ln a_i \ , \ i = 1,2,3 \quad , \tag{3.18}$$

then a_i is called the activity. Equation 3.11 together with 3.12 gives the explicit form of a_i as

$$a_i = x_i \left(\frac{y_{ii}}{x_i^2}\right)^{\omega} \left[x_4 \left(\frac{y_{44}}{x_4^2}\right)^{\omega}\right]^{-1} \tag{3.19}$$

which says that a_i is roughly proportional to the fractional amount x_i. When we use a_i, we can write Equation 3.17 as

$$\frac{a_3}{a_1 a_2} = \exp(-u/kT) \quad . \tag{3.20}$$

This shows that the energy constant u controls the amount of association, a larger -u leading to a larger a_3, i.e., larger association.

When Φ in Equation 3.8 is a minimum and Equation 3.10 holds, we can simplify Φ by forming

$$\Phi \equiv \frac{\beta \hat{G}}{N} = \phi - \sum_{i,j} y_{ij} \frac{\partial \phi}{\partial y_{ij}} = \beta\lambda \quad . \tag{3.21}$$

This means that all terms in Φ cancel each other except the only one $\beta\lambda$. Comparison of Equation 3.21 and 3.16 leads to the relation

$$\lambda = -pv \quad . \tag{3.22}$$

Now we go back to the equations in 3.10, and write it as

$$y_{ij} = \exp\left[\frac{\lambda\beta}{\omega} - \beta\hat{\epsilon}_{ij} + \frac{\beta}{2\omega}(\hat{\mu}_i + \hat{\mu}_j)\right] (x_i x_j)^{(2\omega-1)/(2\omega)} \tag{3.23}$$

When $\beta = 1/kT$ and $\hat{\mu}_i$ are given, this relation and the reduction relations in Equation 2.1 form a set of simultaneous equations to be solved for y_{ij}. We can solve them using the NIM(3).

The energy parameters we need are seven: $\hat{\epsilon}_{12}$, $\hat{\epsilon}_{13}$, $\hat{\epsilon}_{23}$, $\hat{\epsilon}_{14}$, $\hat{\epsilon}_{24}$, $\hat{\epsilon}_{34}$ in Equations 3.4 and u in 3.17. The values of these seven parameters are to be supplied by whatever means before the computation starts. In solving the set of simultaneous equations we fix two values $\hat{\mu}_1$ and $\hat{\mu}_2$. When $\hat{\mu}_1$ and $\hat{\mu}_2$ are given, μ_3 is determined from the association relation Equation 3.17; note $\hat{\mu}_4 = 0$ as in Equation 3.7. We then proceed to solve the equations using NIM. After the iteration has converged, the pressure is derived from the relation in Equation 3.22. The two adjustable parameters $\hat{\mu}_1$ and $\hat{\mu}_2$ can be so chosen that the pressure p and the composition N_A/N_B can take chosen values.

4. Derivation of the Liquidus

Derivation of the liquidus curve was formulated in Section 4 of Reference 2 based on the geometrical construction that the tangent of the Gibbs free energy curve for the liquid

phase goes through the Gibbs free energy point for the solid phase. We can use the similar formulation in the present problem. We assume as in Reference 2, that the solid phase has the fixed composition, $N_A = N_B$, and thus the Gibbs free energy for the solid at T is represented by a single point rather than a curve.

The geometrical construction of Reference 2 leads to the coexistence condition that

$$\mu_1^{(\ell)} + \mu_2^{(\ell)} = \mu_1^{(s)} + \mu_2^{(s)} \tag{4.1}$$

where the superscripts (ℓ) and (s) stand for liquid and solid, respectively. This equation holds in the present case also.

The chemical potentials for the solid state can be calculated using Vieland's method (6), and is written as

$$\mu_1^{(s)} + \mu_2^{(s)} = \mu_1^{(c)} + \mu_2^{(c)} - (T_m - T)\ \Delta S_m \tag{4.2}$$

where (c) indicates the supercooled liquid state of the composition $N_A = N_B$ at T, T_m is the melting temperature of the solid and ΔS_m is the entropy of melting per molecule AB. The value of T_m is to be supplied from experiments.

In the present case we can use Equation 2.19 and simply write μ_3 for $\mu_1 + \mu_2$ in Equation 4.2. Further, we can use Equation 3.14 to write

$$\mu_3^{(\ell)} - \mu_3^{(c)} = \hat{\mu}_3^{(\ell)} - \hat{\mu}_3^{(c)} \tag{4.3}$$

Note a caret on μ on the right-hand side. Combining these three equations, we can write the condition for the liquidus as

$$\hat{\mu}_3^{(\ell)} = \hat{\mu}_3^{(c)} - (T_m - T)\ \Delta S_m \quad . \tag{4.4}$$

Thus the procedure of deriving the liquidus curve is the following. At the temperature T and pressure p, the supercooled state (c) is first solved. This solution gives the value $\hat{\mu}_3^{(c)}$. Then Equation 4.4 is used to derive $\hat{\mu}_3^{(\ell)}$ for the liquid state which coexists with the solid at this T and p. Equation 3.17 is then used to evaluate $\mu_1^{(\ell)} + \mu_2^{(\ell)}$. When we assign a value to $\mu_1^{(\ell)} - \mu_2^{(\ell)}$, all the parameters are ready to solve the simultaneous Equations 3.23 for the liquid state (ℓ). The adjustable value $\hat{\mu}_1^{(\ell)} - \hat{\mu}_2^{(\ell)}$ is determined so that the pressure of the state becomes equal to the desired value p.

5. Choice of the Energy Parameters

In Section 3 we noted that the present formulation has seven energy parameters at our disposal. Among the seven, the three ϵ_{14}, ϵ_{24} and ϵ_{34} are related to vacancies and hence have little effect in the liquidus calculations because the number of vacancies (in the pseudo-lattice model) is always small, less than 10^{-4}, in the present calculations.

In the III-V case, in which no molecular species exists, $\hat{\epsilon}_{13}$ and $\hat{\epsilon}_{23}$ do not appear in the theory and hence $\hat{\epsilon}_{12}$ is the only energy parameter. We know in the III-V case (2) that $\hat{\epsilon}_{12}$ controls the shape of the liquidus curve, making it higher or lower. In the present II-VI case, also, $\hat{\epsilon}_{12}$ controls the liquidus curve in the similar way. When $-\hat{\epsilon}_{12}$ is large the liquidus goes up, except at T_m which is fixed.

The energies $\hat{\epsilon}_{13}$ and $\hat{\epsilon}_{23}$, together with u, control the amount of association. In order to single out the association property, we calculate the special case $\hat{\epsilon}_{13} = \hat{\epsilon}_{23}$, keeping the liquidus symmetric. The calculated results are in Fig. 1, in which the number written next to a curve is the value of the ratio $\hat{\epsilon}_{13}/\hat{\epsilon}_{12} = \hat{\epsilon}_{23}/\hat{\epsilon}_{12}$. For lower curves for which the ratio is positive, and hence $\hat{\epsilon}_{13} = \hat{\epsilon}_{23}$ is negative (i.e., attractive), the liquidus shows the rounded top. For upper curves for which the ratio is negative, i.e.,

$\hat{\epsilon}_{13} = \hat{\epsilon}_{23}$ is positive and repulsive, the liquidus shows a pointed peak. As the shape changes from the rounded top to the pointed top, around -2 of the ratio, the shoulders are almost linear. At -3 and -4 of the ratio, the inflection points are observed. For -5, a phase separation occurs in the liquid phase. The liquidus similar as the -5 case is observed in the Zn-rich side of the Zn-Te binary liquid (7).

Although the upper curves in Fig. 1 are pointed, the peak still has a rounded top with a small radius of curvature. This is in agreement with the thermodynamic requirement (8).

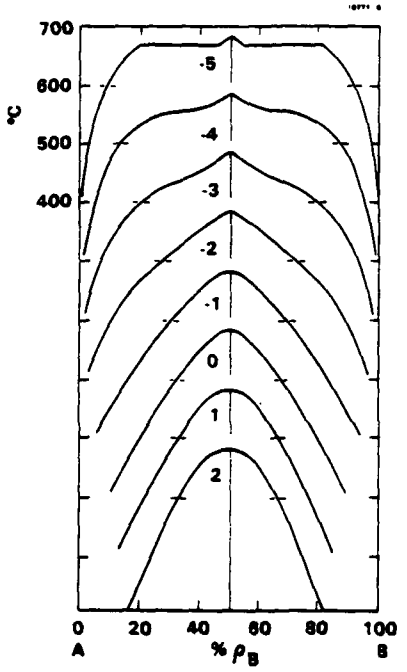

FIG. 1

Liquidus curves for different values of atom-molecule interaction parameters. A horizontal short line marks 600°C for each curve.

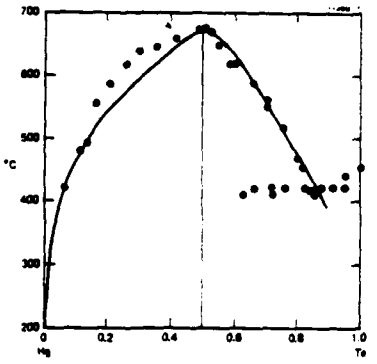

FIG. 2

Hg-Te binary liquidus. Dots are experiments (9).

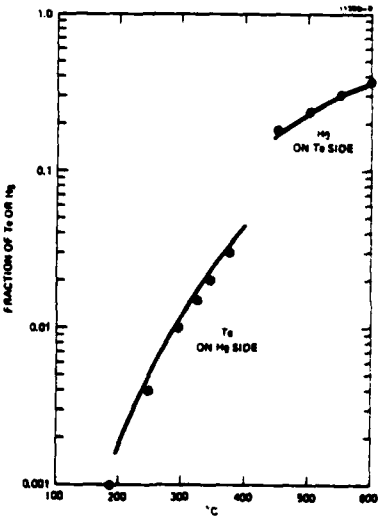

FIG. 3

Replots of the low temperature parts of the Hg-Te liquidus. The vertical axis is the composition of the minority species.

Figure 2 shows the Hg-Te binary liquidus. The dots are Harman's experiments (9). In calculating the theory we used the following values. The melting temperature is Harman's experimental value T_m = 673°C. The entropy of melting at T_m is ΔS_m = 9.2 e.u. which is in Laugier's paper (10). Other energy values are $\hat{\epsilon}_{12}$ = -200/6 cal, $\hat{\epsilon}_{13}/\hat{\epsilon}_{12}$ = -8, $\hat{\epsilon}_{23}/\hat{\epsilon}_{12}$ = -0.5, $\hat{\epsilon}_{14} = \hat{\epsilon}_{24} = \hat{\epsilon}_{34}$ = -1000°, and u = -3000°.

Figure 3 shows the low temperature parts of the liquidus curves for the Hg-rich side and the Te side. The Te values on the Hg side are based on Riley's experiment (11). They are plotted in the logarithmic scale so that a small amount of the minority component is seen more accurately than in Fig. 2. The curves in Fig. 3 are close to linear. It is found by trying many parameter value combinations that the slope of the line in Fig. 3 is controlled by ΔS_m and almost solely by it. For a certain value of ΔS_m, when we change other energy parameters, the line in Fig. 3 goes up or down but the slope remains almost unchanged at the value determined by ΔS_m. The dots in Fig. 3 are experiments and the curves are the theory; they agree well and the theory passes the test which is more severe than Fig. 2. Note that both the Hg-rich and the Te-rich legs agree with experiments and both of them confirm the same value ΔS_m = 9.2 e.u. The fact that 9.2 e.u. is also the independently measured experimental value of ΔS_m in Reference 10 supports the validity of the association model and the consistency of the theory, including Vieland's method of estimating the free energy of the solid state.

Figure 4 is for the Cd-Te binary liquidus. The points are experiments in Reference 7 and the curve is the present theory. The melting temperature is fixed at the experimental value T_m = 1082°C. Other parameters are ΔS_m = 5.0 e.u., $\hat{\epsilon}_{12}$ = -1000/6 cal., $\hat{\epsilon}_{13}/\hat{\epsilon}_{12}$ = -5.5, $\hat{\epsilon}_{23}/\hat{\epsilon}_{12}$ = -3.3, $\hat{\epsilon}_{14} = \hat{\epsilon}_{24} = \hat{\epsilon}_{34}$ = -1000°, and u = -6000°. Figure 5 corresponds to Fig. 3 and plots the amount of Cd in the Te-rich leg of the liquidus on a semi-log scale. The experimental points are due to Harman (12). As was discussed above, the slope of the line in Fig. 5 determines the value of ΔS_m, which we found to be 5.0 e.u. This value of ΔS_m is different from 8.8 e.u. reported in Reference 10. Since our estimate is regarded fairly reliable, further independent experimental measurements of ΔS_m for CdTe are desirable.

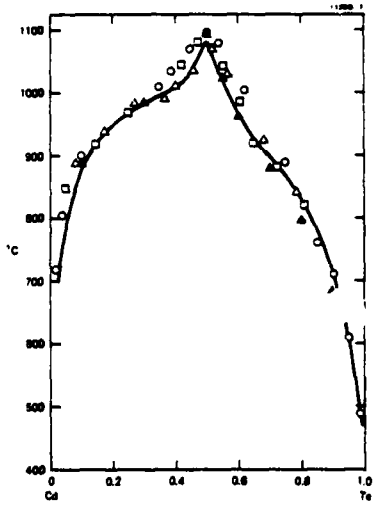

FIG. 4

Cd-Te binary liquidus. Points are experiments (7); curve is present theory.

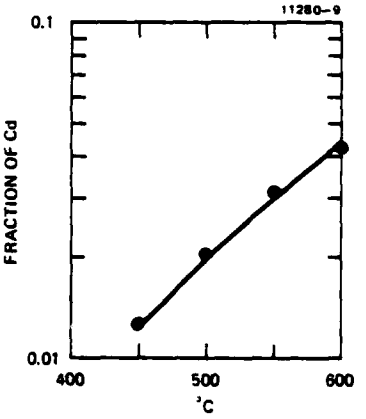

FIG. 5

Amount of Cd in the Te-rich side liquidus.

Although the association model is still controversial (13), the reasonably good agreement with experiments supports its usefulness as a working model.

The pair approximation of CVM can take into account the short range order, i.e., the local atomic arrangement, while the point approximation cannot. The former is recommended in treating the liquid state.

Acknowledgment

Discussions with John W. Cahn of National Bureau of Standards and Lloyd H. DeVaux of Hughes Research Laboratories are cordially acknowledged. Thanks are due to Kevin J. Riley of Santa Barbara Research Center for allowing the paper to use his results before publication.

References

1. G.B. Stringfellow and P.E. Greene, J. Phys. Chem. Solids 30, 1779 (1969).
2. R. Kikuchi, Physica 103B, 41 (1981).
3. R. Kikuchi, J. Chem. Phys. 60, 1070 (1971).
4. R. Kikuchi, J. de Phys. (Paris) 38, C7-307 (1977).
5. E.A. Guggenheim, Mixtures (Oxford University Press, 1952).
6. L.J. Vieland, Acta Met. 11, 137 (1963).
7. J. Steininger, A.J. Strauss, and R.F. Brebrick, J. Electrochem. Soc. 117, 1305 (1970).
8. D.A. Goodman, J.W. Cahn, and L.H. Bennett, to be published.
9. T.C. Harman, "Physics and Chemistry of II-VI Compounds" (M. Aven and J.S. Prener, eds.) p. 767, North Holland Publishers, Amsterdam (1967).
10. A. Laugier, Rev. Phys. Appl. 8, 259 (1973).
11. K.J. Riley, unpublished (1981).
12. T.C. Harman, J. Electronic Materials 9, 945 (1980).
13. M. Hillert and L.-I. Staffansson, Met. Trans. 6B, 37 (1975).

APPENDIX C

THEORETICAL CALCULATION OF Hg-Cd-Te

LIQUIDUS-SOLIDUS PHASE DIAGRAM

Theoretical calculation of Hg–Cd–Te liquidus–solidus phase diagram [a)]

Ryoichi Kikuchi

Hughes Research Laboratories, Malibu, California 90265

(Received 28 October 1981; accepted 22 January 1982)

The liquidus–solidus phase diagram of Hg–Cd–Te is calculated using the pair approximation of the cluster variation method. The work is an extension of previous III–V work and includes association as an additional feature. The liquid phase is approximated by a pseudo-lattice structure and includes molecular species as well as atomic species. Vacancies are also considered in order to take the pressure effect into account. Unlike the regular solution model, the pair method can take into account the short-range order in the liquid phase. Adjustable parameters (mostly energies) are first determined to fit Hg–Te and Cd–Te binary experiments. The association model can explain the asymmetry and the sharp peak at 50% composition. These parameters and several additional ones constitute the one set of parameters (independent of temperature and composition) which are used to calculate the entire ternary liquidus–solidus diagram. Each parameter controls certain features of the diagram. Although the work is still in progress, reasonably good agreement with known experiments has been achieved for both the Hg corner and the Te corner. The chemical potential diagram is discussed.

PACS numbers: 64.70.Dw, 68.45. – v, 81.30.Bx

Ternary phase diagrams of III–V semiconductors were previously calculated[1] using the pair approximation of the cluster variation method (CVM).[2] The work in Ref. 1 gives the same results as those obtained by Stringfellow and Greene,[3] who used the quasichemical approximation of Guggenheim.[4] The present report is an extension of Ref. 1, and includes association[5] and vacancies as additional features. Discussion of associated binary liquids can also be found in Ref. 6. Since the theory is closely related to Ref. 1, the reader is advised to consult Refs. 1 and 6 for additional and pertinent background information. Compared with the previously used regular solution model,[5] the advantage of the pair method is that the short-range order in the liquid phase can be taken into account.

In the liquid phase, x_i indicates the probability of finding an ith species on a lattice point. Since we will discuss both binary and ternary systems, we will make $i = 1, 2,..., 6$ denote Hg, Cd, Te, HgTe, CdTe, and a vacancy throughout the paper. For a Hg–Te binary liquid, we use $i = 1$, 3, 4, and 6 only, and for a Cd–Te binary we use $i = 2$, 3, 5, and 6 only. Along with the x_i's we use the probabilities y_{ij}, for finding i and j species on nearest-neighboring lattice sites. These y_{ij}'s are the basic variables in the pair approximation of the CVM. The two sets of variables are connected by the geometric reduction equation

$$x_i = \sum_j y_{ij}. \tag{1}$$

The equilibrium state of the liquid phase is determined by writing the Helmholtz free energy F in terms of y_{ij}'s, and then minimizing the grand potential $G \equiv F - \Sigma_i \mu_i N_i$ with respect to y_{ij}'s. (We write G for the grand potential, not the Gibbs free energy.) The quantity μ_i is the chemical potential (with respect to an appropriately chosen reference state), and N_i is the total number of the ith species in the system. When G is minimized, we obtain a set of equations

$$y_{ij} = (x_i x_j)^{(z-1)/z} \times \exp\left[\frac{2\lambda\beta}{z} - \beta\epsilon_{ij} + \frac{\beta}{z}(\mu_i + \mu_j)\right], \tag{2}$$

where z is the coordination number, and $\beta = (kT)^{-1}$ and ϵ_{ij} are the energy parameters for an i–j pair. We define ϵ_{ij} in such a way that $\epsilon_{ii} = 0$ for the same subscripts. One advantage of the CVM formulation is that Eqs. (1) and (2) hold for a ternary as well as a binary system, and also for associated as well as nonassociated liquids by appropriately identifying the subscripts. Derivation and discussions of Eq. (2) are in Ref. 1. In Eq. (2), λ is the normalization constant and has the physical meaning of $\lambda = -pv$, where p is the pressure and v is the volume per lattice point.

The mathematical procedure of the problem is to solve y_{ij}'s from the simultaneous nonlinear Eq. (2), together with Eq. (1) for fixed values of ϵ_{ij}, μ_i, β, and z. They are solved by using the natural iteration method (NIM)[7] without further analytical transformations. In the NIM, the first input is a set of guess values of x_i. We use these values on the right-hand side of Eq. (2) to calculate y_{ij} as the output. These y_{ij}'s are used in Eq. (1) to obtain the next input set, x_i. It was proved[7] that at each iteration cycle the G value decreases, and hence the iteration procedure always converges.

In deriving the liquidus curve theoretically, we need the relation between the free energies of the liquid and solid phases. The chemical potential, $\mu^{(s)}$, for solid HgTe (or CdTe) is derived from $\mu^{(l)}$ in the supercooled liquid state of the 50% composition by using Vieland's formula,[8] expressed as

$$\mu^{(s)} = \mu^{(l)} - (T_m - T)\Delta S_m, \tag{3}$$

where T_m is the melting point and ΔS_m is the entropy of melting per molecule.

For the Hg-Te binary system, the important adjustable parameters are ϵ_{13}, ϵ_{14}, ϵ_{34}, ΔS_m and U_1, where U_1 controls

 0022-5355/82/050129-04$01.00

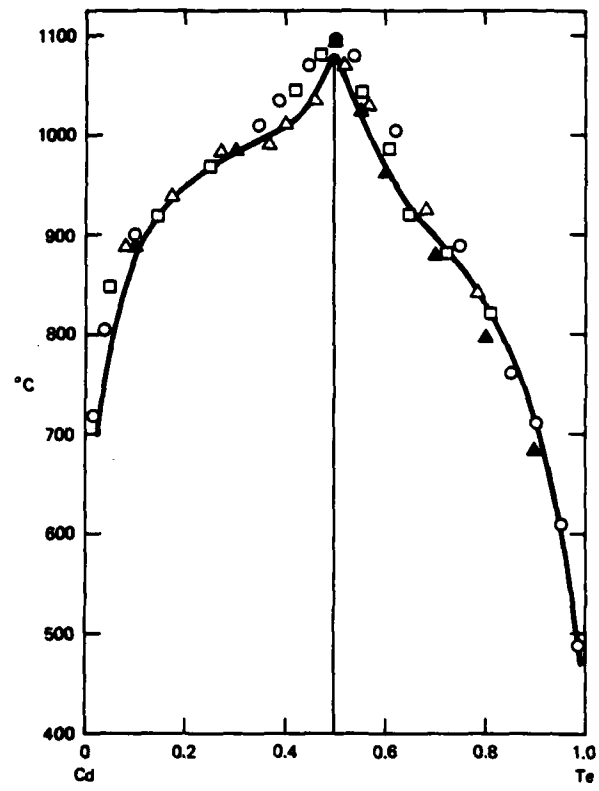

FIG. 1. Cd–Te binary liquidus. The curve is the present theory, and the points are experiments shown in Ref. 9.

the amount of association and connects μ_i's as

$$\mu_1 + \mu_3 - \mu_4 = U_1. \tag{4}$$

Details of this equation are found in Ref. 6. Figures 1 and 2 compare the theory (solid curves) of binary liquidus with experiments. Two features of liquidus curves, which are different from the III–V cases, are the asymmetry and the sharp peak at the 50% composition. The theory can derive asymmetry when $\epsilon_{14} \neq \epsilon_{34}$. The atomic pair interaction ϵ_{13} is attractive (i.e., negative). When ϵ_{14} and ϵ_{34} are repulsive (i.e., positive), the liquidus shows a peak at the 50% composition.[6] When $-U_1$ is large, the association property increases and the peak becomes sharper. Then when $-\epsilon_{14}/\epsilon_{13}$ is larger, the left shoulder of the Hg–Te liquidus goes up, and when $-\epsilon_{13}$ is smaller, the entire liquidus curve becomes lower (except that T_m at the 50% composition is anchored). The value of ΔS_m controls the shape of the leg parts of the liquidus curves in Figs. 1 and 2.

The values of the parameters we used in calculating the curves in Figs. 1 and 2 are: $\epsilon_{13} = -200/6$ cal, $\epsilon_{14}/\epsilon_{13} = -8.0$, $\epsilon_{34}/\epsilon_{13} = -0.5$, $U_1 = -3000$ °, $\epsilon_{23} = -1000/6$ cal, $\epsilon_{25}/\epsilon_{23} = -5.5$, $\epsilon_{35}/\epsilon_{23} = -3.3$, $U_2 = -6000$°, ΔS_m(HgTe) = 9.2 e.u., T_m(HgT) = 673 °C, ΔS_m(CdTe) = 5.0 e.u, T_m(CdTe) = 1082 °C, $\epsilon_{i6} = -1000$°, $i = 1, 2, \ldots, 5$, and $\epsilon_{66} = 0$. The energy units are left as they were used in computations. The value of z is chosen as 6 in the numerical work; however, $z = 4$ or 8 does not change the results very much.

In calculating binary liquidus curves, several cases were noticed in which different combinations of some parameters led to practically the same shape. Therefore, the above values of the parameters are not altogether unique.

However, the value of ΔS_m(HgTe) is believed to be accurate because 9.2 e.u. leads to a good agreement in both Hg-

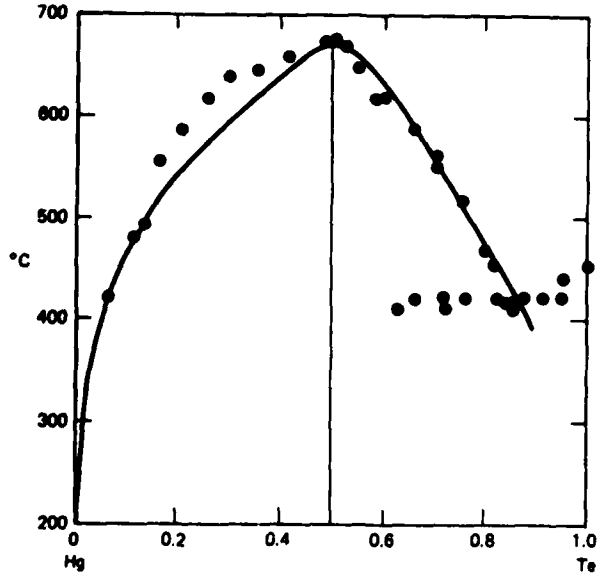

FIG. 2. Hg-Te binary liquidus, showing the present theory (curve) and experiments in Ref. 10 (points).

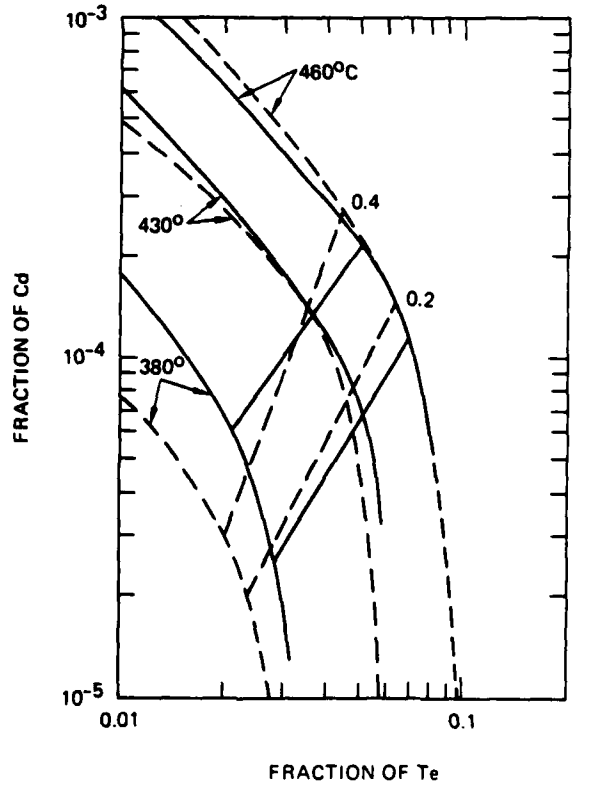

FIG. 3. The Hg corner of the ternary Hg–Cd–Te liquidus. The solid curve is the present theory, and the broken curves are Riley's experiments, Ref. 12. The numbers 0.2 and 0.4 are the values of x in the solid phase $(HgTe)_{1-x}(CdTe)_x$.

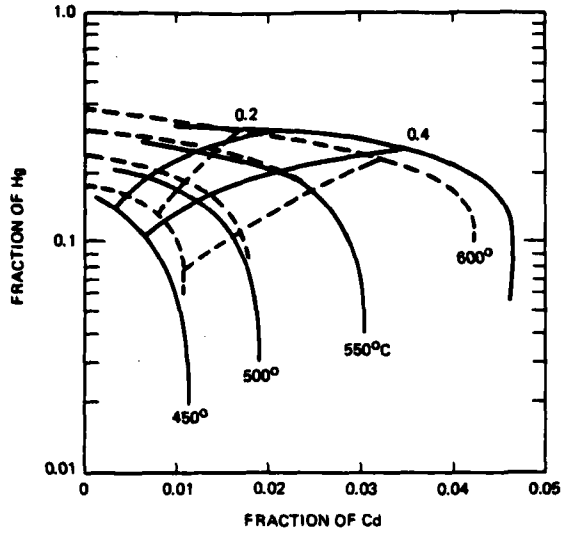

FIG. 4. The ternary Hg–Cd–Te liquidus near the Te corner. The solid curves are the present theory, and the broken curves are the experiments of Harman in Ref. 13. The numbers 0.2 and 0.4 have the same meaning as in Fig. 3.

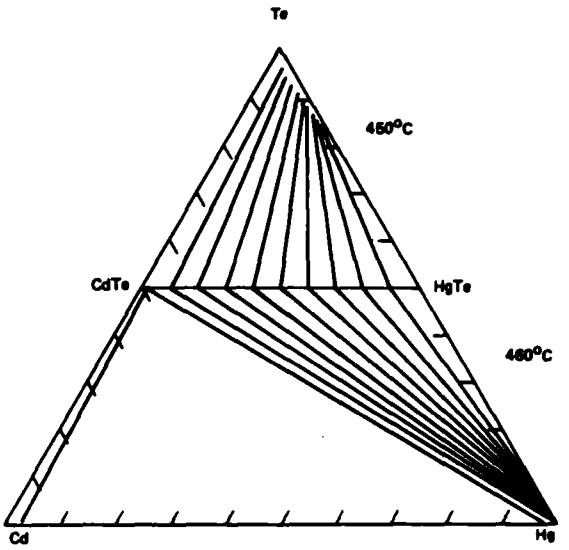

FIG. 6. The Gibbs diagram of the Hg–Cd–Te liquidus and solidus. The upper Te-rich side is for 450 °C, and the lower part is for 460 °C. Note the phase separation in the lower part.

rich and Te-rich leg parts and also is the value reported by Laugier.[11]

For the ternary system (as was done in Ref. 1) we need ϵ_s, the interaction of a Hg–Cd pair on one of two fcc sublattices which constitute the zincblende structure. Besides ϵ_s, adjustable parameters are ϵ_{12} for the Hg–Cd pair, ϵ_{15} for the Hg–CdTe pair, ϵ_{45} for the HgTe–CdTe pair, and ϵ_{24} for the Cd–HgTe pair.

In comparing with other experiments, we first examined the Hg corner. The value of ϵ_s adjusts the general shape of the curves, and the best choice we could make was $\epsilon_s = 0$. The values of ϵ_{12} and ϵ_{15} were adjusted to bring the Cd concentration to the right range. The values we chose to plot in Fig. 3 were $\epsilon_{12} = 500°$ and $\epsilon_{15} = 900°$. For these energy values, Cd species exist more or less equally in the atomic Cd form, and the molecular CdTe form.

After these values are determined we move to the Te-corner in Fig. 4. The shape of the curve is adjusted by ϵ_{45}. In the region of Fig. 4, HgTe predominates over CdTe; thus, when ϵ_{45} is attractive, CdTe increases (the contribution of atomic Cd is negligible). We chose the value $\epsilon_{45} = -120°$ to draw Fig. 4. Figure 5 replots the data in Fig. 4 in a different way. The circles are Harman's experiments[13] for temperatures ranging between 450° and 550 °C. Although the experimental points of different temperatures lie on one curve, and the

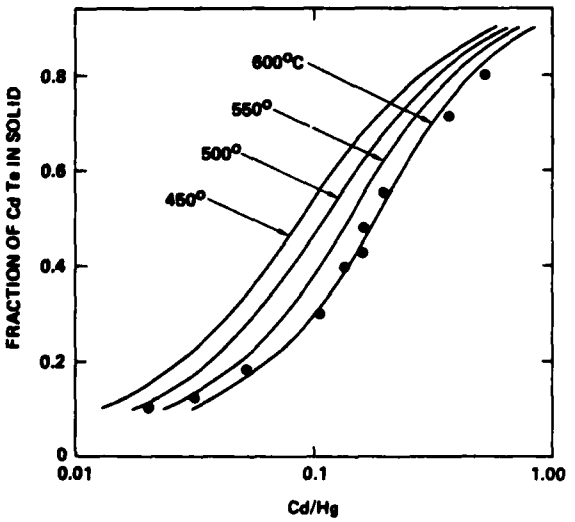

FIG. 5. The Hg–Cd–Te liquidus and solidus in the Te-rich side. This is a replot of Fig. 4. The experimental points are those of Harman, in Ref. 13.

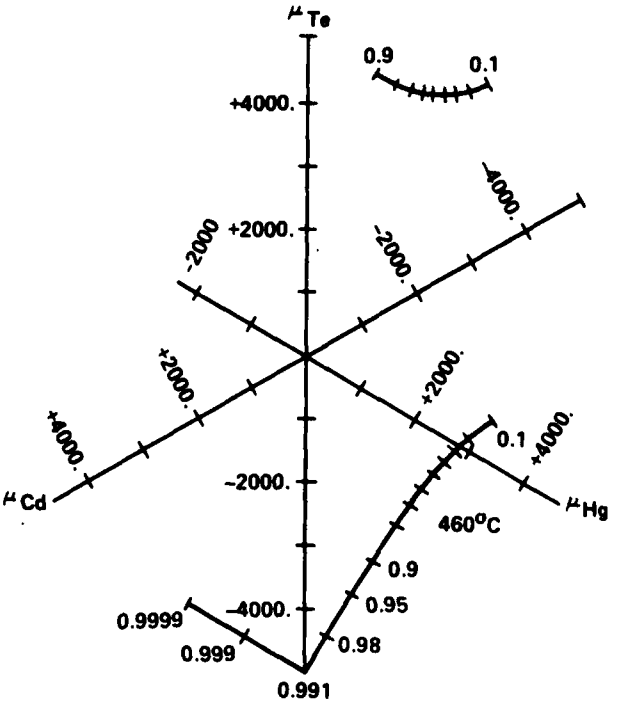

FIG. 7. The chemical potential diagram corresponding to Fig. 6.

600 °C theoretical curve fits the experiments well, the theoretical curves for other temperatures are shifted.

It should be pointed out that the values of ϵ_s, ϵ_{12}, and ϵ_{15}, which have been determined in Fig. 3, have a strong effect on Fig. 4. The fact that the same set of values of ϵ_s, ϵ_{12}, and ϵ_{15} leads to a satisfactory agreement with experiments in both Figs. 3 and 4 can be counted as a merit of the theory. The value of ϵ_{45} determined from Fig. 4 has practically no effect on Fig. 3 because the amount of HgTe in the Fig. 3 region is much smaller than the amount of Hg. Since no detailed experimental data were available for the Cd-rich region, we left ϵ_{24} undetermined for the Cd–HgTe interaction and used $\epsilon_{24} = 0$ in computation.

Figure 6 is the Gibbs diagram of the liquidus–solidus. Note especially the tie line which goes all the way across from the Hg corner to the point near CdTe, in agreement with the report of Ref. 14. Since our value of $\epsilon_{12} = 500°$ shows the repulsion between Hg and Cd, there is a phase separation in the liquid phase. In Fig. 6 the state of Hg = 0.976, Cd = 0.024 coexists with the state of Hg = 0.027, Cd = 0.968. (These values are not reliable because $\epsilon_{24} = 0$ is tentative.)

Figure 7 shows the chemical potential diagram as it corresponds to Fig. 6. The chemical potentials for Hg, Cd, and Te are adjusted (linearly shifted) so that the sum of the three is zero. In that case, μ_1, μ_2, and μ_3 can be plotted[1] in the star diagram of Fig. 7. The upper curve is for the Te corner and the lower curve is for the Hg–Cd side. Each point on the two curves represents the coexisting states of the liquid and the solid. A number next to a mark on the curves is the composition x in the solid phase, $(HgTe)_{1-x}(CdTe)_x$. The point to be noted is that a tie line in Fig. 6 is perpendicular[1] to the μ curve at the corresponding x point. The phase separation near the Cd–Hg edge in Fig. 5 is represented by the discontinuous change of slope in the bottom part of Fig. 7.

The pair approximation has been known for many years, and is known to give more reliable results than the regular solution method. The difficulty, however, in applying the pair treatment to a system of many components was that a large number of variables had to be calculated by solving nonlinear equations. This difficulty was solved by the NIM.[7] Different from the Newton–Raphson method, the NIM does not need matrix inversion, and it guarantees positivity of all probability variables being calculated. The large number of variables does not cause any problem.

Although the association model used in this paper is still controversial,[15] the good agreement between experiments and the present theory, which uses one set of parameters, suggests the usefulness of the model as a working hypothesis.

The author wishes to express his thanks to Lloyd deVaux of Hughes Research Laboratories for the discussions and his continued interest in this work, and also to Kevin Riley of Santa Barbara Research Center for allowing the paper to use his experimental results before publication.

[a]Supported by U. S. Army Research Office.

[1]R. Kikuchi, Physica 103B, 41 (1981).
[2]R. Kikuchi, Phys. Rev. 81, 988 (1951).
[3]G. B. Stringfellow and P. E. Greene, J. Phys. Chem. Solids 30, 1779 (1969).
[4]E. A. Guggenheim, *Mixtures* (Oxford University, Oxford, 1952).
[5]T. Tung, L. Golonka, and R. F. Brebrick, J. Electrochem. Soc. 128, 1601 (1981).
[6]R. Kikuchi, Calphad 6, 1 (1982).
[7]R. Kikuchi, J. Chem. Phys. 60, 1071 (1974).
[8]L. J. Vieland, Acta Metall. 11, 137 (1963).
[9]J. Steininger, A. J. Strauss, and R. F. Brebrick, J. Electrochem. Soc. 117, 1305 (1970).
[10]T. C. Harman, *Physics and Chemistry of II-VI Compounds*, edited by M. Aven and J. S. Prener (North-Holland, Amsterdam, 1967), p. 767.
[11]A. Laugier, Rev. Phys. Appl. 8, 259 (1973).
[12]K. J. Riely, Santa Barbara Research Center (private communication), 1981.
[13]T. C. Harman, J. Electron. Mater. 9, 945 (1980).
[14]J. E. Bowers, J. L. Schmit, C. J. Speerschneider, and R. B. Maciolek, IEEE Trans. Electron. Devices ED27, 52 (1980).
[15]M. Hillert and L.-I. Staffansson, Metall. Trans. 6B, 37 (1975).

APPENDIX D

THEORY OF SOLID HgCdTe WITH DEFECTS

1. INTRODUCTION

In the liquidus calculations of III-V and II-VI semiconductors in References 1, 2 and 3 by the author, and also in those by Brebrick et al.[4], the solid phase was treated as stoichimetric without lattice defects. In actuality, lattice defects are important since the electrical properties of the semiconductor are affected by the defects. In this appendix we formulate the Hg-Cd-Te solid phase, including lattice defects.

The solid Hg-Cd-Te lattice is shown in Figure 1. It is made of two interpenetrating fcc sublattices. On the white fcc sublattice, Hg and Cd atoms are distributed, while the black fcc sublattice is occupied by Te atoms. For this examination we allow vacancies in both sublattices, and also we include antiatoms, which means Te atoms on the HgCd sublattice and Hg or Cd atoms on the Te sublattice.

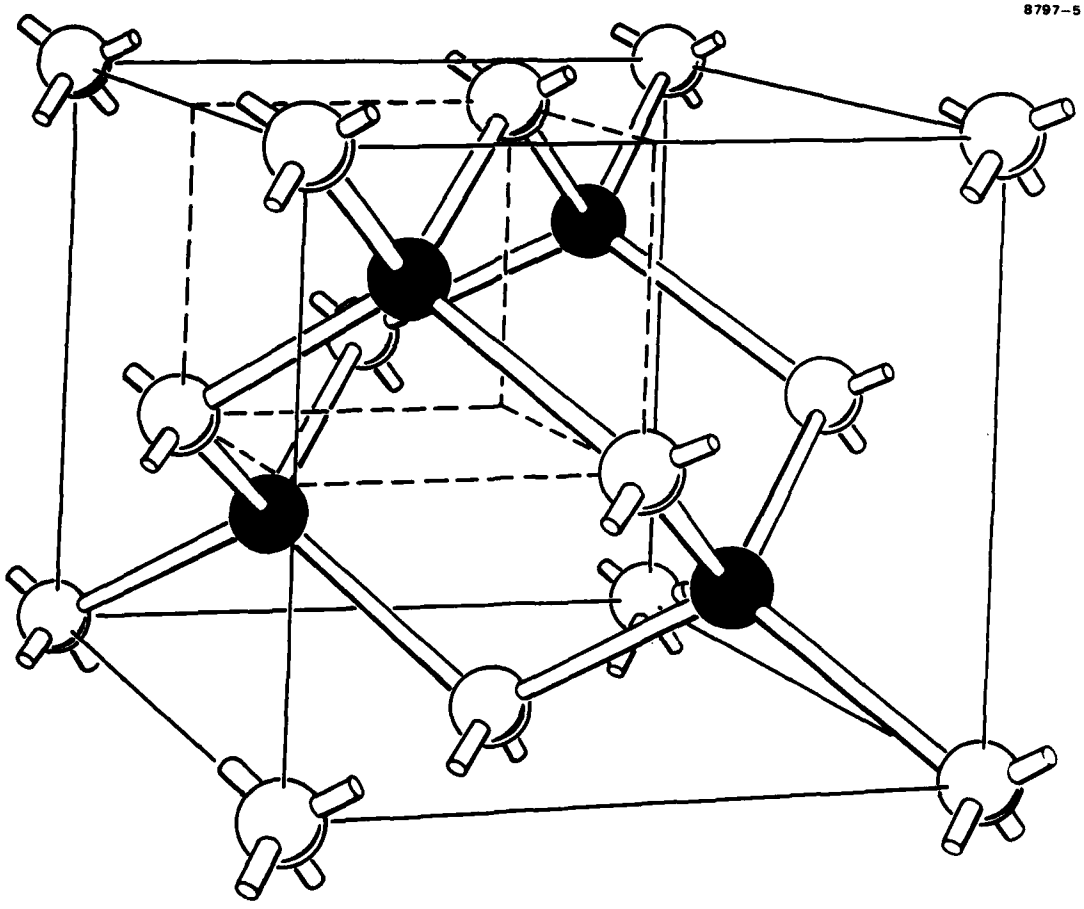

Figure 1. Structure of the Hg-Cd-Te crystal.

In calculating the free energy, we use the pair approximation of the cluster variation method (CVM)[5]. Although the two sublattices are both of the fcc structure, each fcc lattice is disordered by itself, and hence there is no frustration effect which is characteristic in the ordered fcc structure. Therefore, the pair approximation is expected to be a reliable method.

In contrast to the ordinary pair approximation, we use two kinds of pairs, intrasublattice and intersublattice; thus the entropy expression of the present formulation has not been used before.

2. VARIABLES

We use the designation I and II for the HgCd sublattice and the Te sublattice. On each lattice point we have either a Hg, Cd, or Te atom or a vacancy; these four species are designated by i = 1,2,3 and 4.

The probability of finding an i^{th} species on the sublattice I is written as $x_{I,i}$. This is a "point" variable. The probability of finding an i-j nearest-neighbor pair in the I sublattice is written as $y_{I,ij}$; this is the variable for an intrasublattice pair. The corresponding variables, $x_{II,i}$ and $y_{II,ij}$ are similarly defined for the sublattice II. Another pair variable, z_{ij}, is for the probability of finding an i^{th} species on the sublattice I and a j^{th} species on a nearest-neighboring II sublattice (note the order of the two subscripts); z_{ij} is an intersublattice variable. Note that z_{ij} and z_{ji} are different, while $y_{I,ij} = y_{I,ji}$.

These variables are related by the following relations:

$$x_{I,i} = \sum_j y_{I,ij} = \sum_j z_{ij} \quad , \tag{2.1a}$$

$$x_{II,i} = \sum_j y_{II,ij} = \sum_j z_{ji} \quad . \tag{2.1b}$$

The normalization relations are

$$1 = \sum_{i,j} y_{I,ij} = \sum_{i,j} y_{II,ij} = \sum_{i,j} z_{ij} \quad . \tag{2.2}$$

In subsequent sections we minimize the grand potential under constraints. The constraints written in Equation (2.1) can be treated using Lagrange multipliers, $\alpha_{I,i}$ and $\alpha_{II,i}$ as

$$12 \sum_i \alpha_{I,i} \left[\sum_j y_{I,ij} - \sum_j z_{ij} \right] + 12 \sum_j \alpha_{II,j} \left[\sum_i y_{II,ij} - \sum_i z_{ij} \right]$$

$$= 6 \sum_{i,j} \left(\alpha_{I,i} + \alpha_{I,j} \right) y_{I,ij} + 6 \sum_{i,j} \left(\alpha_{II,i} + \alpha_{II,j} \right) y_{II,ij}$$

$$- 12 \sum_{i,j} \left(\alpha_{I,i} + \alpha_{II,j} \right) z_{ij} \quad . \tag{2.3}$$

This expression will be used in Equation (3.10).

3. GRAND POTENTIAL

The entropy expression can be derived by using, for example, Barker's procedure[6]:

$$S/kN = 15\left[\sum_i \mathcal{L}\left(x_{I,i}\right) + \sum_i \mathcal{L}\left(x_{II,i}\right)\right]$$
$$-6\left[\sum_{i,j}\mathcal{L}\left(y_{I,ij}\right) + \sum_{i,j}\mathcal{L}\left(y_{II,ij}\right)\right] - 4\sum_{i,j}\mathcal{L}\left(z_{ij}\right) + 14 \quad , \tag{3.1}$$

where k is the Boltzman constant, N is the number of lattice points in one of the fcc sublattices, and $\mathcal{L}(x)$ is defined as

$$\mathcal{L}(x) \equiv x\ell nx - x \quad . \tag{3.2}$$

In writing the energy expression, we need two kinds of energy parameters: ϵ_{ij} for an intrasublattice pair and u_{ij} for an intersublattice pair. Using these parameters, we can write the total energy of the system as

$$E/N = 6\sum_{i,j}\epsilon_{ij}\left[y_{I,ij} + y_{II,ij}\right] + 4\sum_{i,j} u_{ij}\, z_{ij} \quad . \tag{3.3}$$

We assume that a vacancy does not contribute potential energy, so that

$$\epsilon_{i4} = \epsilon_{4i} = u_{i4} = u_{4i} = 0 \quad \text{for } i = 1,2,3,4 \tag{3.4}$$

The grand potential, Ω, is defined as

$$\Omega \equiv E - TS - \sum_i \mu_i N_i \quad , \tag{3.5}$$

where μ_i is the chemical potential and N_i is the total number (both of the i^{th} species). For the vacancy i = 4, we define $\mu_4 = 0$, since we do not need the chemical potential for a vacancy. Using the variables $x_{I,i}$ and $x_{II,i}$, we can write

$$N_i = N \left(x_{I,i} + x_{II,i} \right) \quad . \tag{3.6}$$

When we combine the two terms, $E - \sum \mu_i N_i$ in Equation (3.5), it is convenient to define

$$\hat{\varepsilon}_{ij} \equiv \varepsilon_{ij} - (\varepsilon_{ii} + \varepsilon_{jj})/2.$$
$$\hat{u}_{ij} \equiv u_{ij} - (u_{ii} + u_{jj})/2. \tag{3.7a}$$

and

$$\hat{\mu}_i \equiv \mu_i - 2u_{ii} - 6\,\varepsilon_{ii} \quad . \tag{3.7b}$$

Then we can write

$$\left[E - \sum_i \mu_i N_i \right] / N$$
$$\equiv 6 \sum_{i,j} \hat{\varepsilon}_{ij} \left[y_{I,ij} + y_{II,ij} \right] + 4 \sum_{i,j} \hat{u}_{ij}\, z_{ij} - \sum_i \hat{\mu}_i \left(x_{I,i} + x_{II,i} \right), \tag{3.8}$$

where each summation goes over i = 1,2,3,4 and j = 1,2,3,4. From Equation (3.7), the parameters with carets have the properties:

$$\hat{\varepsilon}_{ii} = \hat{u}_{ii} = 0 \quad \text{and} \quad \hat{\mu}_4 = 0 \tag{3.9a}$$

$$\hat{\varepsilon}_{i4} = \hat{\varepsilon}_{4i} = -\varepsilon_{ii}/2$$
$$\hat{u}_{i4} = \hat{u}_{4i} = -u_{ii}/2 \quad . \tag{3.9b}$$

It is convenient to use these energy parameters with carets because in the limit of no vacanies, the individual ε_{ii} and u_{ii} do not contribute to the state of the system.

Combining the energy and chemical potential terms in Equation (3.8) and the entropy expression in Equation (3.1), the grand potential, Ω, in Equation (3.5), together with the constraint terms, is written explicitly as follows:

$$\begin{aligned}\Phi \equiv \beta\Omega/N = {} & 6\beta \sum_{i,j} \hat{\varepsilon}_{ij} \left[y_{I,ij} + y_{II,ij}\right] + 4\beta \sum_{i,j} \hat{u}_{ij}\, \hat{z}_{ij} \\ & - \beta \sum_{i} \hat{\mu}_{i} \left[x_{I,i} + x_{II,i}\right] \\ & - 15 \left[\sum_{i} \mathcal{L}(x_{I,i}) + \sum_{j} \mathcal{L}(x_{II,j})\right] \\ & + 6 \left[\sum_{i,j} \mathcal{L}(y_{I,ij}) + \sum \mathcal{L}(y_{II,ij})\right] + 4 \sum_{i,j} \mathcal{L}(z_{ij}) - 14 \\ & + \beta\lambda_{z} \left(1 - \sum_{i,j} z_{ij}\right) + \beta\lambda_{I} \left(1 - \sum_{i,j} y_{I,ij}\right) + \beta\lambda_{II} \left(1 - \sum_{i,j} y_{II,ij}\right) \\ & + 6 \sum_{i,j} \left(\alpha_{I,j} + \alpha_{I,j}\right) y_{I,ij} + 6 \sum \left(\alpha_{II,i} + \alpha_{II,j}\right) y_{II,ij} \\ & - 12 \sum_{i,j} \left(\alpha_{I,i} + \alpha_{II,j}\right) z_{ij} \quad , \end{aligned} \tag{3.10}$$

where the λ terms are for the normalizations and the α terms are the constraints derived in Equation (2.3).

4. MINIMIZATION OF THE GRAND POTENTIAL

The equilibrium state of the system is obtained as a minimum of the grand potential, Ω, or Φ in Equation (3.10). In minimizing it, we regard $y_{I,ij}$, $y_{II,ij}$ and z_{ij} as independent. We treat $x_{I,i}$ and $x_{II,i}$ as averages of y's and z's; the weights are arbitrary, but we use the following expressions:

$$x_{I,i} = \frac{1}{4}\left(3\sum_j y_{I,ij} + \sum_j z_{ij}\right)$$
$$x_{II,j} = \frac{1}{4}\left(3\sum_i y_{II,ij} + \sum_i z_{ij}\right) . \qquad (4.1)$$

Differentrations of Φ in Equation (3.10) with respect to $y_{II,ij}$ and z_{ij} lead to the following equations:

$$\ell n\ y_{I,ij} = \beta\lambda_I/6 + \ell n\ \hat{y}_{I,ij}$$
$$\ell n\ y_{II,ij} = \beta\lambda_{II}/6 + \ell n\ \hat{y}_{II,ij} \qquad (4.2)$$
$$\ell n\ z_{ij} = \beta\lambda_z/4 + \ell n\ \hat{z}_{ij} ,$$

where we separated out the normalization factors, x's, and the quantities with carets are defined as

$$\ell n\ \hat{y}_{I,ij} = \frac{15}{16}\ell n\ (x_{I,i}\ x_{I,j}) + \beta\left[-\hat{\varepsilon}_{ij} + \frac{1}{16}(\hat{\mu}_i + \hat{\mu}_j)\right] - \alpha_{I,i} - \alpha_{I,j}$$
$$\ell n\ \hat{y}_{II,ij} = \frac{15}{16}\ell n(x_{II,i}x_{II,j}) + \beta\left[-\hat{\varepsilon}_{ij} + \frac{1}{16}(\hat{\mu}_i + \hat{\mu}_j)\right] - \alpha_{II,i} - \alpha_{II,j}$$
$$\ell n\hat{z}_{ij} = \frac{15}{16}\ell n(x_{I,i}x_{II,j}) + \beta\left[-\hat{u}_{ij} + \frac{1}{16}(\hat{\mu}_i + \hat{\mu}_j)\right] + 3\ (\alpha_{I,i} + \alpha_{II,j}). \qquad (4.3)$$

The equilibrium state is solved from Equation (4.2) and (4.3), and the constraint relations in Equations (2.1) and (2.2).

When these equations are solved, Φ in Equation (3.10) can be simplified as

$$\Phi = \Phi - \sum_{i,j} y_{I,ij} \frac{\partial \Phi}{\partial y_{I,ij}} - \sum_{i,j} y_{II,ij} \frac{\partial \Phi}{\partial y_{II,ij}} - \sum_{ij} z_{ij} \frac{\partial \Phi}{\partial z_{ij}}$$

(4.4)

$$= \beta \left(\lambda_z + \lambda_I + \lambda_{II}\right) = \beta \Omega / N \quad .$$

On the other hand, since the $\sum_i \mu_i N_i$ term in Equation (3.5) is the Gibbs free energy, we can identify Ω as the difference between the Helmholtz and Gibbs free energies, so that

$$\Omega = -pV \quad , \tag{4.5}$$

where V is the total volume of the system. From the last two equations, we can derive the pressure expression as

$$p = - \left(\lambda_z + \lambda_I + \lambda_{II}\right) N/V \quad . \tag{4.6}$$

Since we will need it later, let us derive the chemical potential expressions from Equation (4.3) by eliminating α's. Making i = j, we obtain

$$\hat{\mu}_i = kT\left[-\frac{15}{2} \ln \left(x_{I,i}\, x_{II,i}\right) + 3 \ln \left(y_{I,ii}\, y_{II,ii}\right) + 2 \ln z_{ii}\right]$$

(4.7)

$$- \frac{1}{2} \left(\lambda_z + \lambda_I + \lambda_{II}\right) \quad .$$

This holds for I = 1,2,3,or 4. The λ terms can be rewritten from the i = 4 case as

$$\frac{1}{2}\left(\lambda_z+\lambda_I+\lambda_{II}\right) = kT\left[-\frac{15}{2}\ln \left(x_{I,4}x_{II,4}\right) + 3\ln \left(y_{I,44}y_{II,44}\right) +2\ln z_{44}\right].$$

(4.8)

5. ITERATIVE SOLUTION OF THE EQUATIONS

The set of equations in the previous section is solved iteratively. The method is called the Natural Iteration Method.[7] The flow chart of the iteration procedure is shown in Figure 2. In using this scheme we fix the values of the energies, $\hat{\epsilon}_{ij}$, $\hat{u}_{ij}$, the chemical potentials, $\hat{\mu}_i$, and the temperature, β. The three chemical potential values control the equilibrium composition and the pressure.

In the flow chart of Figure 2, the second step is called the Minor Iteration. It solves the Lagrange multipliers (α's) using the following procedure. The variable $\alpha_{I,i}$ is contained in both the y_I terms and z terms of Equation (2.1a), as is seen in Equation (4.3). Using (4.2) in (2.1a), we write the latter as

$$e^{\beta\lambda_I/6}\, e^{-\alpha_{I,i}} \sum_j e^{\alpha_{I,i}}\, \hat{y}_{I,ij} = e^{\beta\lambda z/4}\, e^{3\alpha_{I,i}} \sum_j e^{-3\alpha_{I,i}}\, \hat{z}_{ij} \quad . \tag{5.1}$$

Since $y_{I,ij}$ and z_{ij} are individually normalized to unity, one of the four equations, i = 1,2,3,4, in Equation (2.1a) is redundant. This means that we need only three α_I's. Or we may choose, for example,

$$\alpha_{I,3} = 0 = \alpha_{II,3} \quad . \tag{5.2}$$

Then we can eliminate the normalization factors λ's in Equation (5.1) and write

$$e^{-\alpha_{I,i}} \frac{\sum_i e^{\alpha_{I,i}} \hat{y}_{I,ij}}{\sum_j \hat{y}_{I,3j}} = e^{3\alpha_{I,i}} \frac{\sum_i e^{-3\alpha_{I,i}} \hat{z}_{ij}}{\sum_j \hat{z}_{ij}} \quad . \tag{5.3}$$

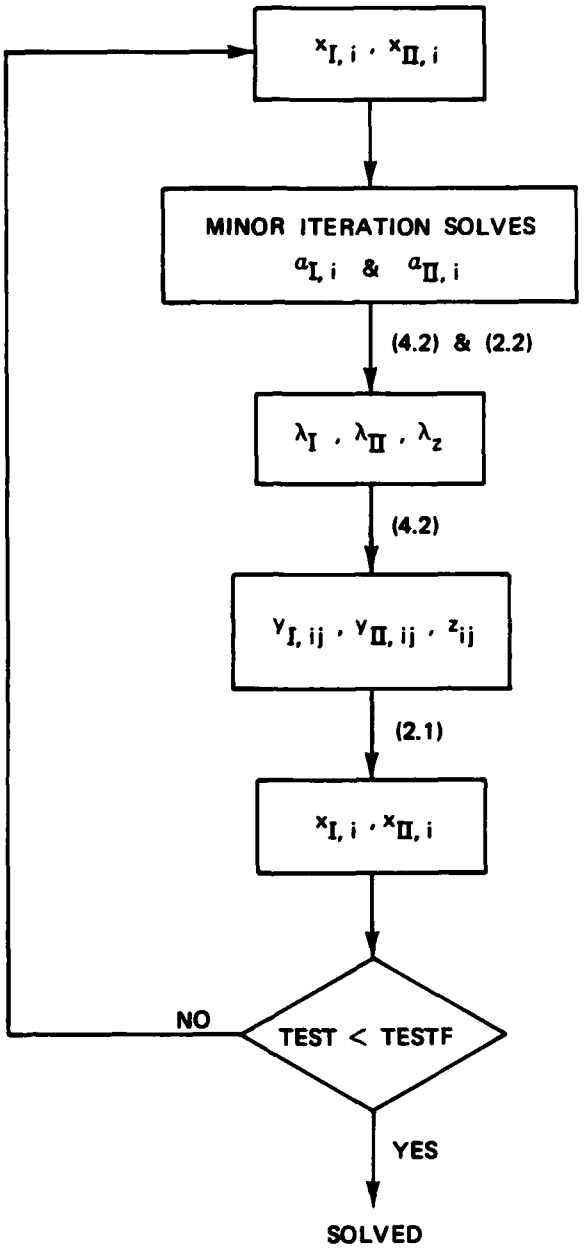

Figure 2. Flow chart of the Natural Iteration Method.

When we use this expression as the iterative equation for $\alpha_{I,i}$, we use $\alpha_{I,i}^{(input)}$ for the $\alpha_{I,i}$ written inside the summation signs, and the outside $\alpha_{I,i}$ is written as $\alpha_{I,i}^{(output)}$. Thus, we write

$$\alpha_{I,i}^{(output)} = \alpha_{I,i}^{(input)} + \frac{\gamma}{4} \ell n \left[\frac{\sum_j \hat{y}_{I,ij}}{\sum_j \hat{y}_{I,3j}} \quad \frac{\sum_j \hat{z}_{3j}}{\sum_j \hat{z}_{ij}} \right]. \qquad (5.4a)$$

In this equation, we use a damping factor, γ. We assign to γ a certain constant value between 0 and 1 in the iteration calculation. When $\gamma = 0$, the output α is equal to the input α and the iteration does not proceed. When $\gamma = 1$, the $\alpha_{I,i}^{(output)}$, which is the next input value, may sometimes overshoot. Usually, $\gamma = 0.5$ leads to stable convergence of the iteration.

For $\alpha_{II,i}$, the equation corresponding to Equation (5.4a) is

$$\alpha_{II,j}^{(output)} = \alpha_{II,j}^{(input)} + \frac{\gamma}{4} \ell n \left[\frac{\sum_i \hat{y}_{II,ij}}{\sum_i \hat{y}_{II,i3}} \quad \frac{\sum_i \hat{z}_{i3}}{\sum_i \hat{z}_{ij}} \right]. \qquad (5.4b)$$

The chemical potential controls the composition as follows. We first combine $x_{I,i}$ and $x_{II,i}$ and define

$$x_i = (x_{I,i} + x_{II,i})/2. \qquad (5.5)$$

Using x_i's, we define

$$\eta_2 \equiv x_1 - x_2$$
$$\eta_3 \equiv x_1 + x_2 - x_3 \quad . \qquad (5.6)$$

Then, η_2 signifies the Hg-Cd composition, and η_3 represents the deviation from the stoichiometry. Using η's, we can write the chemical potential terms in the grand potential as

$$\sum_i \hat{\mu}_i \left(x_{I,i} + x_{II,i}\right) = \hat{\mu}_u \eta_2 + \hat{\mu}_w \eta_3 + \hat{\mu}_v \left(1 - x_4\right) , \qquad (5.7)$$

where

$$\hat{\mu}_u \equiv \left(\hat{\mu}_1 - \hat{\mu}_2\right)/2$$

$$\hat{\mu}_w \equiv \left(\hat{\mu}_1 + \hat{\mu}_2\right)/4 - \hat{\mu}_3/2 \qquad (5.8a)$$

$$\hat{\mu}_v \equiv \left(\hat{\mu}_1 + \hat{\mu}_2\right)/4 + \hat{\mu}_3/2$$

or

$$\hat{\mu}_1 = \hat{\mu}_v + \hat{\mu}_w + \hat{\mu}_u$$

$$\hat{\mu}_2 = \hat{\mu}_v + \hat{\mu}_w - \hat{\mu}_u \qquad (5.8b)$$

$$\hat{\mu}_3 = \hat{\mu}_v - \hat{\mu}_w \quad .$$

From Equation (5.7), we see that the value of $\hat{\mu}_v$ controls $1 - x_4$; as μ_v increases, $1 - x_4$ increases and the vacancy concentration decreases. The value lof $\hat{\mu}_u$ controls the Hg-Cd composition; as $\hat{\mu}_u$ increses $x_1 - x_2$ increases. As the value $\hat{\mu}_w$ increases, the non-stoichiometry $x_1 + x_2 - x_3$ increases.

When we treat a ternary system, we expect it to reduce to the binary case when one of the ternary components reduces to zero. For example, when x_2 reduces to zero, $\hat{\mu}_2$ goes to $-\infty$, whereas $\hat{\mu}_1$ and $\hat{\mu}_2$ remain finite. We can establish the correspondence between the ternary and the binary case by this procedure.

6. SUMMARY

The Hg-Cd-Te crystalline state is formulated using the pair approximation of the CVM, including vacancies and antiatoms, but without interstitial atoms. The crystal is made of two fcc sublattices I and II. On each lattice point, one of the four species is found: Hg, Cd, and Te atoms and a vacancy. The treatment uses nearest-neighbor intersublattice potentials, u_{ij}, and nearest-neighbor intrasublattice potentials, ϵ_{ij}. The basic variables are intersublattice pair probabilities, z_{ij}, and intrasublattice pair probabilities, $y_{I,ij}$ and $y_{II,ij}$.

In order to solve the equilibrium state, the grand potential, $\Omega \equiv E - TS - \sum_i \mu_i N_i$, is written in terms of y's and z's, and is then minimized with respect to the variables. The resulting equations are solved for given values of T and μ_i's by an iterative technique.

This solid state treatment is a part of the work on the liquidus-solidus calculation in Appendix E.

REFERENCES

1. R. Kikuchi, Physica 103B, 41 (1981).

2. R. Kikuchi, CALPHAD 6, 1 (1982).

3. R. Kikuchi, J. Vac. Sci. Techn. 21, 129 (1982).

4. See, for example, T. Tung, C.-H. Su, P.-K. Liao and R.F. Brebrick, J. Vac. Sci. Tech. 21, 117 (1982).

5. R. Kikuchi, Phys. Rev. 81, 988 (1951).

6. J.A. Barker, Proc. Roy. Soc. A216, 45 (1953).

7. R. Kikuchi, J. Chem. Phys. 60, 1071 (1974).

APPENDIX E

HgCdTe LIQUIDUS AND SOLIDUS, INCLUDING

LATTICE DEFECTS IN SOLID

A. INTRODUCTION

The liquidus and solidus of the binary Hg-Te and Cd-Te systems and the ternary Hg-Cd-Te have been calculated by the author[1,2] using the pair approximation of the cluster variation method (CVM). In these calculations, the free energy, F, of the binary solid state was represented by a point in the F vs. composition space because the solid phase was assumed to be stoichiometric and free from any lattice defects. Since the lattice defects are of practical importance, we included vacancies and antiatoms in the solid phase in Appendix D of the present report. This appendix reports the procedure of combining the new solid phase in Appendix D and the liquid phase of Reference 2 to obtain the liquidus and the solidus.

In the ternary liquid treatment of Appendix C, not many equations were written because of the page limitation. Actually, the equations in Appendix B for the binary liquid can be used for the ternary liquid as well without much change. Thus, we may refer to Appendix B when equations for a ternary liquid are needed.

B. COEXISTENCE CONDITIONS

When two phases coexist, one of the conditions of coexistence is that the chemical potentials of each component are equal in the two phases; i.e.,

$$\mu_i^{(\ell)} = \mu_i^{(s)} \qquad i = 1, 2 \text{ and } 3, \qquad (2.1)$$

where 1, 2 and 3 denote Hg, Cd and Te species. It should be mentioned here that the previous work of the Hg-Cd-Te liquidus and solidus[2] could not use Equation (2.1) because the solid phase was represented by a singular structure, as was mentioned in the previous section, and because $\mu_i^{(s)}$ was indeterminate.

The second condition of coexistence is that the pressure of the liquid and that of the solid are the same. Since our models of the liquid and the solid both contain vacancies, we can calculate pressures of both phases and equate them for coexistence.

When we compare chemical potentials in the liquid and solid phases, we need to determine the reference levels in the two phases. We use Vieland's equation[3], as was done in Reference 2. It is written for binary cases as follows:

$$\mu_i(s,i3) + \mu_3(s,i3) = \mu_i(sc\ell,i3) + \mu_3(sc\ell,i3) - (T_m - T)\,\Delta S_m, \quad i = 1 \text{ and } 2 \tag{2.2}$$

where s and sc^{ℓ} in supercript stand for solid and supercooled liquid, respectively, and i3 indicates that this equation is for the i-3 binary case. In the last term, T_m is the melting temperature, and ΔS_m is the entropy of melting (per molecule) of HgTe (i = 1) or CdTe (i = 2) solid.

C. STEPS OF LIQUIDUS - SOLIDUS CALCULATION

The liquidus-solidus calculations are done in the following steps. The temperature T and the pressure p are fixed throughout the calculation. In this and subsequent sections we use the names i = 1, ..,6 for atomic Hg, Cd, Te, molecular HgTe, CdTe and a vacancy in the liquid phase.

(1) First, we solve the Hg-Te and Cd-Te binary liquid states for the 50-50 composition. This state is unstable below the melting temperature, T_m, and was called the supercooled state in Section 2, with the designation sc^{ℓ} in Equation (2.2). We calculate the sum, $\mu_i(s,i3) + \mu_3(s,i3)$, for a binary solid phase from the left-hand side of Vieland's relation (Equation 2.2).

(2) Then, we solve the binary solid states, Hg-Te and Cd-Te, and $\hat{\mu}_i(s,i3) + \hat{\mu}_3(s,i3)$ are obtained. The superscript (s,i3) indicates that this is the i3 binary solid state (i = 1 or 2).

(3) Next, we solve the ternary solid state. As we remarked in Section 5 of Appendix D, $\hat{\mu}_u(s)$ controls the Hg:Cd ratio and $\hat{\mu}_w(s)$ controls the (Hg + Cd): Te stoichimetry. The third chemical potential parameter, $\hat{\mu}_v(s)$, controls the number of vacancies and thus the pressure. By

selecting these three chemical potential parameters, we make the solid phase take the desired composition and the prescribed pressure, p_o. For this state, the three values, $\hat{\mu}_i$, in Equation (5.8b) of Appendix D are written as $\hat{\mu}_i(s,123)$ to note that it is for the ternary case.

(4) In the solid phase, μ_i and $\hat{\mu}_i$ are related by Equation (3.7b) of Appendix D:

$$\hat{\mu}_i(s) = \mu_i(s) - 2u_{ii} - 6\varepsilon_{ii} \quad . \tag{3.1}$$

We assume that u_{ii} and ε_{ii} remain the same, independent of the ternary composition. Then we can write

$$\begin{aligned} \mu_i(s,123) + \mu_3(s,123) = {} & \mu_i(s,i3) + \mu_3(s,i3) \\ & + \left(\hat{\mu}_i(s,123) + \hat{\mu}_3(s,123)\right) \\ & - \left(\hat{\mu}_i(s,i3) + \hat{\mu}_3(s,i3)\right) \\ & i = 1 \text{ and } 2 \quad . \end{aligned} \tag{3.2}$$

On the right-hand side the first two terms are calculated using the Vieland formula (Equation 2.2), and the terms with carets are calculated in solving the solid phases. Thus, we can evaluate the left-hand side quantity.

(5) In the coexisting states, μ_i's are equal in the liquid and the solid phases, as was stated in Equation (2.1). Thus we can replace the μ's on the left-hand side of Equation (3.2), by the corresponding μ's for the liquid phase. For the first two terms of the right-hand side of Equation (3.2), we use Equation (2.2). Then we can write.

$$\begin{aligned} \mu_i(\ell) + \mu_3(\ell) = {} & \mu_i(sc\,\ell,i3) + \mu_3(sc\,\ell,i3) - (T_m - T)\,\Delta S_m \\ & + \left(\hat{\mu}_i(s,123) + \hat{\mu}_3(s,123)\right) \\ & - \left(\hat{\mu}_i(s,i3) + \hat{\mu}_3(s,i3)\right) \\ & i = 1 \text{ and } 2 \quad . \end{aligned} \tag{3.3}$$

Since both $\mu_i^{(\ell)}$ and $\mu_i^{(sc\ell,i3)}$ are for the liquid phase, we can use Equation (3.b) of Appendix B and place carets on them to write

$$\hat{\mu}_i^{(\ell)} + \hat{\mu}_3^{(\ell)} = \hat{\mu}_i^{(sc\ell,i3)} + \hat{\mu}_3^{(sc\ell,i3)} - (T_m - T)\,\Delta S_m + \left(\hat{\mu}_i^{(s,123)} + \hat{\mu}_3^{(s,123)}\right) - \left(\hat{\mu}_i^{(s,i3)} + \hat{\mu}_3^{(s,i3)}\right) \qquad i = 1 \text{ and } 2 \qquad (3.4)$$

(6) We choose $\hat{\mu}_3^{(\ell)}$. Then, combining with Equation (3.4), we know $\hat{\mu}_i^{(\ell)}$ and $\hat{\mu}_2^{(\ell)}$. Using these three $\hat{\mu}_i^{(\ell)}$ values, we can solve the liquid state. When the liquid state is solved, we examine the pressure. We then vary $\hat{\mu}_3^{(\ell)}$ to come to the preassigned value, p_o, of the pressure. By calculating $\mu_3^{(\ell)}$ from $\hat{\mu}_3^{(\ell)}$ using Equation (3.6) and (3.15) of Appendix B, we get

$$\mu_3^{(\ell)} = \hat{\mu}_3^{(\ell)} + \omega\varepsilon_{33} - \varepsilon_3 \quad . \qquad (3.5)$$

Note that these are different from the solid relation in Equation (3.1).

(7) Since we know the value of $\hat{\mu}_3^{(s)}$ in Step (3), we can calculate $\mu_3^{(s)}$ from Equation (3.1). We then plot $\mu_3^{(s)}$ and $\mu_3^{(\ell)}$ against $\hat{\mu}_w^{(s)}$ used in Step 3. We vary $\hat{\mu}_w^{(s)}$ and find the value for which

$$\mu_3^{(s)} = \mu_3^{(\ell)} \quad . \qquad (3.6)$$

This point is the coexistence point. Note that in going from Equation (3.2) to Equation (3.3), we use the relationship

$$\mu_i^{(s)} + \mu_3^{(s)} = \mu_i^{(\ell)} + \mu_3^{(\ell)} \text{ for } i = 1 \text{ and } 2 \; . \qquad (3.7)$$

The combination of Equations (3.6) and (3.7) are equivalent to the coexistence condition (Equation 2.1).

D. SUMMARY

We have described the procedures of calculating the liquidus-solidus of the Hg-Cd-Te system. For the solid phase, the method in Appendix D is used and the lattice defects (vacancies and autiatoms) are included. The liquid phase is modeled using a pseudo-lattice structure, as was done in Reference 1 and 2.

The detailed steps, (1) through (7), of computing the liquidus and solidus for the coexistence condition are described in Section 3.

The main results are shown in Figures 10, 11 and 12 of the main text of this report.

REFERENCES

1. R. Kikuchi, CALPHAD 6, 1 (1982).
2. R. Kikuchi, J. Vac. Sci. Techn. 21, 129 (1982).
3. L.J. Vieland, Acta Metall. 11, 137 (1963).

END

FILMED

10-83

DTIC